FINAL REPORT

Evaluation of UWB and Lower Adjacent Band Interference to C-Band Earth Station Receivers

11 February 2004

Prepared For:

Coalition of C-Band Constituents

ALION
SCIENCE AND TECHNOLOGY

8100 Corporate Drive
Lanham, MD 20785-2231
301-918-1000
www.alionscience.com

Executive Summary

Working for the Coalition of C-Band Constituents (CCBC), Alion Science & Technology has conducted an extensive investigation of how UWB will affect C-band satellite reception. By understanding these effects, means of co-existence between the incumbent C-band users and the new UWB unlicensed service may be proposed.

At the currently allowed UWB power limits, using modeled UWB device densities likely to be encountered in consumer deployment, and simulations verified with actual C-band signals, C-band reception will increasingly fail due to interference arising from UWB proliferation. As UWB begins to appear in quantities typical of consumer applications, the combined effects of UWB devices will overpower C-band reception and render it impossible.

SECTION 1 Introduction 1-1
1.1 Background 1-1
1.2 Objective 1-2
1.3 Approach 1-2
1.3.1 Task 1. Modeling and Simulation 1-3
1.3.2 Task 2. Laboratory Testing 1-4

SECTION 2 Earth Station Modeling 2-1
2.1 General 2-1
2.2 C-Band Ground Stations 2-1
2.3 Modeled C-Band Earth Station Receivers 2-1
2.3.1 General 2-1
2.3.2 Earth Station Receivers 2-2
2.3.2.1 FM 2-3
2.3.2.2 PSK 2-5
2.3.2.3 QPSK 2-5

SECTION 3 UWB Signal Environment 3-1
3.1 General 3-1
3.2 UWB Devices 3-1
3.2.1 Imaging System 3-1
3.2.1.1 Ground Penetrating Radar Imaging Systems 3-1
3.2.1.2 Wall Imaging Systems 3-2
3.2.1.3 Through-wall Imaging Systems 3-2
3.2.1.4 Surveillance Systems 3-2
3.2.1.5 Medical Imaging Systems 3-2
3.2.2 Vehicular Radar Systems 3-2
3.2.3 Communications and Measurement Systems 3-3
3.3 UWB Signal Environments 3-3
3.3.1 General 3-3
3.3.2 UWB Deployments 3-3
3.3.2.1 Spatial Characteristics 3-3
3.3.2.2 Propagation Path Loss 3-4
3.3.2.3 Received Power Distribution 3-7
3.3.2.4 UWB Time/Power Characterization 3-11

SECTION 4 Modeling and Simulation Results 4-1
4.1 Introduction 4-1

SECTION 5 Validation Testing 5-1
5.1 Introduction 5-1
5.2 Testing Methodology 5-1
5.3 Desired Signal Conditions 5-2
5.4 Undesired Signal Conditions 5-5
5.5 UWB Signal Source 5-6
5.6 Receivers Under Test 5-7
5.7 UWB Test Results for the 8PSK Receiver 5-8
5.8 UWB Test Results for QPSK 5-9
5.9 UWB Test Results for the Analog Receiver 5-9
5.10 WiFi Test Results 5-11
5.11 Computer Receiver Model Validation 5-11

SECTION 6 SUMMARY OF RESULTS AND CONCLUSIONS 6-1
6.1 Summary of Results 6-1

6.2 Conclusions 6-7

ATTACHMENT 1

Model TFP1001 Impulse Source User Instructions.....1

SECTION 1
Introduction

1.1 Background

On February 14, 2002, the Federal Communication Commission (FCC) adopted a *First Report and Order* ("R&O") in the matter of Revision of Part 15 of the Commission's rules Regarding Ultra-Wideband Transmission Systems. This R&O amended Part 15 to permit the marketing and operation of products incorporating UWB technology.

UWB radio systems can employ pulse modulation where extremely narrow (short) bursts of RF energy are modulated and emitted to convey information.[1] Because of the very short duration of these pulses, the emission bandwidths from these systems are large and often exceed one gigahertz (GHz).[2]

In some cases, "impulse" transmitters are employed where the pulses do not modulate a carrier. Instead, the radio frequency emissions generated by the pulses are applied to an antenna, and the resonant frequency of the antenna determines the center frequency of the radiated emission. The frequency response characteristics of the antenna provide band-pass filtering, further affecting the shape of the radiated signal.

UWB devices can be used for precise measurement of distances or locations and for obtaining the images of objects buried under ground or behind surfaces. UWB devices can also be used for wireless communications, particularly for short-range high-speed data transmissions suitable for broadband access to networks.

Several categories of UWB devices are permitted under the revised Part 15 including imaging systems,[3] vehicular radars and indoor and outdoor communication systems. Because of their wide operating bandwidths, UWB devices operate in frequency bands that are allocated both to U.S. Government and to non-government public and commercial operations. Operation of federal government radio stations is regulated by the National Telecommunications and Information Administration (NTIA), while operation of stations by private industry, by state and local governments and by the public is regulated by the FCC. The standards and operating requirements that were recently adopted were based in large measure on standards that NTIA

[1] The rules adopted in the *R&O* also permit UWB devices to comply with the minimum bandwidth requirement due to the use of a high speed data rate or the use of other modulation techniques instead of the width of the pulse or impulse signal.

[2] Typical pulse widths used by UWB devices currently are on the order of 0.1-2 nanoseconds, or less, in width. The emission spectrum appears as a fundamental lobe with adjacent side lobes that can decrease slowly in amplitude. The rise time of the leading edge of the pulse and the passband of the radiating antenna are major factors in determining the bandwidth of the UWB emission.

[3] Imaging systems consist of GPRs, wall imaging systems, through-wall imaging systems, surveillance systems, and medical imaging systems.

found to be necessary to protect against interference to federal government operations. The FCC has indicated that it will review the standards for UWB devices, and issue a further rule making in the future as additional information becomes available and additional types of UWB operations and technology become known.

The Commission established in Part 15 technical standards and operating restrictions for three types of UWB devices based on their potential to cause interference. These three types of devices are: 1) imaging systems including Ground Penetrating Radar (GPR), wall imaging systems, through-wall imaging systems, surveillance systems and medical imaging devices; 2) vehicular radar systems; and 3) communications and measurement systems consisting of indoor-only devices and hand held devices that may be operated anywhere.

1.2 Objective

The overall objective of this investigation was to determine C-Band receiver degradation arising from UWB and lower-adjacent-band (3.65-3.9 GHz) unlicensed services, as well as a technology demonstration of the interference effects on various C-Band systems.

1.3 Approach

A combination of laboratory testing and computer modeling and simulation was utilized to demonstrate the effect of UWB and lower adjacent band unlicensed devices on C-Band FSS ground station receiver performance. A sample of analog and digital receivers of interest were identified and modeled. The performance of the models developed was then verified and validated (V&V) utilizing laboratory testing with appropriate desired and undesired interfering UWB and lower adjacent band signals. Once the performance of the receiver models was verified and validated, an operational aggregate environment of multiple potentially interfering emitters was then prepared for input to the simulation. This interfering signal environment was developed using Monte-Carlo techniques to characterize the distribution of emitters in the environment. The results of the simulation were used to identify appropriate degradation criteria for UWB and representative lower-adjacent-band interfering signals, and to show the impact of multiple interfering signals on the video picture quality for selected cases of interest.

The Approach has been broken down into two general tasks: Modeling and Simulation, and Laboratory Testing.

1.3.1 Task 1. Modeling and Simulation

The specific objective of this task was to characterize the performance of several typical FSS receivers in the presence of interference from UWB and lower adjacent band interferers. For the UWB case, spectral characteristics were determined from published technical parameters for representative systems. Adjacent band interference was assumed to have spectral characteristics equivalent to IEEE 802.11b wireless networking devices, translated to the lower adjacent frequency range.

The general approach was to use MATLAB/Simulink to develop dynamic simulations of the FSS desired signals and receivers and an aggregate interfering environment. Laboratory measurements were then utilized to verify the performance of the receiver models versus individual interfering signals.

Five receiver models, representing five different typical analog and digital video FSS receivers were created in Simulink. The characteristics of each receiver model such as modulation type, bandwidth, and error correction features were specified within Simulink to match the characteristics of the representative systems. Each receiver model included components for RF/IF filtering (to include both frequency selectivity and time waveform distortion effects) and demodulation (for example, analog FM or QPSK). When appropriate, the models also included components for error correction (for example, concatenated Viterbi and Reed-Solomon decoding). The simulations were designed to produce the following outputs:

- Analog signal-to-distortion ratio (SDR) – Ratio between the power in the desired signal and the power in the error signal, expressed in decibels. For our purposes the error signal is the difference between the source and recovered baseband signals, after amplitude normalization.
- Digital bit-error rate (BER) – As calculated using the native SIMULINK bit-error rate block. Include mean, variance, and temporal trends where available.

An UWB signal generator model and a lower adjacent band signal generator model were created in Simulink. The models generated interfering waveforms that were considered to be typical. In addition, Monte Carlo techniques were used to generate "aggregate" waveforms; that is, waveforms that represent an environment containing multiple interferers. These interference models have adjustable parameters called *test parameters*. In some cases, the test parameters represented random variables associated with coupling loss or antenna gain. The test parameters were also varied in the simulations to fully characterize their effects on performance.

The following assumptions were made regarding the aggregate interference environment:

1) UWB sources are independent (i.e., uncorrelated)
2) Emission source characteristics such as pulse repetition frequency (PRF) and initial phase within the pulse repetition cycle are stationary random variables.
3) Random spatial source distribution
4) Located within an annular ring centered on the victim receiver
5) Inner (R_{min}) and outer (R_{max}) radii (eg., from 30m to 5km) to be determined by analysis as part of design of experiment (DOE).
6) Mean interference source density varies from d_{min} to d_{max} (eg., from 1 to 1,000 units per square kilometer), in steps to be defined during DOE.

The simulation model was validated by comparing the results for a particular simulation with results measured in the lab. The validated model was then exercised repeatedly for each receiver model. The interference signal type was varied, and all test parameters were varied.

1.3.2 Task 2. Laboratory Testing

Laboratory testing was used to characterize the effect of the LNB on interfering signals prior to their reaching the receiver, and to perform validation of the receiver models versus the selected UWB and lower adjacent-band interfering signals.

During the LNB characterization tests, the changes in the UWB signal as it passed through a typical C-Band LNB were characterized. A spectrum analyzer and digitizing oscilloscope were used to measure the frequency and time domain characteristics, respectively of the UWB signal applied to the LNB input and of the resulting LNB output. The spectrum analyzer was also used to measure the attenuation of lower adjacent band signals by the LNB.

A UWB signal source was utilized for the LNB test, along with appropriate spectrum analyzer, digitizing oscilloscope, and test controller.

For the receiver model validation tests, a desired signal and varying levels of UWB and lower adjacent band interference were applied to the input of a satellite earth station receiver and the output of the receiver was monitored to identify the degradation, if any, produced by the interfering signal. Specific desired signal parameters (modulation, power level at receiver input, and information content) and interfering signal parameters (pulse timing, power level at receiver input) were varied to determine the point at which the degradation ceases to be observable and the point at which the degradation is catastrophic.

For the laboratory tests, interference effects on receiver performance was evaluated based on observed degradation in picture quality.

SECTION 2
Earth Station Modeling

2.1 General

Five generic C-Band receivers were modeled to predict the effects of UWB on representative C-Band Earth Stations.

2.2 C-Band Ground Stations

C-Band is defined as the frequency range from 3.7 - 4.2 GHz. Satellites operating in this band are located in geostationary orbit and can be spaced as close as two degrees apart in space. There are currently over 20 satellites utilized by video and television broadcasters for dissemination of programming materials in the United States.

C-Band FCC domestic satellite are limited to 24 transponders operating at 10 to 17 watts each. Typical ground station receive antennas are 3.7 to 10 m in diameter. More than 250 channels of video and 75 audio services are available today from the C-Band satellites over North America. Virtually every cable programming and over-the-air broadcast television service is delivered via C-Band. Typical C-Band earth station technical characteristics are shown in Table 2-1.

Table 2-1
Typical C-Band Earth Station Characteristics

Frequency Range	3.7-4.2 GHz
Antenna Size (diameter)	4.5 meters
Antenna Gain (Peak)	44.1 dBi
Antenna Elevation Angle	5 –50 degrees
Antenna Azimuth	95-270 degrees
Modulation Types	FM, QPSK, 8-PSK
Data Rate	40-75 Mb/s
Desired Signal Level	-81 dBm

2.3 Modeled C-Band Earth Station Receivers

2.3.1 General

Five different receiver configurations were developed for this measurement/analysis effort. Each of these types of receivers is described below along with a summary of modeling assumptions.

2.3.2 Earth Station Receivers

The receiver models described in this section were created and their performance analyzed using the block-oriented MATLAB/Simulink software. Each model represents a complete transmit-receive cycle, with system noise, interference, and a path loss calculated for geostationary altitude. In the following diagrams the lower half of the signal path represents the receiver of interest. Details vary slightly with each model, but the following features constitute a common simulation approach.

- A primary information source, represented by a random number generator
- Block and convolutional source encoding (for all digital receivers)
- Primary modulation (QPSK, 8-PSK, or FM)
- Constant geosynchronous orbital path loss (195 dB)
- Antenna module
    - Entry point for both desired and interference signals
    - Nominal main-lobe gain for desired signals
    - Antenna pattern effects incorporated into UWB interference model
    - Thermal noise and coupling losses
- Receiver front end module
    - Primary demodulation (i.e., to baseband)
    - Thermal and phase noise
- Block and convolutional decoding of received signal (digital only)
- Comparison with source; quantify receiver performance
    - BER for digital receiver models
    - S/D ratio for analog FM

For the purposes of this simulation effort, identical antenna models were paired with each Earth Station receiver. The most significant variations between the receiver models are listed in the following table.

Table 2-2
Receiver Model Parameters

Receiver Model	Modulation	Channel Data Rate	FEC Reed Solomon (n, k)	FEC-Viterbi (n/k)
FSS-FM	FM	10.75 MHz/V	N/A	N/A
FSS-QPSK1	QPSK	41.471 Mb/s	(188, 204)	3/4
FSS-QPSK2	QPSK	47.2 Mb/s	(188, 204)	7/8
FSS-QPSK3	QPSK	1.5 Mb/s	(188, 204)	3/4
FSS-8PSK	8-PSK	73.725 Mb/s	(188, 204)	8/9

2.3.2.1 FM

The FM receiver depicted in Figure 2-1 is conceptually the simplest of our simulation models. The random source data is directly modulated by the "FM Modulator" block with a modulation constant of 10.75 MHz per volt, then amplified to the appropriate transmit signal strength. The desired signal undergoes geostationary path-loss attenuation before injection into the antenna, where it is mixed with a signal representing the aggregate UWB interference (Figure 2-2). The combined signal enters the "Receiver Front End" block, where it encounters the LNA and system noise sources prior to FM demodulation. The demodulated signal is compared with the source data, and the difference is used to calculate an analog signal-to-distortion (S/D) ratio.

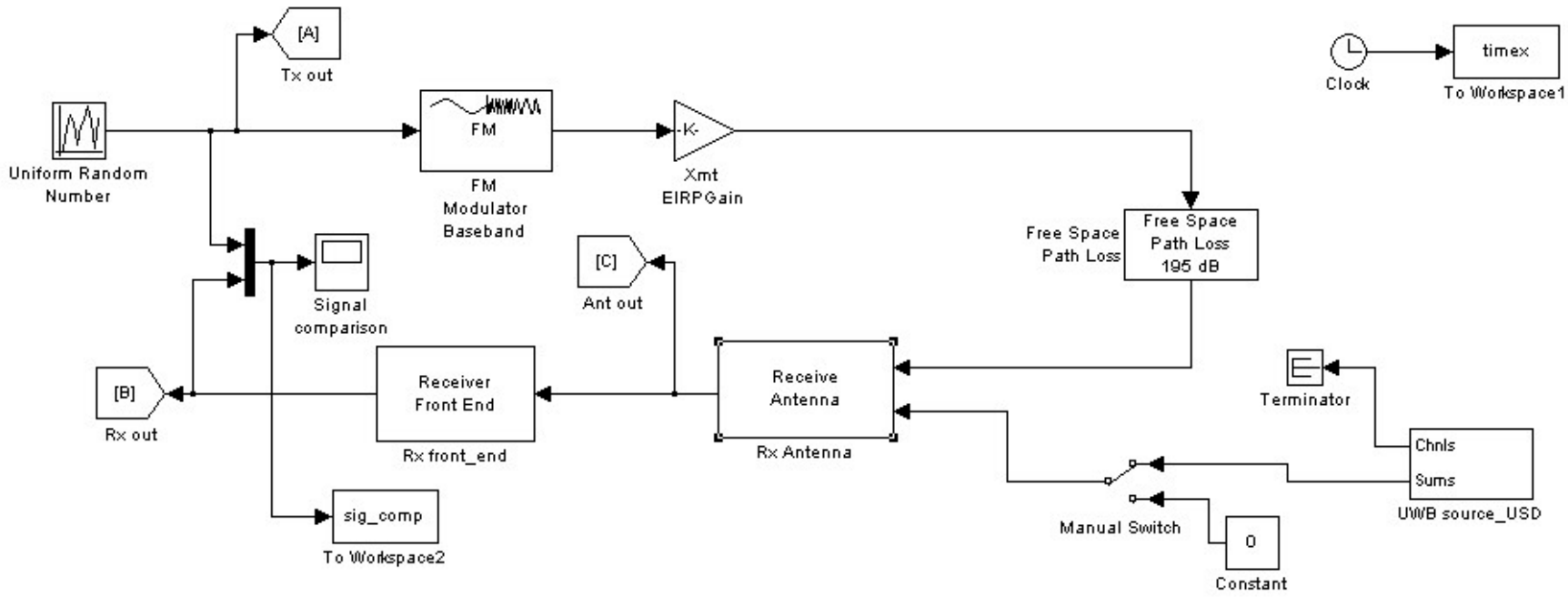

Figure 2-1. FM Receiver Block Diagram

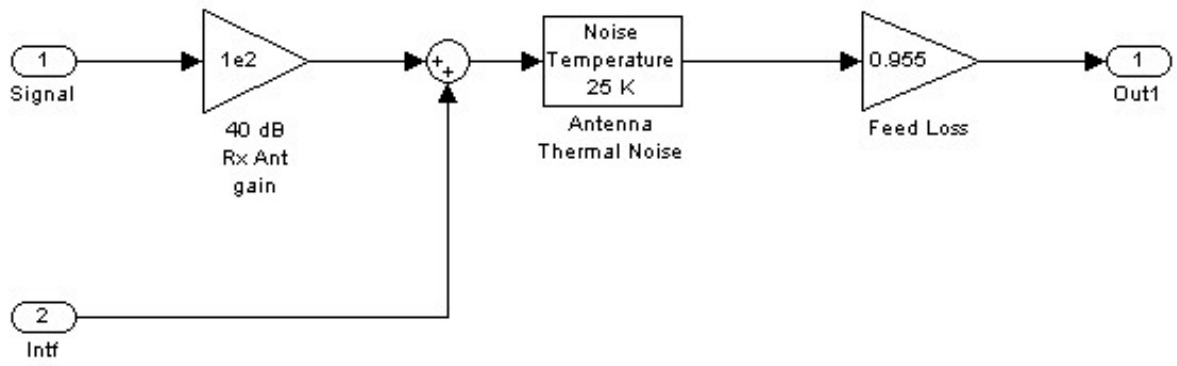

Figure 2-2 Earth Station Antenna Representation

2.3.2.2 PSK

In the model depicted in Figure 2-3 the random-integer source data stream is subjected to two stages of forward error-correction encoding; a (188, 204) Reed-Solomon algorithm followed by 8/9 rate convolutional encoding. The encoded signal is then phase-modulated by "M-PSK Modulator" (M=8) before amplification, transmission, and receive-path attenuation. As in the FM model, the received signal is mixed with UWB interference in the "Antenna" block, amplified and demodulated in the "Receiver Front End" block. The demodulated signal is subjected to Viterbi, then Reed-Solomon decoding before comparison with the source via the "Error Rate Calculation" block to determine the system bit-error rate.

2.3.2.3 QPSK

Figure 2-4 depicts one of three conceptually similar Earth Station receivers, which differ from that of Figure 2-3 only in modulation type, quadrature phase shift keying (QPSK), source data rates, and in the parameters of the Reed-Solomon and Viterbi forward error-correction coding algorithms to be applied.

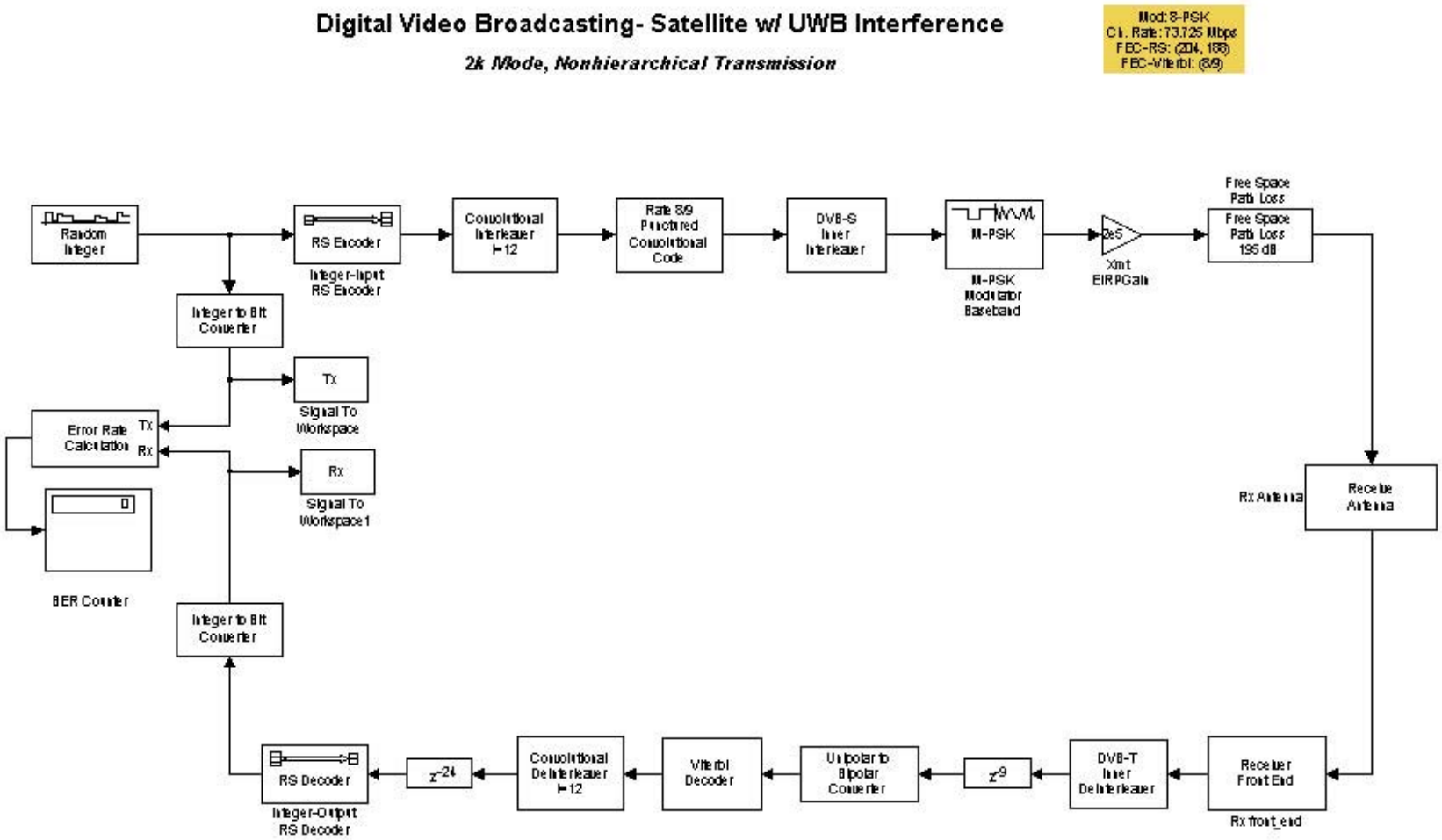

Figure 2-3. 8-PSK Receiver Block Diagram

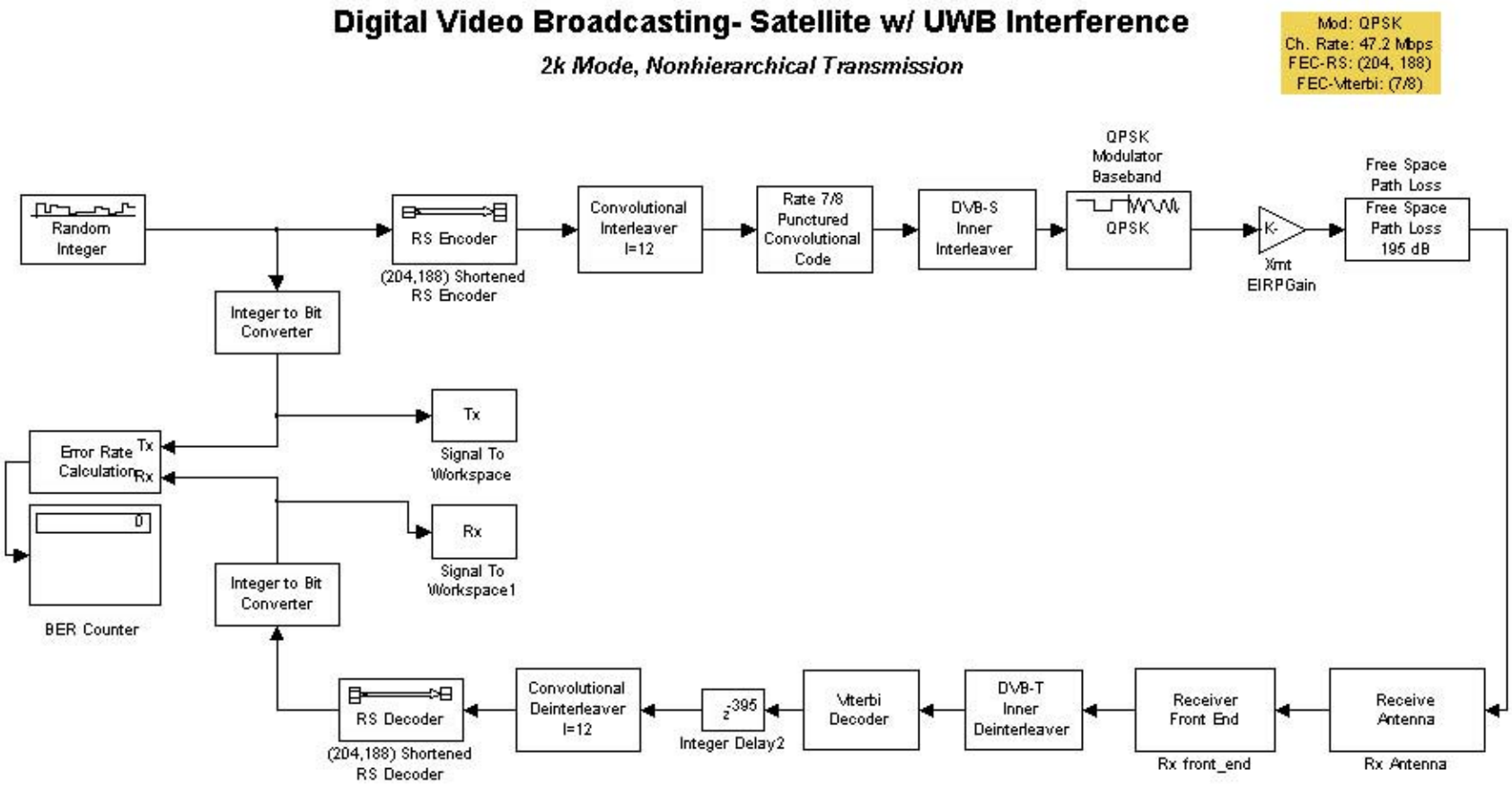

Figure 2-4. QPSK Receiver #2 Block Diagram

SECTION 3
UWB Signal Environment

3.1 General

UWB radio systems typically use extremely narrow pulse (impulse) modulation or swept frequency modulation that employs a fast sweep over a wide bandwidth. Because of the type of modulation employed, the emission bandwidths of UWB devices generally exceed one gigahertz and may be greater than ten gigahertz. In some cases, these pulses do not modulate a carrier. Instead, the radio frequency emissions generated by the pulses are applied to an antenna, the resonant frequency of which determines the center frequency of the radiated emission. The standards and operational restrictions that were applied to UWB devices are described below.

3.2 UWB Devices

UWB devices predominantly fall under imaging, radar, and communication and measurement applications. The following paragraphs describe typical characteristics of thee application.

3.2.1 Imaging Systems

GPRs and other imaging devices may operate under Part 15 of the Commission's rules subject to certain frequency and power limitations. All imaging systems are subject to coordination with NTIA through the FCC. Coordination may not take longer than 15 business days from the receipt of the coordination request by NTIA, and special temporary authorizations may be expedited when circumstances warrant. The operation of imaging systems in emergencies involving safety of life or property may take place following a notification procedure.[4] The operators of imaging devices, other than medical imaging devices, must be eligible for licensing under Part 90 of our rules. Medical imaging systems must be used at the direction of, or under the supervision of, a licensed health care practitioner. Imaging systems include:

3.2.1.1 Ground Penetrating Radar Imaging Systems

GPRs must be operated with their -10 dB bandwidth below 960 MHz or within the frequency band 3.1-10.6 GHz. GPRs operate only when in contact with, or within close proximity of, the ground for the purpose of detecting or obtaining the images of buried objects. The energy from the GPR is intentionally directed down into the ground for this purpose. Operation is restricted

[4] The notification procedure is described in 47 C.F.R. § 2.405(a)-(e).

to law enforcement, fire and rescue organizations,[5] to scientific research institutions, to commercial mining companies, and to construction companies.[6]

3.2.1.2 Wall Imaging Systems

Wall imaging systems must be operated with their -10 dB bandwidth below 960 MHz or within the frequency band 3.1-10.6 GHz. Wall-imaging systems are designed to detect the location of objects contained within a "wall." Typical uses include examining a concrete structure, the side of a bridge, or the wall of a mine. Operation is restricted to law enforcement, fire and rescue organizations, to scientific research institutions, to commercial mining companies, and to construction companies.

3.2.1.3 Through-Wall Imaging Systems

These systems must be operated with their -10 dB bandwidth below 960 MHz or within the frequency band 1.99-10.6 GHz. Through-wall imaging systems detect the location or movement of persons or objects that are located on the other side of a structure such as a wall. Operation is limited to law enforcement, fire and rescue organizations.

3.2.1.4 Surveillance Systems

These systems must be operated with their -10 dB bandwidth within the frequency band 1.99-10.6 GHz. Surveillance systems operate as "security fences" by establishing a stationary RF perimeter field and detecting the intrusion of persons or objects in that field. Operation is limited to law enforcement, fire and rescue organizations, to public utilities and to industrial entities.[7]

3.2.1.5 Medical Imaging Systems

These devices must be operated with their -10 dB bandwidth within the frequency band 3.1-10.6 GHz. A medical imaging system may be used for a variety of health applications to "see" inside the body of a person or animal. Operation must be at the direction of, or under the supervision of, a licensed health care practitioner.

3.2.2 Vehicular Radar Systems

Vehicular radars are limited to operation on terrestrial transportation vehicles. The -10 dB bandwidth must be within the 22-29 GHz band and directional antennas must be employed. The

[5] As used in the FCC MO&O, law enforcement, fire and emergency rescue organizations refers to parties eligible to obtain a license from the FCC under the eligibility requirements specified in 47 C.F. R. § 90.20(a)(1).

[6] As detailed later in this MO&O, the provisions regarding who may operate a GPR and for what purpose were further interpreted in an *Order* adopted on July 12, 2002. *See Order* in ET Docket No. 98-153, 17 FCC Rcd 13522 (2002).

[7] As used in the FCC MO&O, the reference to public utilities and industrial entities refers to the manufacturers licensees, petroleum licensees and power licensees defined in 47 C.F.R. § 90.7.

center frequency of the emission and the frequency at which the highest radiated emission occurs must be greater than 24.075 GHz. These devices detect the location and movement of objects near a vehicle, enabling features such as near collision avoidance, improved airbag activation, and suspension systems that better respond to road conditions. Attenuation of the emissions below 24 GHz is required above the horizontal plane in order to protect space borne passive sensors operating in the 23.6-24.0 GHz band.[8]

3.2.3 Communications and Measurement Systems

This category encompasses a wide variety of other UWB devices, such as high-speed home and business networking devices as well as storage tank measurement devices subject to certain frequency and power limitations. The devices must operate with their -10 dB bandwidth within the frequency band 3.1-10.6 GHz. The equipment must be designed to ensure that operation only can occur indoors, or it must be hand held in which case it may be operated anywhere. Hand held devices may be employed for such activities as peer-to-peer operation.

3.3 UWB Signal Environments

3.3.1 General

The MatLab receiver models were executed in a variety of UWB signal environments, with the number and distribution of UWB sources, as well as, variations in the pulse repetition frequency (PRF), pulse duration, and transmitter power. To minimize the time required for implementing changes in the signal sources, an external, large-scale signal environment simulation model was developed using Microsoft Visual Basic. The time/power characteristics of the UWB sources developed with this external signal environment simulation model were used to construct the equivalent UWB sources for input to the MatLab receiver models. The description of the signal environments developed for this analysis is provided below.

3.3.2 UWB Deployments

3.3.2.1 Spatial Characteristics

Three signal source deployments were developed with 1000 UWB transmitters uniformly distributed, normally distributed, and inverse normally distributed about the earth station receiver subject to the following constraints:

[8] The specific attenuation requirements are described in 47 C.F.R. § 15.515(c).

$$.03 \text{ km} < r \square 5 \text{ km}$$
$$0 < \square \square 2 \square$$
$$0 < z \square 100 \text{ m}$$

Figure 3-1 shows the uniform distribution of UWBs. This represents a baseline deployment of UWB transmitters. Figure 3-2 shows the normal distribution of UWBs. This represents an earth station deployed at the center of a dense UWB deployment configuration. Figure 3-3 shows the inverse normal distribution of UWBs. This distribution could represent an earth station with a surrounding interference protection zone. Figures 3-4, 3-5, and 3-6 show the corresponding density of emitters about the earth station averaged over 100 meter range bins.

3.3.2.2 Propagation Path Loss

A mix of $1/r^2$, $1/r^3$, $1/r^4$ fall-off was used for propagation path loss: $1/r^2$ corresponds to free-space path loss; $1/r^3$ fall-off represents propagation through foliage; $1/r^4$ represents losses through walls, obstacles, etc. Table 1 shows the percentage of UWB transmitters modeled using each propagation mode for each of five range bins.

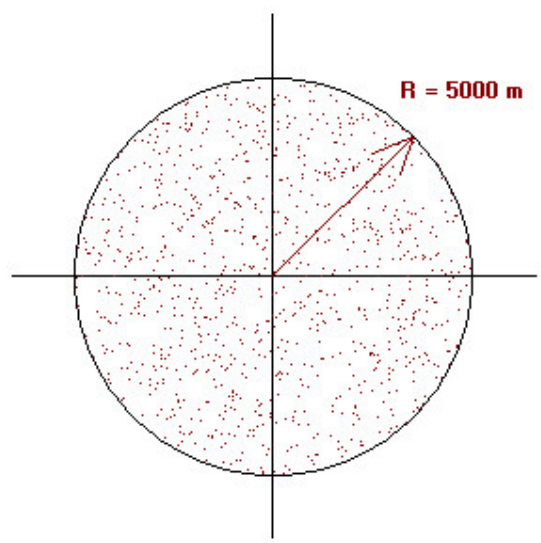

Figure 3-1. Uniform Distribution of UWB Transmitters about the Earth Station.

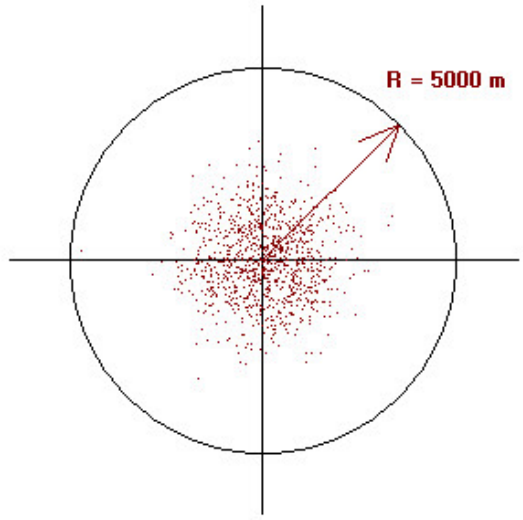

Figure 3-2. Normal Distribution of UWB Transmitters about the Earth Station.[9]

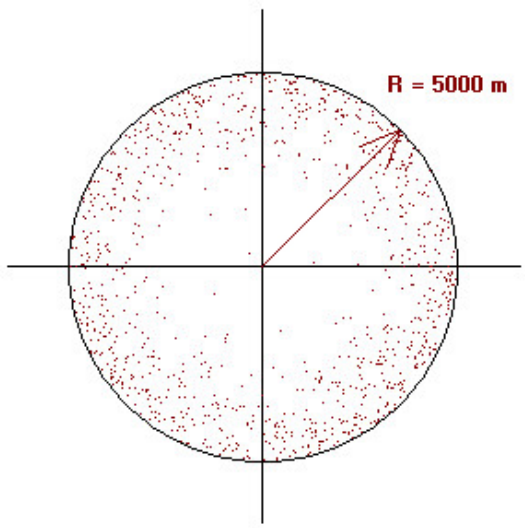

Figure 3-3. Inverse Normal Distribution of UWB Transmitters about the Earth Station.[10]

---

[9] The Normal Distribution of UWBs was generated using the transformation :

$$X = \square \ (-2 \ln(W_1))^{1/2} \ \ \mathrm{Cos}\,(2\square W_2)$$

$$Y = \square \ (-2 \ln(W_1))^{1/2} \ \ \mathrm{Sin}\,(2\square W_2),$$

where W_1 and W_2 are independent and sampled from uniform distributions. X and Y each have a Gaussian distribution with $\square$ set to 1000 meters.

[10] The Inverse Normal Distribution of UWBs was generated using the transformation :

$$X = 1000.\ (\ 7 - (-4 \ln (W_1))^{1/2} \ \ \mathrm{Cos}\,(2\square W_2)$$

$$Y = 1000.\ (\ 7 - (-4 \ln (W_1))^{1/2} \ \ \mathrm{Sin}\,(2\square W_2),$$

where W_1 and W_2 are independent and sampled from uniform distributions.

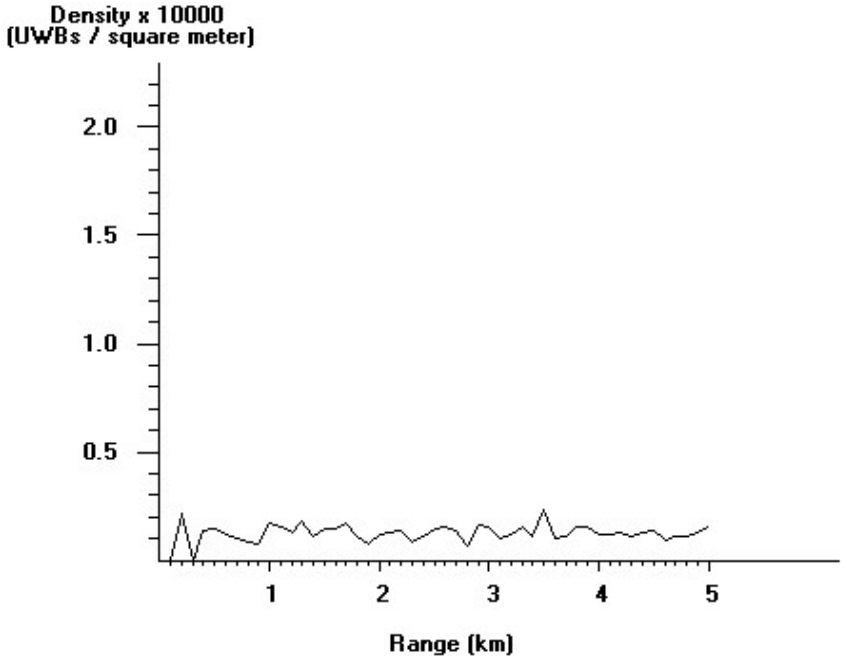

Figure 3-4. Density Averaged Over 100 Meter Range Bins for Uniform Distribution of UWB Transmitters about the Earth Station.

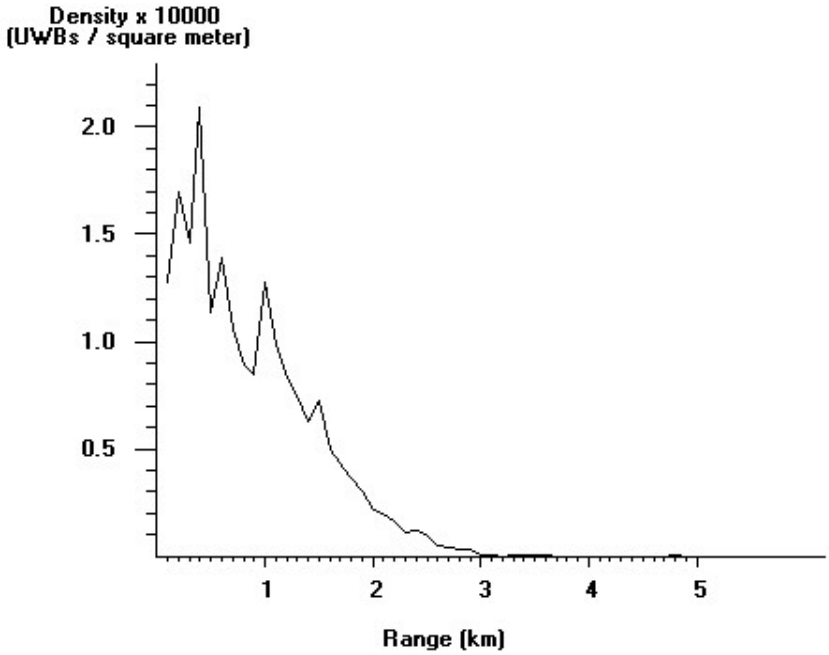

Figure 3-5. Density Averaged Over 100 Meter Range Bins for Normal Distribution of UWB Transmitters about the Earth Station.

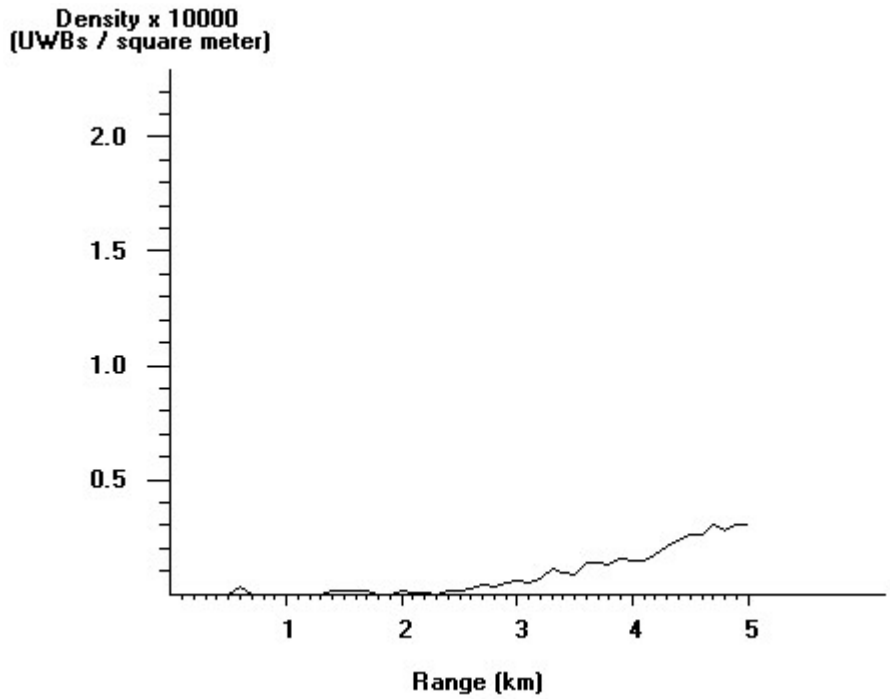

Figure 3-6. Density Averaged Over 100 Meter Range Bins for Inverse Normal Distribution of UWB Transmitters about the Earth Station.

Table 3-1
Propagation Mode as a Function of Range from the Earth Station.

Range Bin (km)	Propagation Mode		
	Percent $1/r^2$	Percent $1/r^3$	Percent $1/r^4$
0 – 1	90	5	5
1 – 2	70	15	15
2 – 3	50	25	25
3 – 4	30	35	35
4 – 5	10	45	45

3.3.2.3 Received Power Distribution

The received power at the earth station receiver was computed using the relation:

$$P_R = PSD_T + 10Log(BW_R) + G_T - L_P + G_R,$$

where,

P_R = power received, in dBm,

PSD_T = power spectral density of UWB transmitter, in dBm/MHz (- 41.3 dBm/MHz.),
BW_R = earth station receiver bandwidth, in MHz,
G_T = UWB transmitter antenna gain, in dBi,
L_P = path loss, in dB, and
G_R = earth station antenna gain, in dBi.

It was assumed that each UWB emitter radiated using a unity gain isotropic source. The antenna coupling between each UWB emitter and the earth station was computed as follows. First, a vector was constructed to represent the earth station antenna-pointing angle:

$$\mathbf{A} = a_1\,\mathbf{i} + a_2\,\mathbf{j} + a_3\,\mathbf{k},$$

where

$$a_1 = \sin(249°),$$
$$a_2 = \cos(249°),$$
$$a_3 = \tan(5°).$$

Similarly, a vector **B** was constructed from the origin to each UWB:

$$\mathbf{B} = b_1\,\mathbf{i} + b_2\,\mathbf{j} + b_3\,\mathbf{k}$$

For the uniform deployment of UWBs, the **i** and **j** components (b_1 and b_2) were selected randomly from uniform distributions subject to the constraint .03 km < r □ 5 km, where $r = (b_1^2 + b_2^2)^{1/2}$. The **k** component ($b_3$) was selected randomly from a uniform distribution subject to the constraint 0 < z □ 100 m. The cosine of the angle between the vectors **A** and **B** was computed using:

$$\text{Cos}(\square) = (a_1 b_1 + a_2 b_2 + a_3 b_3) / (|\mathbf{A}| \cdot |\mathbf{B}|),$$

The angle □ was then used in conjunction with the FCC off-axis gain constraint to assign the appropriate gain value:

$$G = 32 - 25\,\text{Log}(\square)\ \text{dBi} \qquad 1° \square \square \square 48°$$

$$G = -10\ \text{dBi} \qquad 48° < \square$$

The x, y, and z coordinates of each UWB emitter were used to compute the off-axis angle of the UWB device relative to the boresight angle of the earth station antenna. This angle was then used in conjunction with the off-axis gain constraints to estimate the antenna coupling between each UWB device and the earth station antenna.

Note that all UWB devices were precluded from off-boresight angles of less than 3°; this resulted in a maximum antenna coupling of 20 dBi. An arbitrary earth station antenna azimuth angle of 249° was selected for the analysis. An earth station antenna elevation angle of 5° was used to protect the edges of the satellite arc, and additional values of 7.5°, 10°, 12.5°, and 15° were also used for the 8PSK receiver cases.

Propagation path loss, L_P, was computed using the relation:

$$L_P = L_R + L_F - 27.56,$$

where,

L_R = path loss due to distance separation, in dB, and
L_F = path loss due to frequency, in dB

L_R was computed using the relation:

$$L_R = K \, \mathrm{Log}(r),$$

with r in meters, and K set to either 20, 30, or 40 for propagation modes of $1/r^2$, $1/r^3$, and $1/r^4$, respectively.

L_F was computed using the relation:

$$L_F = 20 \, \mathrm{Log}(f_{ES}),$$

where f_{ES} is in MHz.

Figure 3-7 shows resulting distribution in received power at the earth station from the uniformly distributed deployment of UWBs; Figure 3-8 shows the received power distribution resulting from the normally distributed deployment; Figure 3-9 shows the received power distribution resulting from the inverse normal distribution. As can be seen in Figures 3-7, 3-8, and 3-9, there are three clusters corresponding to the 3 propagation modes (i.e., $1/r^2$, $1/r^3$, $1/r^4$).

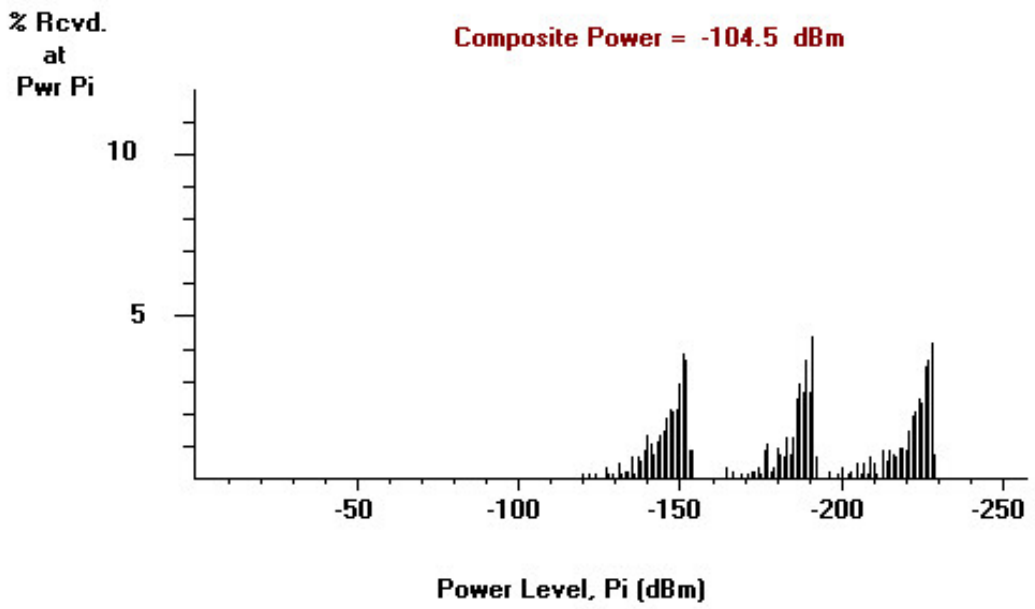

Figure 3-7. Percent of UWB Signals Received as a function of Received Power Level, Pi at the Earth Station (Uniform Distribution of UWBs).

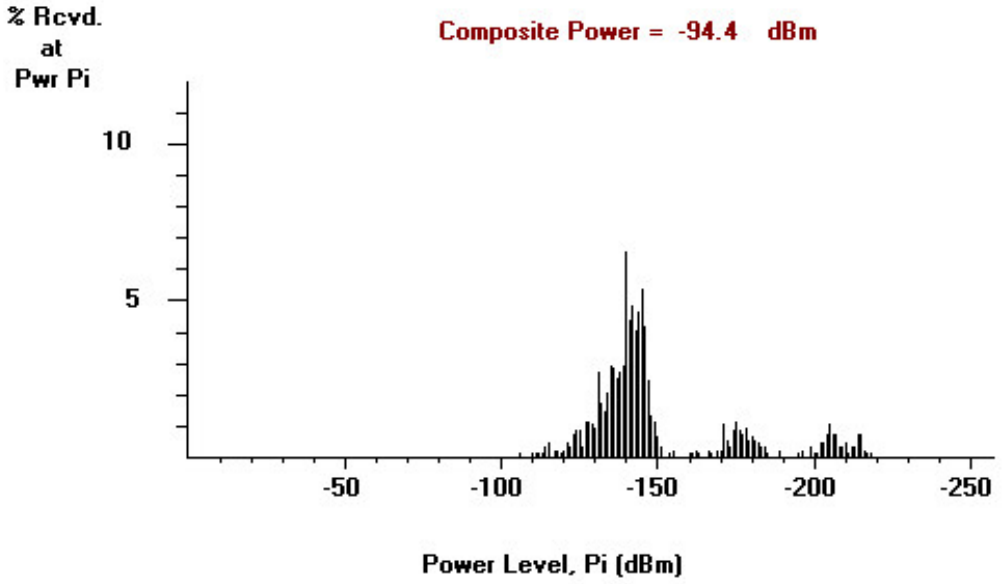

Figure 3-8. Percent of UWB Signals Received as a function of Received Power Level, Pi at the Earth Station (Normal Distribution of UWBs).

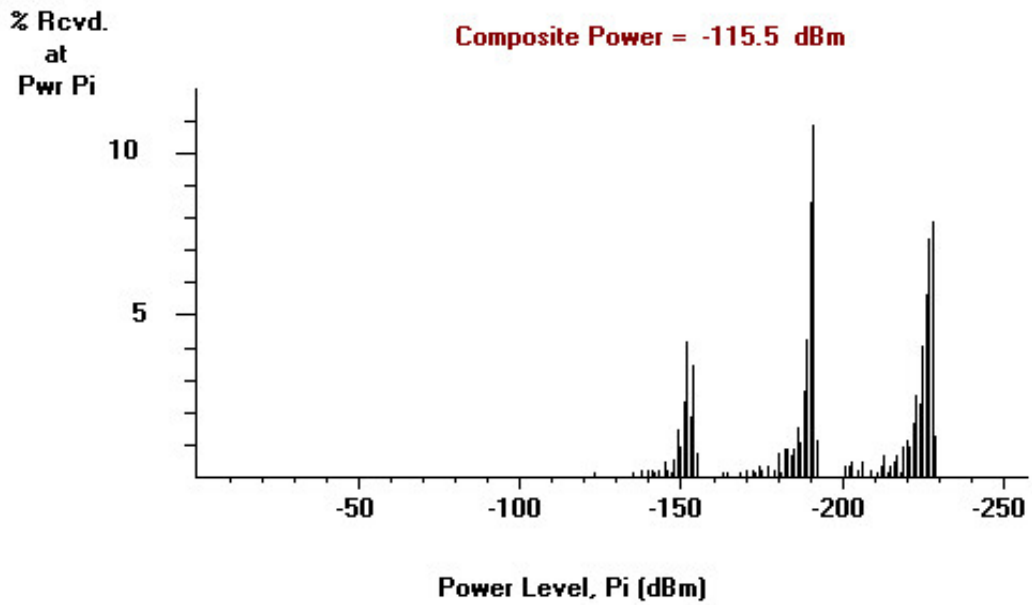

Figure 3-9. Percent of UWB Signals Received as a function of Received Power Level, Pi at the Earth Station (Inverse Normal Distribution of UWBs).

With the normal distribution, there is a smoothing between the modes, and the number of sources in the $1/r^2$ propagation mode is dominant since most UWBs are nearer to the earth station (See Table 1). Conversely, with the inverse normal distribution, most are mixed between $1/r^3$ and $1/r^4$ propagation modes. Note that the composite power is also given in Figures 3-7, 3-8, and 3-9. The composite power is the sum of all signals assuming random phase (powers add in watts) and continuous operation (i.e., duty cycle = 1.0).

3.3.2.4 UWB Time/Power Characterization

The 1000 UWB sources were modeled to transmit Gaussian Monocycle pulses of duration ranging from 0.25 - 1.0 ns, resulting in emission bandwidths in the neighborhood of 1 to 4 GHz. The Gaussian Monocycle is of the form[11]:

$$V(t) \approx (t/\square) \exp(-(t/\square)^2)$$

[11] Alan Petroff and Paul Withington, "Time Modulated Ultra-Wideband (TM-UWB) Overview, " presented at Wireless Symposium/Portable by Design, Feb. 25, 2000.

Figure 3-10 illustrates the Gaussian Monocycle. The mean PRF of each UWB source was set such that the source duty cycle equaled 0.20. For example, if the pulse-width of a given source was 0.5 ns, then the mean PRF was set to 400 MHz. To include the effects of dithering, the PRF of each source was varied pseudo-randomly by 20% about the mean.

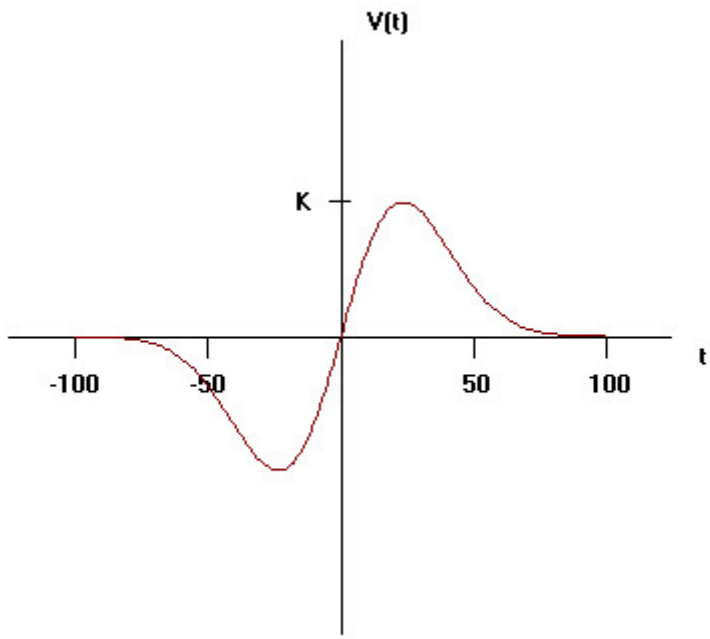

Figure 3-10. Gaussian Monocycle Pulse

Transmissions from each UWB were then scheduled for a period of 125 ns. This interval corresponds roughly to 40 complete periods of operation. The time-of-arrival, phase, and power of each signal was used to establish the composite electric field at the earth station during each 0.01 ns interval throughout the duration of the simulation.

Figure 3-11 shows the number of active UWB Sources during each 0.01 ns interval. As can be seen, a steady-state condition exists after about 20 ns with approximately 200 UWBs transmitting at any given time. This is expected since there are 1000 UWB sources and the transmit characteristics (pulse-width and PRF) were set to yield a 20% duty cycle. Figure 3-12 shows the corresponding composite power at the earth station antenna terminals throughout the 120 ns simulation for the Gaussian distribution of UWB transmitters. The numeral –101.5 just above the curve is the average power level in dBm. The corresponding average power levels for the Uniform and the Inverse Gaussian distributions were –111.5 dBm, and –122.5 dBm, respectively. Each of these values is roughly 7 dB less than the averages shown on Figures 3-7,

3-8, and 3-9. This 7 dB difference is associated with the duty cycle of the UWBs (i.e., 10 Log (0.2) ~ -7 dB). To see the time variation of the power more clearly, the composite power during a 10 ns interval is shown in Figure 3-13. Figures 3-14, 3-15, and 3-16 show the percent of time that the composite received power from the UWBs is at a given level for the normal distribution, the uniform distribution, and the inverse normal distribution of UWB transmitters, respectively. The time/power characteristics shown if Figures 3-14, 3-15, and 3-16 were then used to specify signal sources within Simulink to emulate the UWB signal environments.

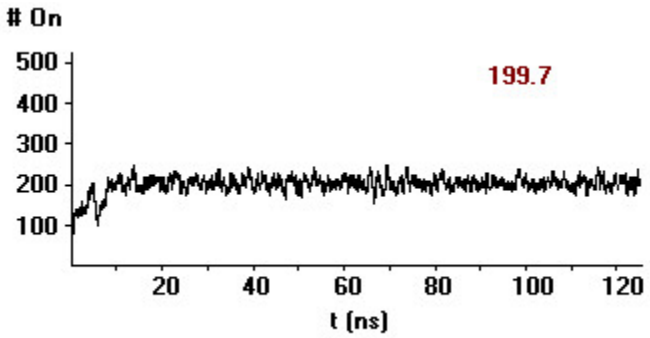

Figure 3-11. Number of Active UWB Sources during each 0.01 ns interval. (The average number on during the 125 ns simulation was 199.7.)

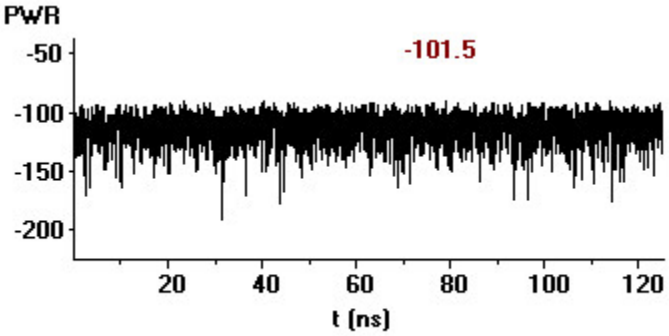

Figure 3-12. Composite Power at the Earth Station Antenna Terminals for the Gaussian Distribution of UWB transmitters. (The average value is -101.5 dBm.)

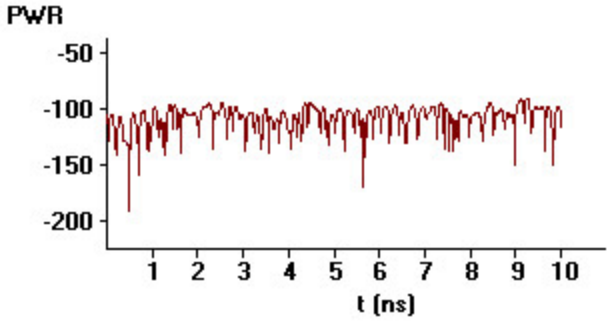

Figure 3-13. Composite Power at the Earth Station Antenna Terminals for the Gaussian Distribution of UWB Transmitters over a 10 ns interval.

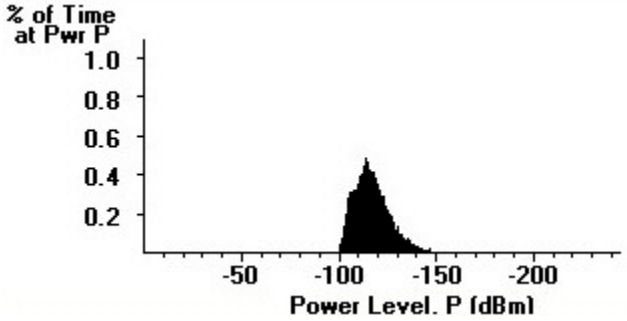

Figure 3-14. Percent of Time at Power Level, P for the Uniform Distribution of UWB Transmitters.

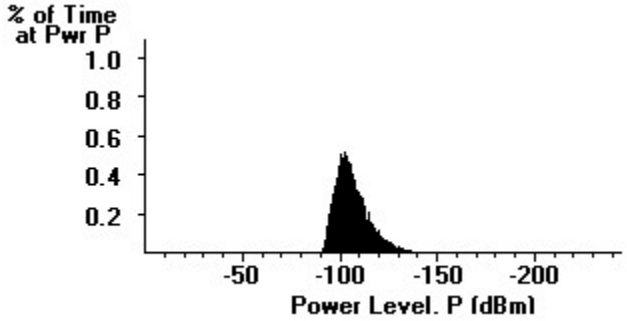

Figure 3-15. Percent of Time at Power Level, P for the Gaussian Distribution of UWB Transmitters.

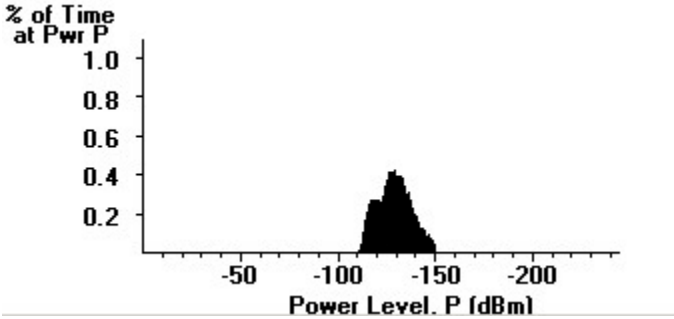

Figure 3-16. Percent of Time at Power Level, P for the Inverse Gaussian Distribution of UWB Transmitters.

SECTION 4
Modeling and Simulation Results

4.1 Introduction

Figures 4-1 through 4-45 show the performance of the five representative receivers in terms of bit-error rate (BER) versus aggregate power, BER versus D/U, and BER versus effective UWB Population, for three UWB deployment configurations: Uniform, Gaussian, Inverse Gaussian. Specifically, Figures 4-1 through 4-9 show the performance of the FM receiver; Figures 4-10 through 4-18 show the performance of the PSK receiver; Figures 4-19 through 4-27 show the performance of the QPSK Receiver #1; Figures 4-29 through 4-36 show the performance of QPSK Receiver #2; and Figures 4-37-4-45 show the performance of QPSK Receiver #3. The distinction between the 3 QPSK receivers is discussed in Section 2.

In addition, a parametric study of the effect of earth station antenna elevation angle versus BER performance was conducted for the 8-PSK receiver in a Uniform deployment. BER vs aggregate UWB Power curves for antenna elevation angles of 7.5°, 10°, 12.5°, and 15° are shown in Figures 4-46 through 4-49 respectively.

In comparing the PSK receiver results, of BER versus aggregate interference power for the 3 distributions (Figure 4-10 – Uniform, Figure 4-13 - Gaussian, and Figure 4-16 – Inverse Gaussian), it is seen that the BER departs from zero with the aggregate power shifted to –108 dBm, -94 dBm, and –95 dBm, respectively for Uniform, Gaussian, and Inverse Gaussian. This represents an increase in power level from predicted average power level by 8 dB, 6 dB, and 22 dB respectively, for Uniform, Gaussian, and Inverse Gaussian. (See page 3-11.). It should be recognized that these shifts are not uniform because the time distribution of power is different for the three different deployments – see Figure 3-13, 3-14, and 3-15.

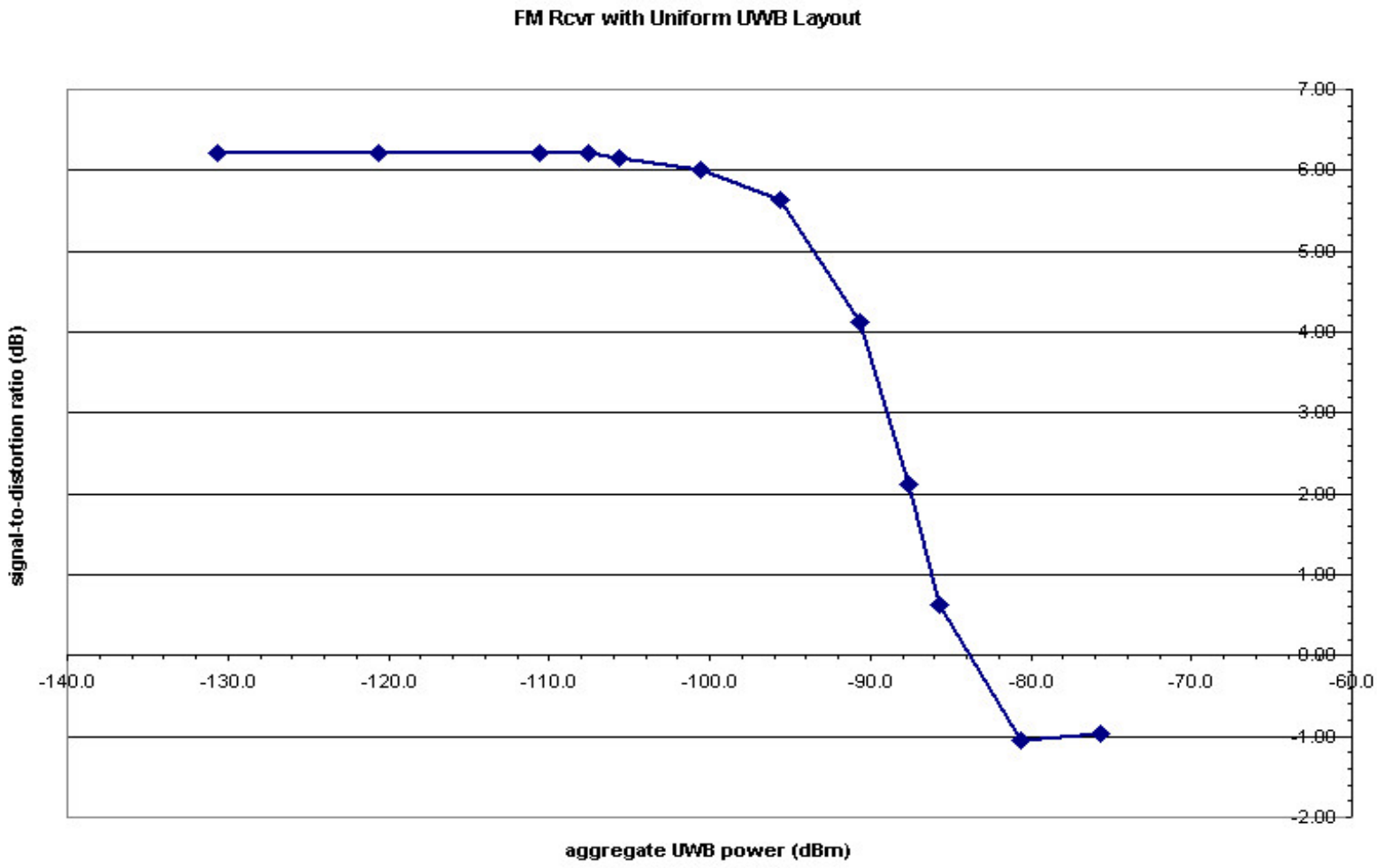

Figure 4-1 FM Receiver Performance (BER vs Aggregate Power) with 1000 UWB Sources Uniformly Dstributed about Earth Station.

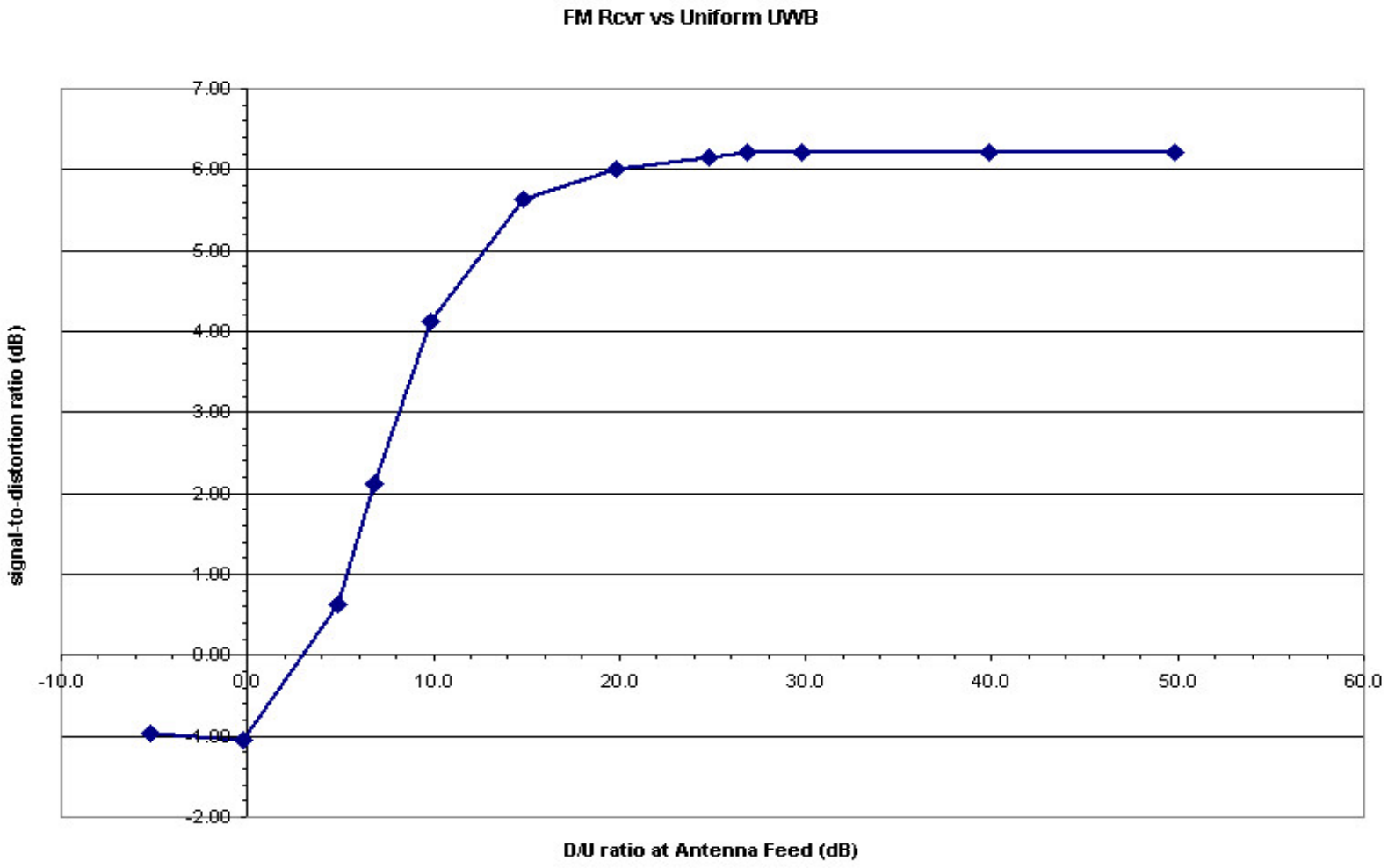

Figure 4-2 FM Receiver Performance (BER vs D/U) with 1000 UWB Sources Uniformly Distributed about Earth Station.

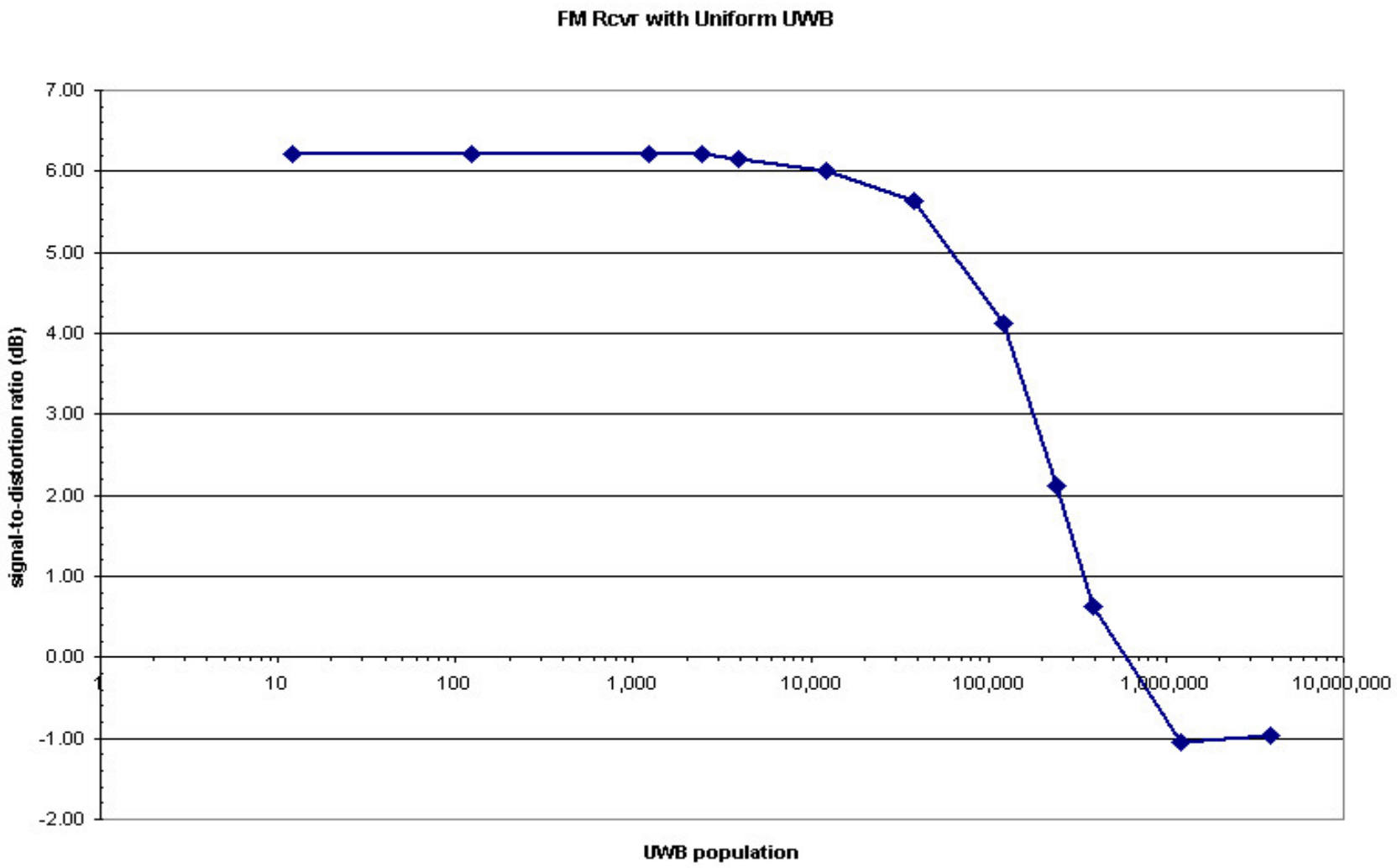

Figure 4-3 FM Receiver Performance (BER vs Effective Population) with 1000 UWB Sources Uniformly Distributed about Earth Station.

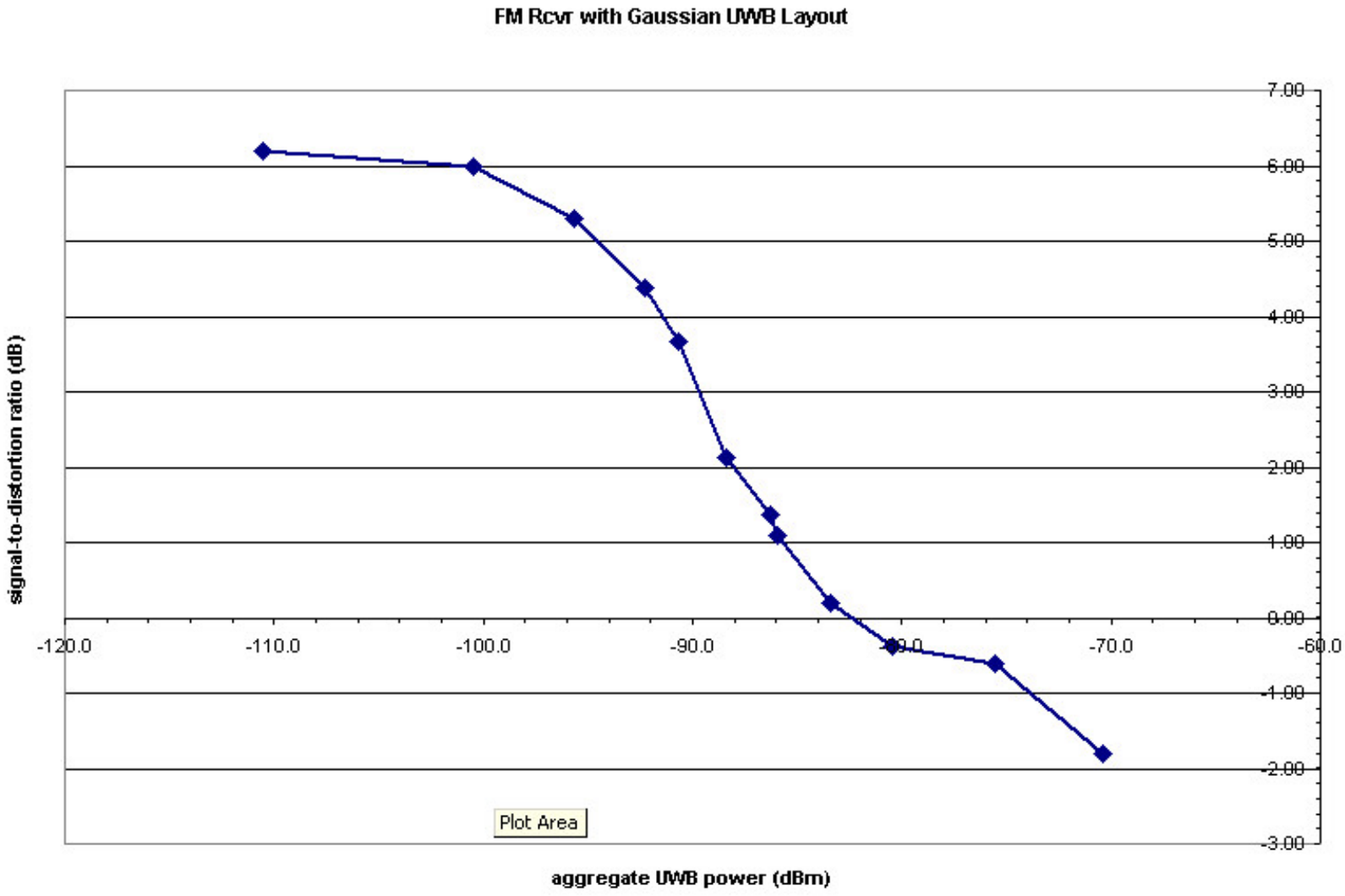

Figure 4-4 FM Receiver Performance (BER vs Aggregate Power) with 1000 UWB Sources Gaussian distributed about Earth Station.

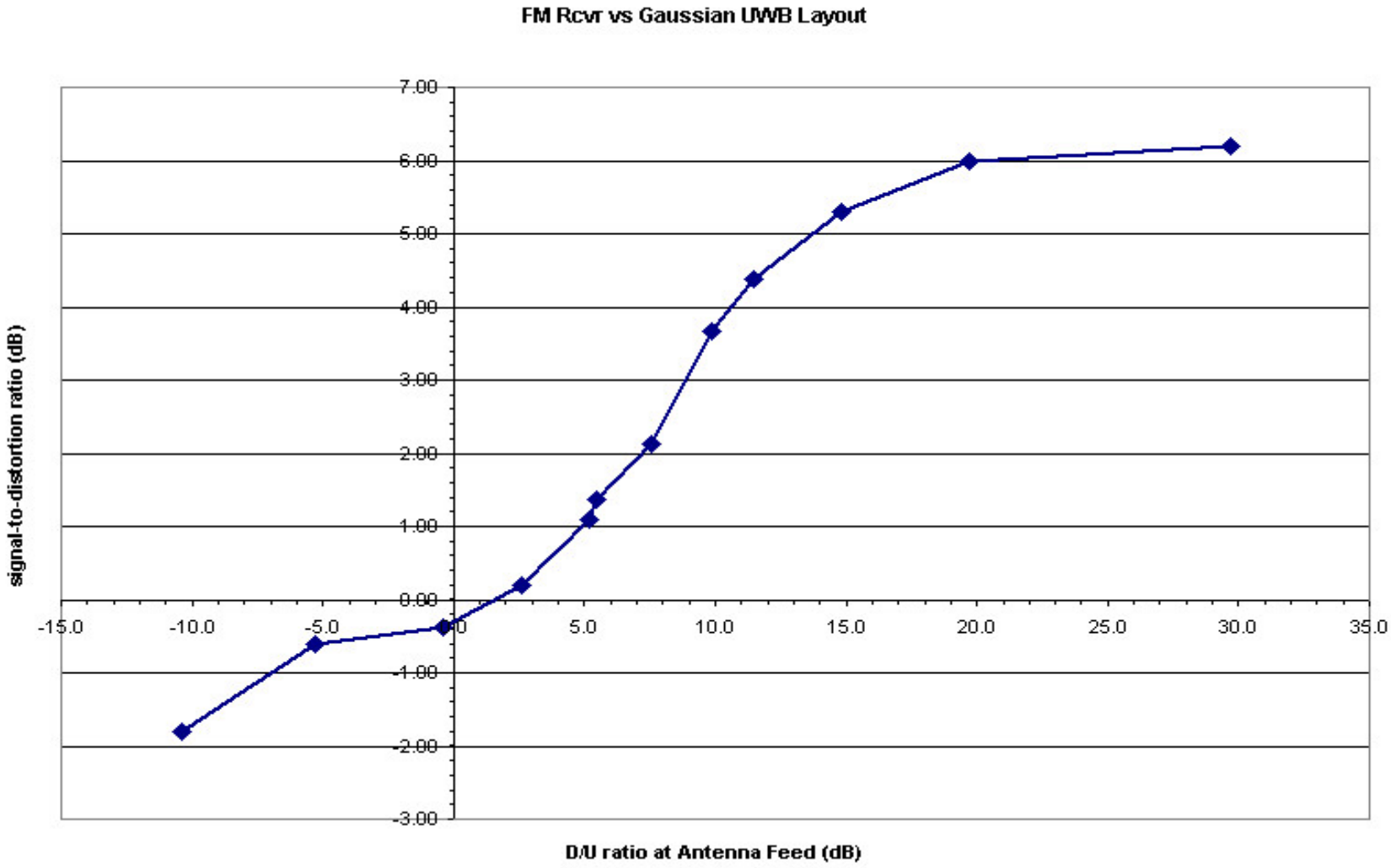

Figure 4-5 FM Receiver Performance (BER vs D/U) with 1000 UWB Sources Gaussian distributed about Earth Station.

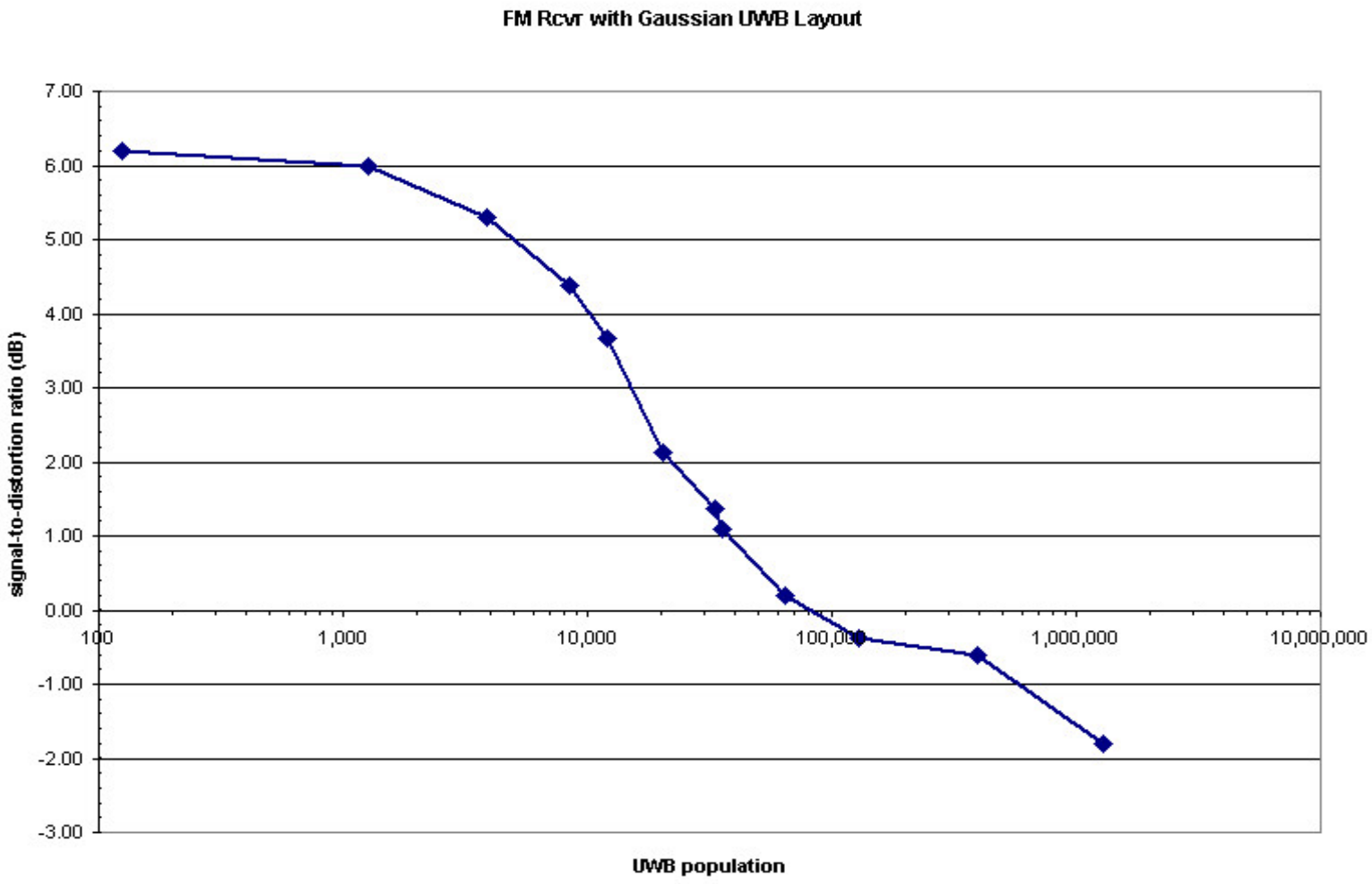

Figure 4-6 FM Receiver Performance (BER vs Effective Population) with 1000 UWB Sources Gaussian distributed about Earth Station.

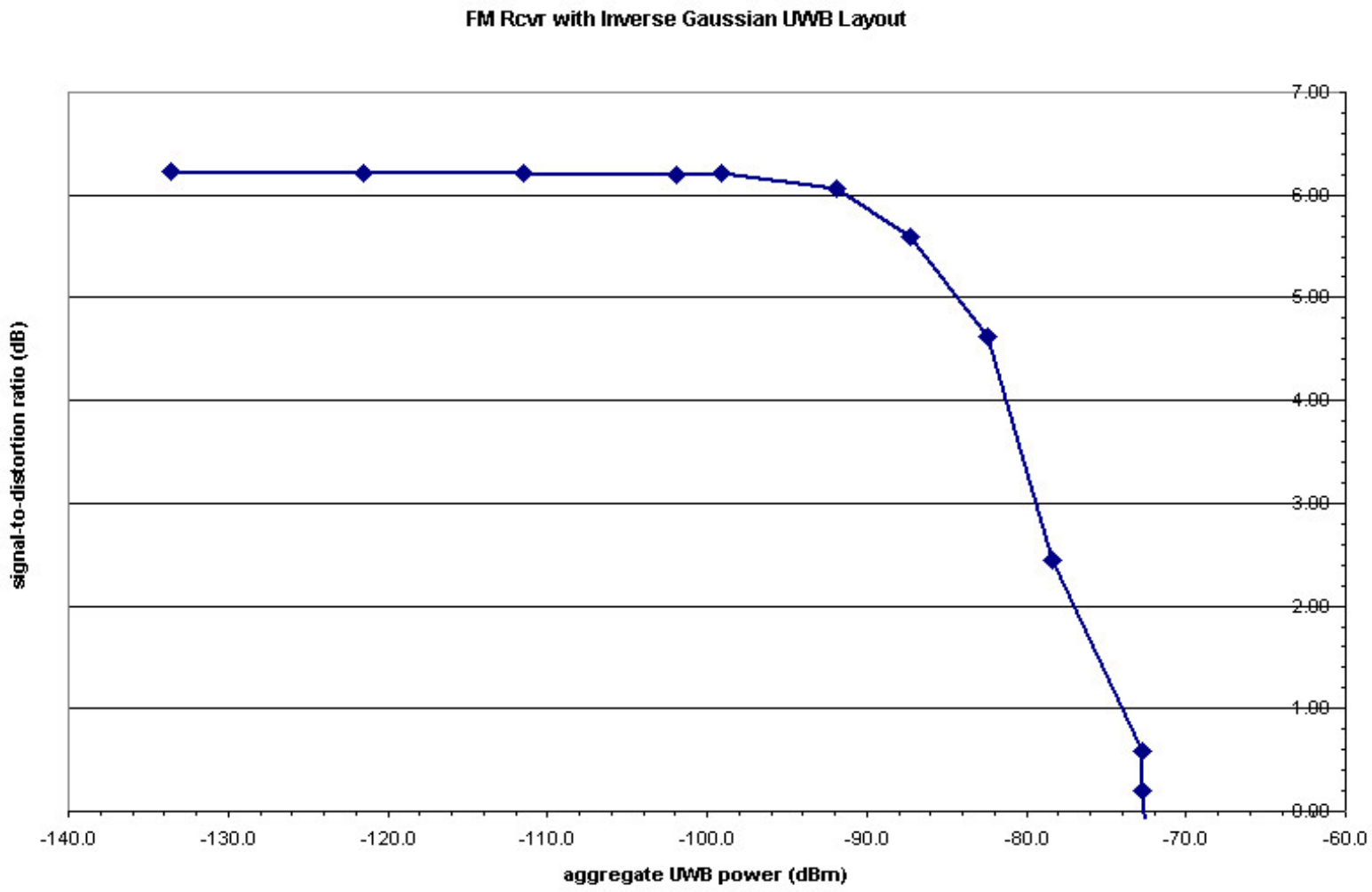

Figure 4-7 FM Receiver Performance (BER vs Aggregate Power) with 1000 UWB Sources Inverse Gaussian Distributed about Earth Station.

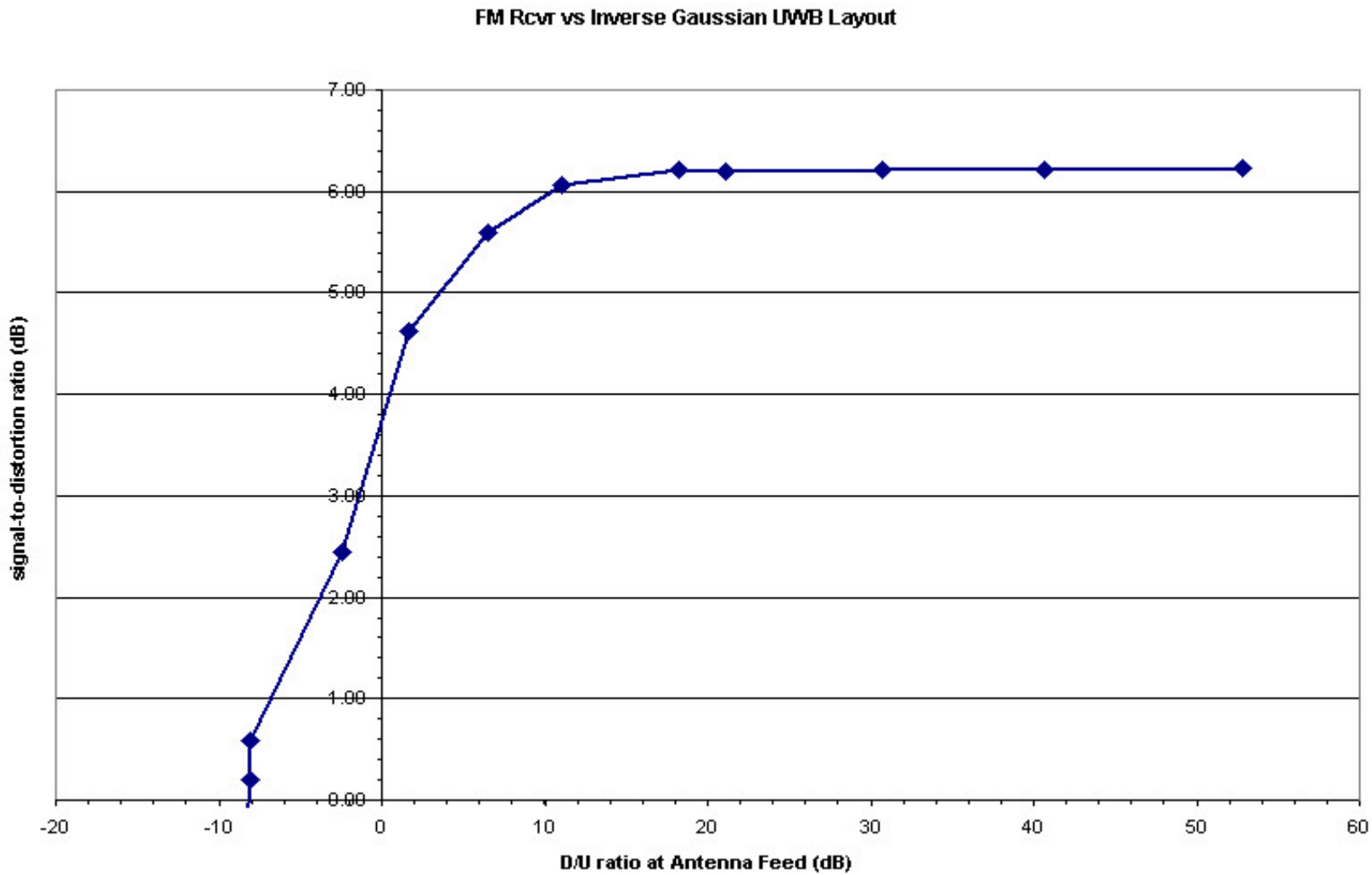

Figure 4-8 FM Receiver Performance (BER vs D/U) with 1000 UWB Sources Inverse Gaussian Distributed about Earth Station.

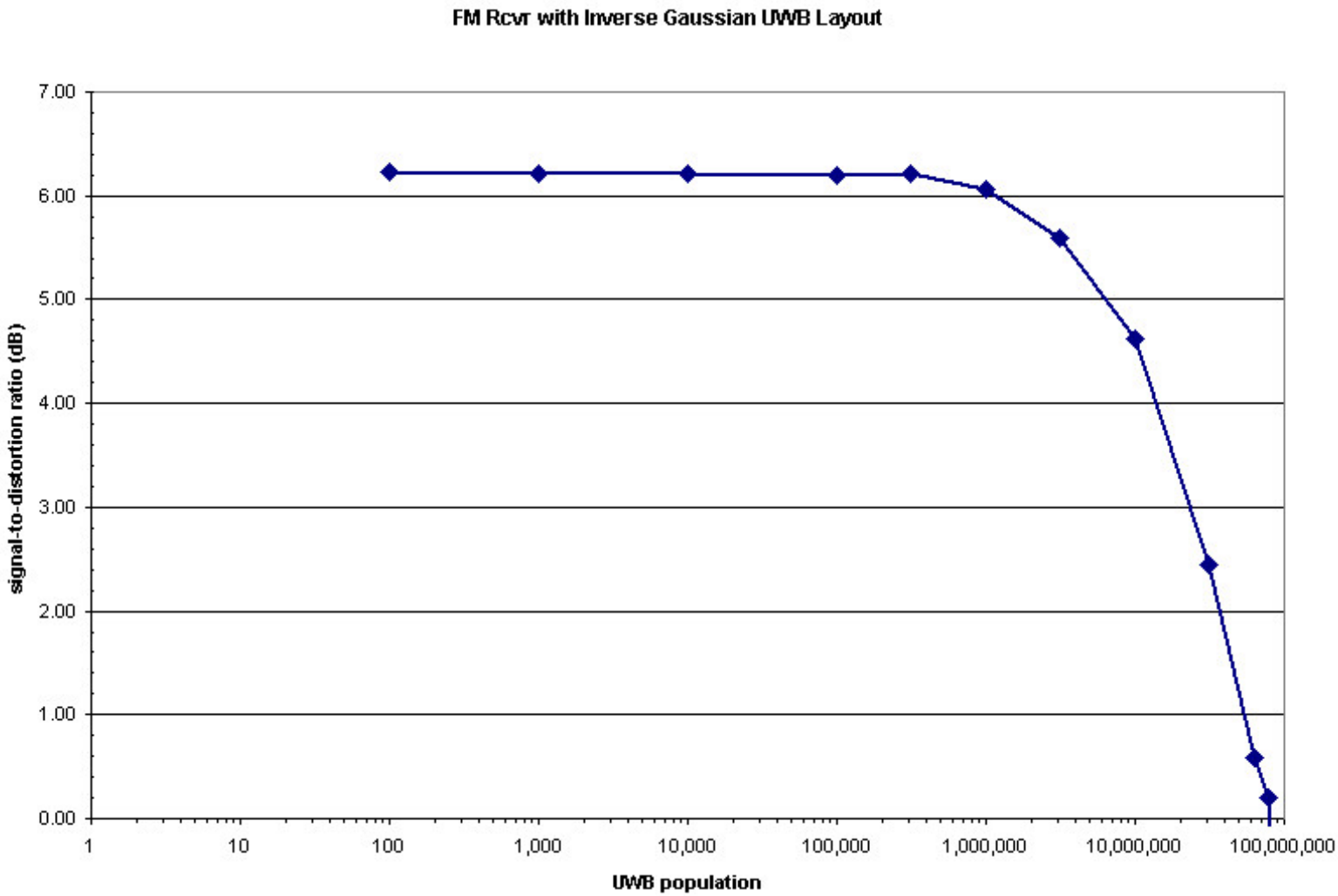

Figure 4-9 FM Receiver Performance (BER vs Effective Population) with 1000 UWB Sources Inverse Gaussian Distributed About Earth Station.

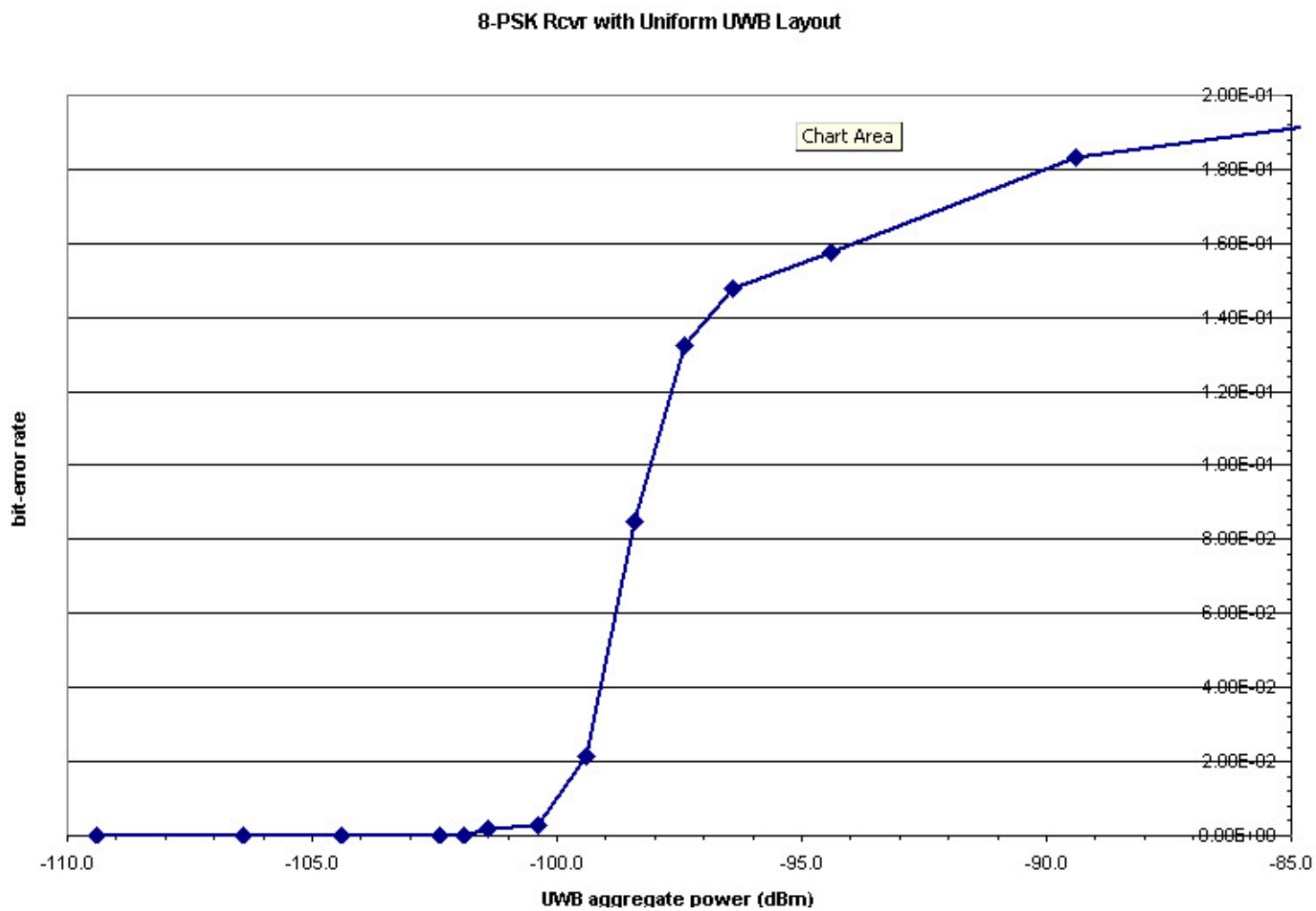

Figure 4-10 8-PSK Receiver Performance (BER vs Aggregate Power) with 1000 UWB Sources Uniformly Dstributed About Earth Station.

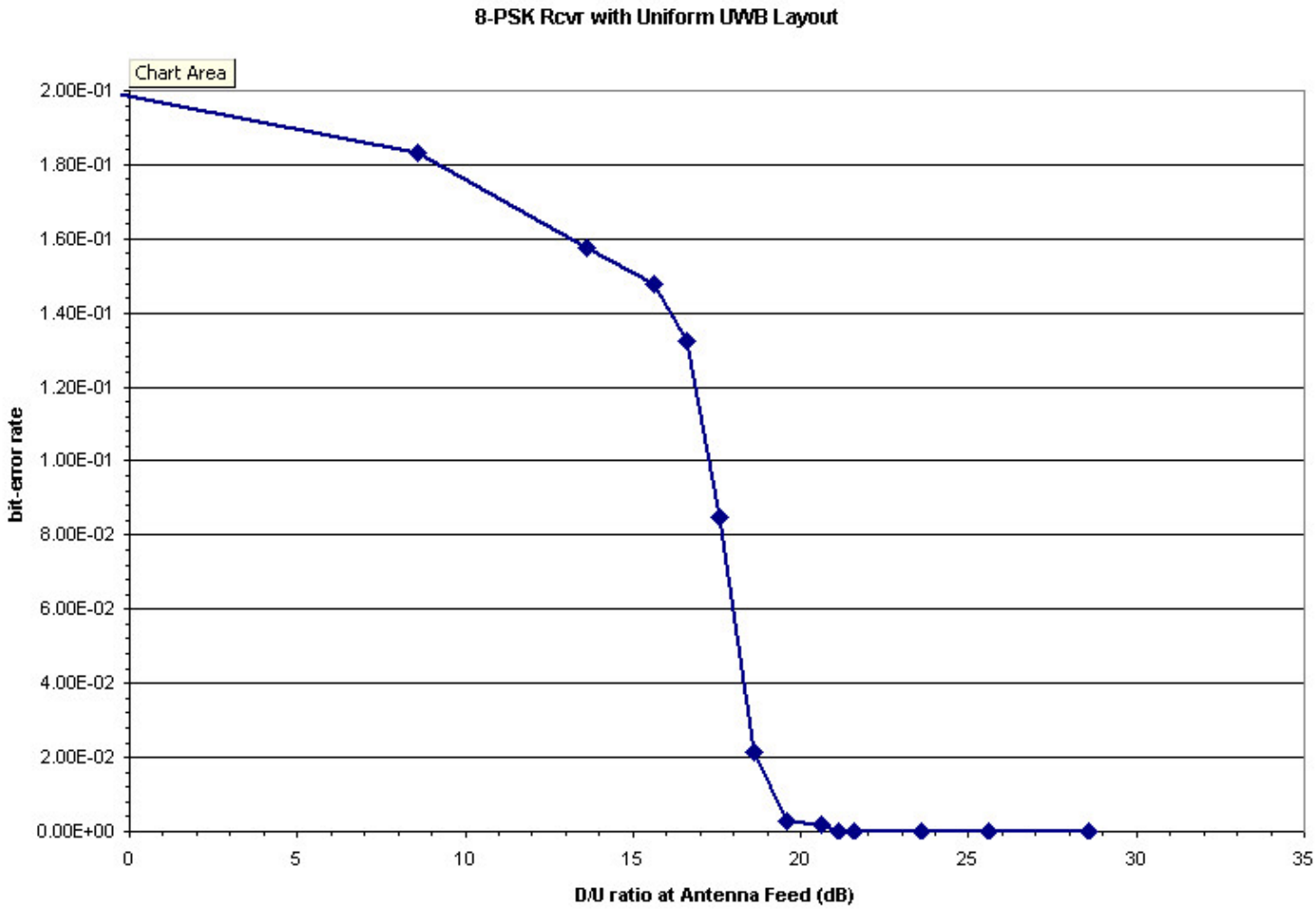

Figure 4-11 8-PSK Receiver Performance (BER vs D/U) with 1000 UWB Sources Uniformly Distributed About Earth Station.

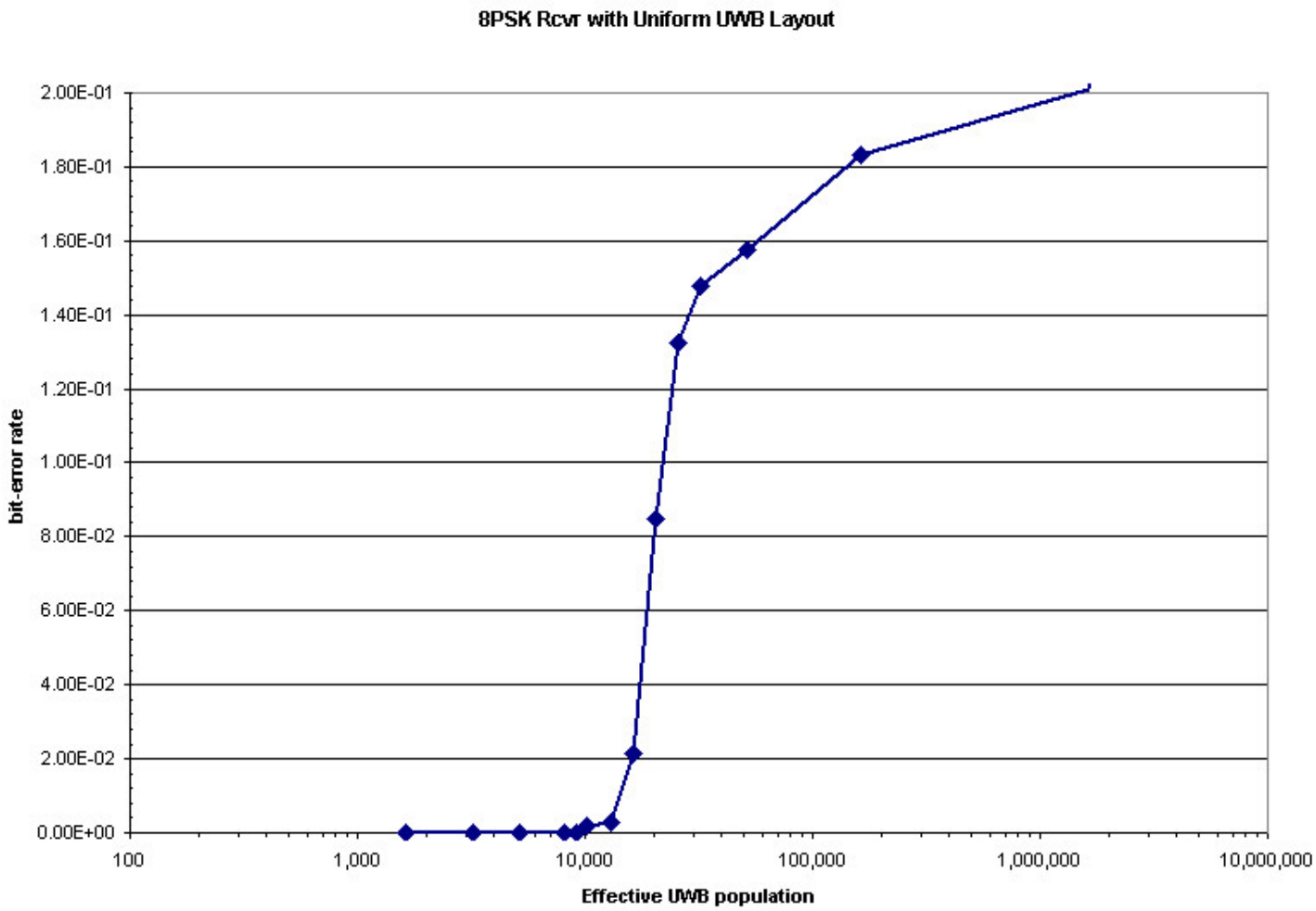

Figure 4-12 8-PSK Receiver Performance (BER vs Effective Population) with 1000 UWB Sources Uniformly Distributed About Earth Station.

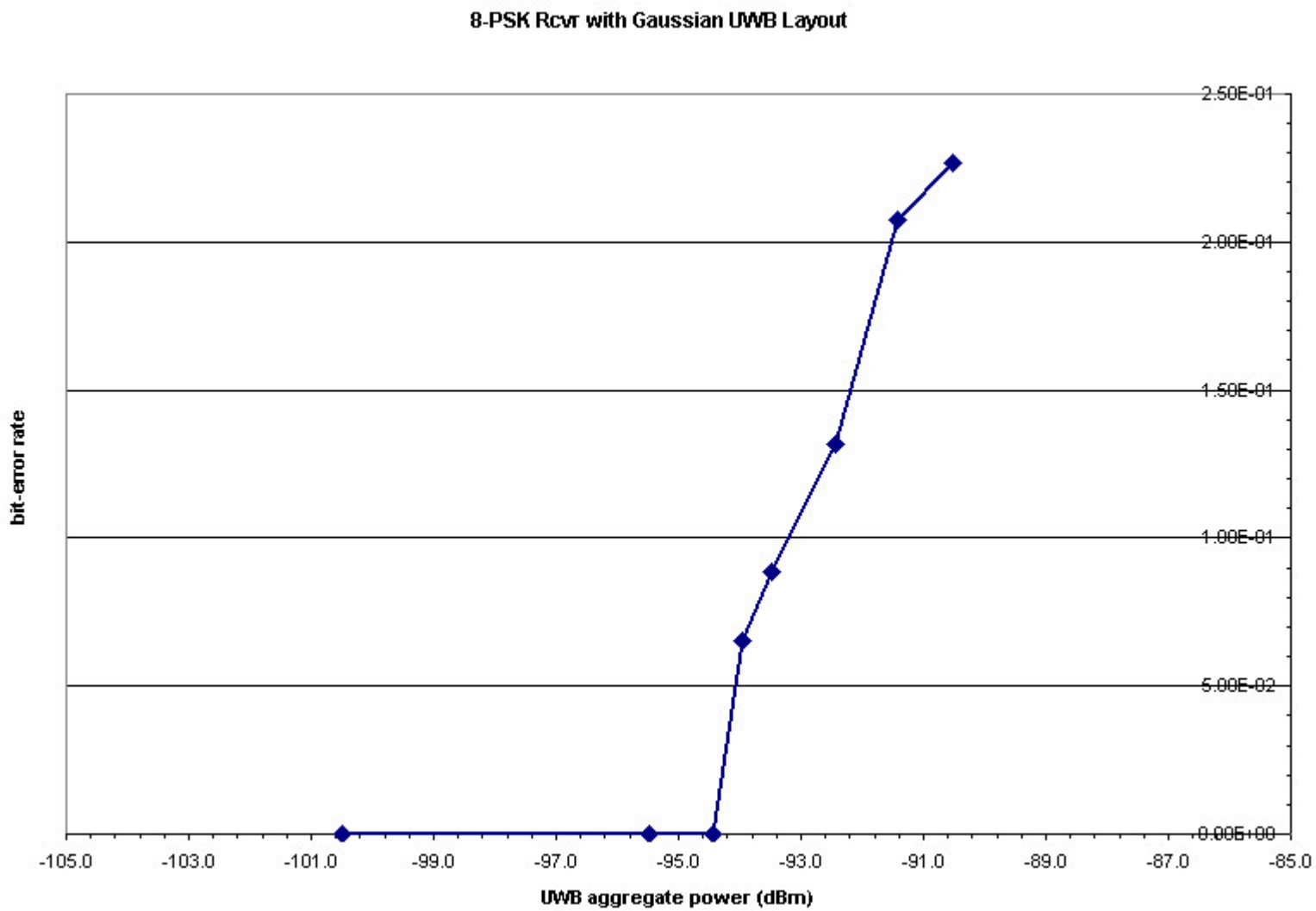

Figure 4-13 8-PSK Receiver Performance (BER vs Aggregate Power) with 1000 UWB Sources Gaussian Distributed About Earth Station.

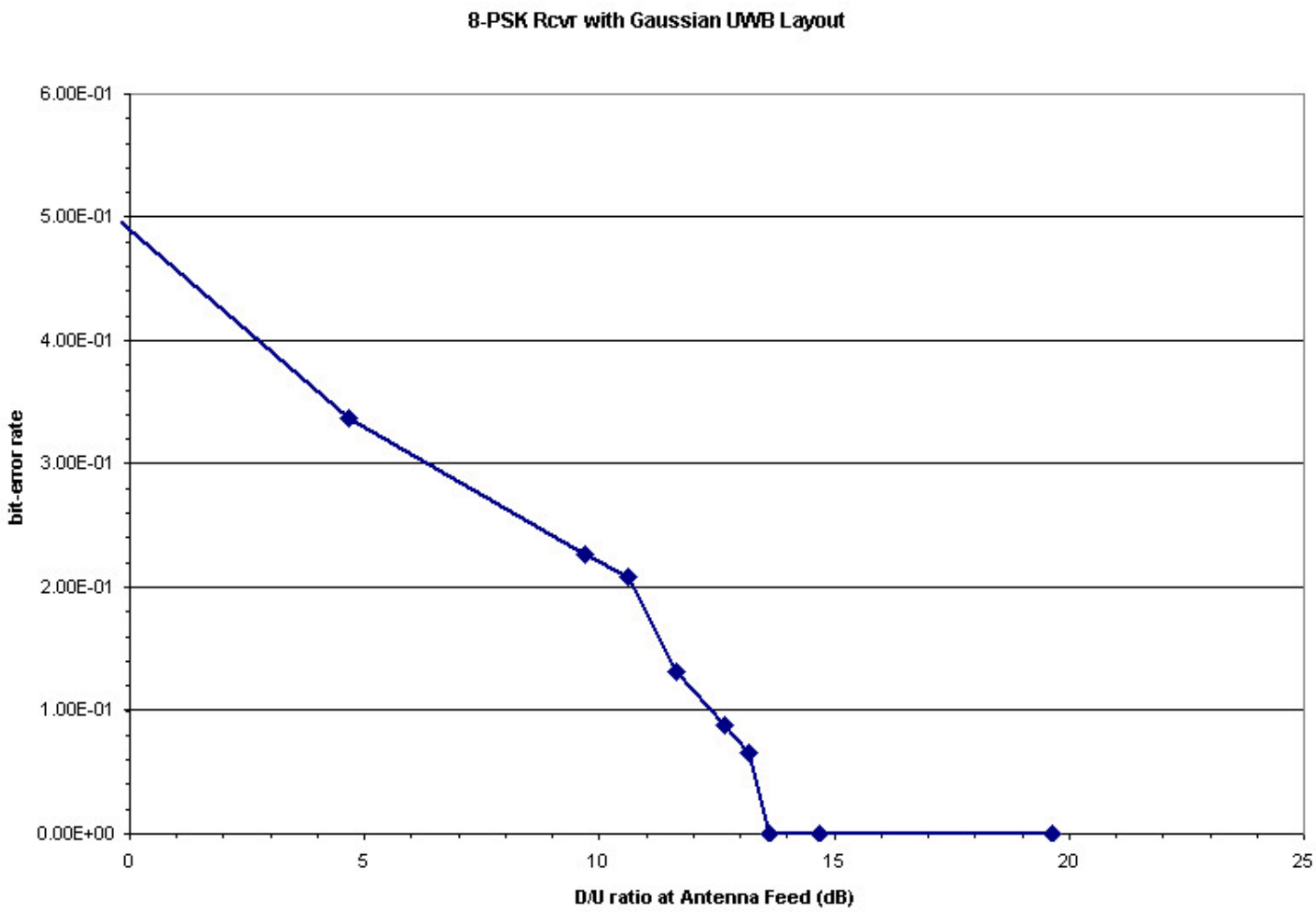

Figure 4-14 8-PSK Receiver Performance (BER vs D/U) with 1000 UWB Sources Gaussian Distributed About Earth Station.

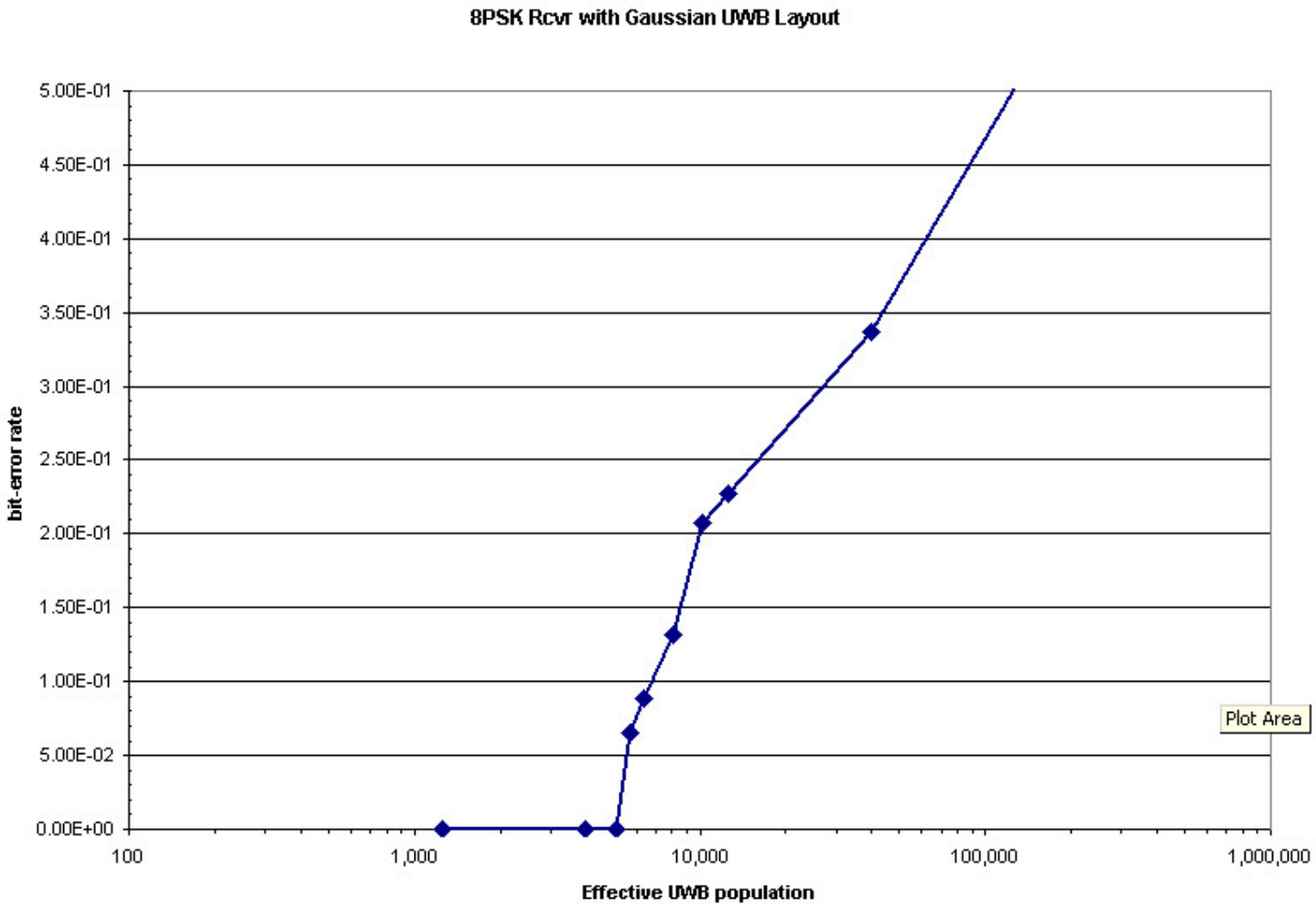

Figure 4-15 8-PSK Receiver Performance (BER vs Effective Population) with 1000 UWB Sources Gaussian Distributed About Earth Station.

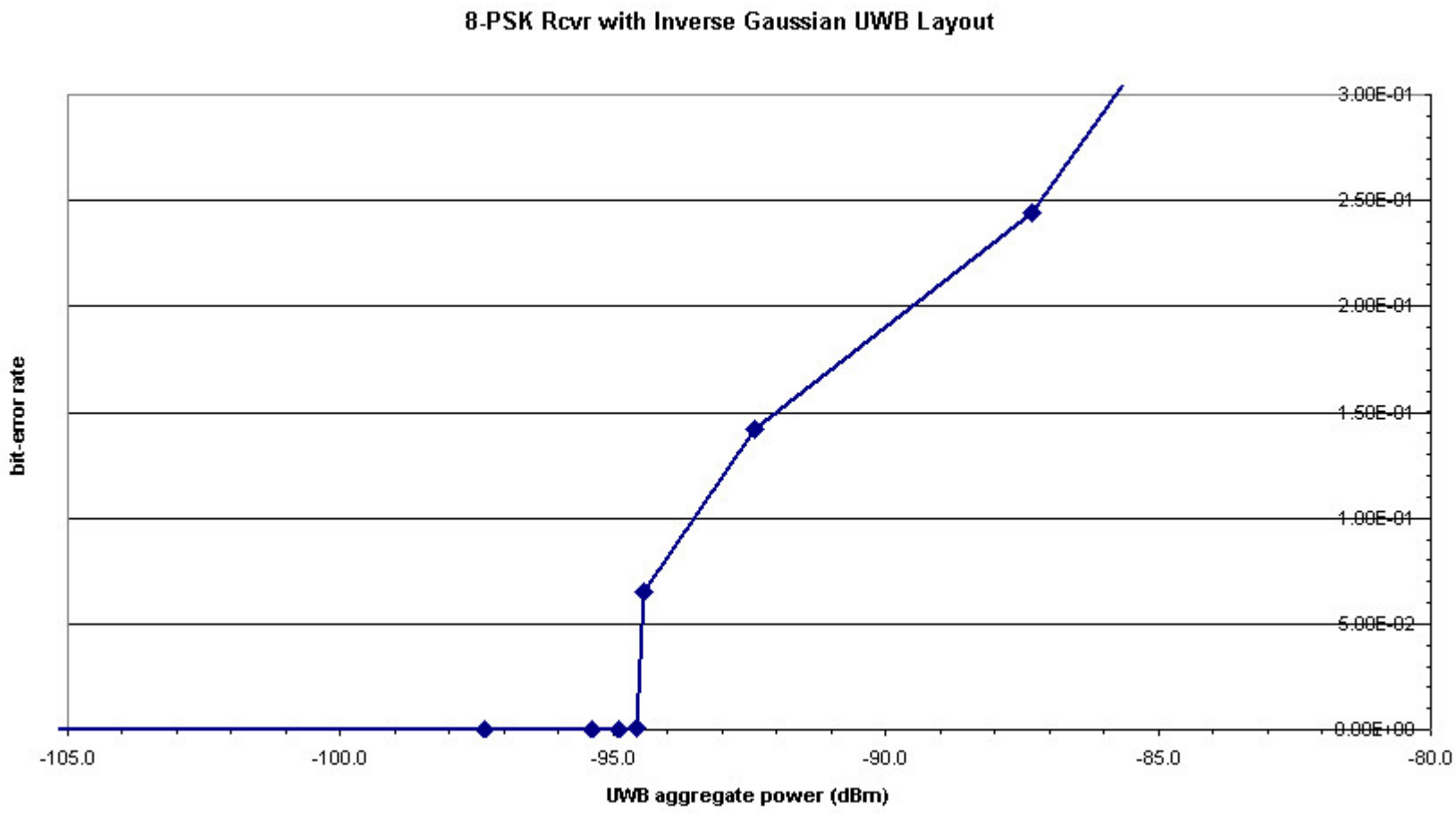

Figure 4-16 8-PSK Receiver Performance (BER vs Aggregate Power) with 1000 UWB Sources Inverse Gaussian Distributed About Earth Station.

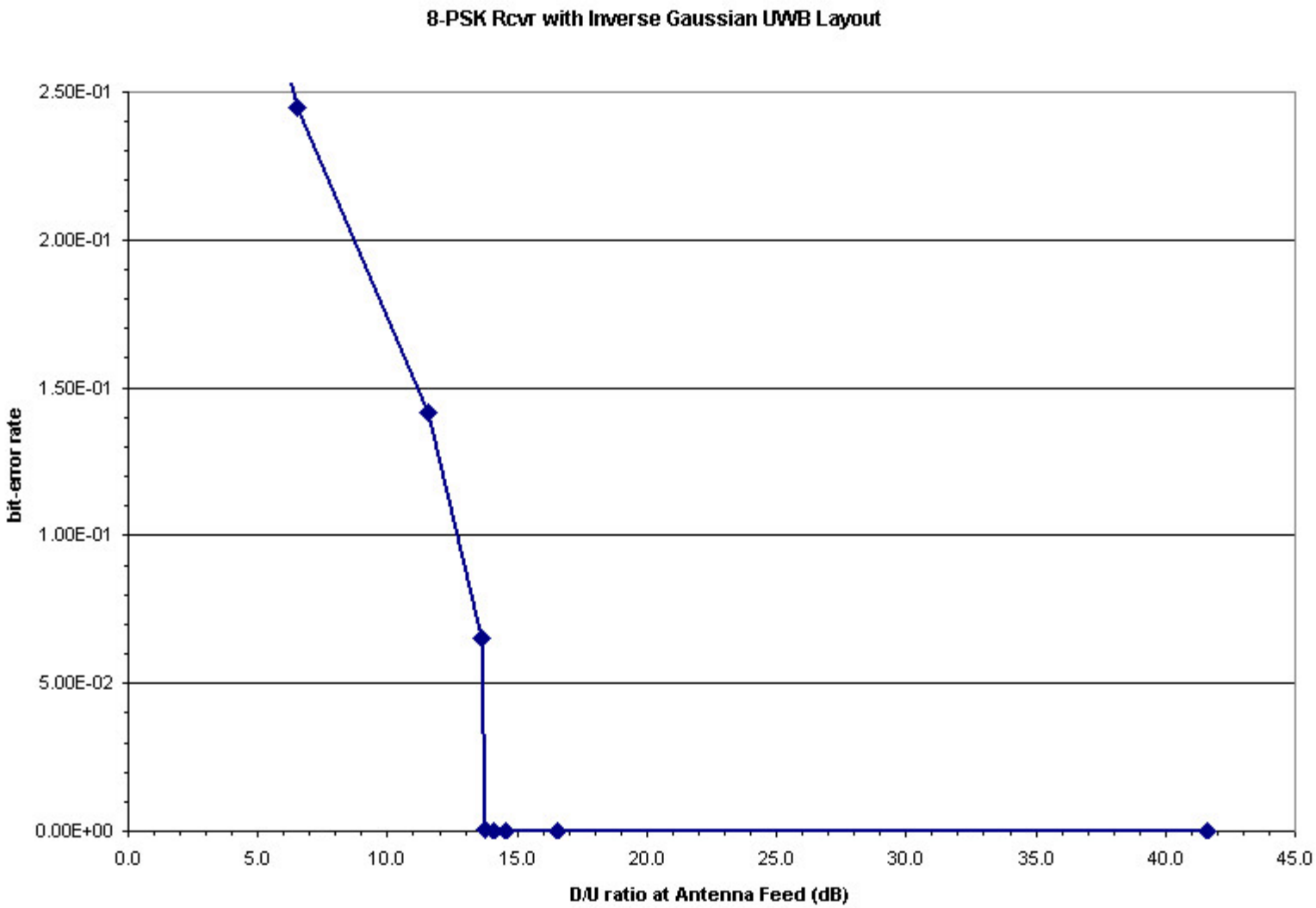

Figure 4-17 8-PSK Receiver Performance (BER vs D/U) with 1000 UWB Sources Inverse Gaussian Distributed About Earth Station.

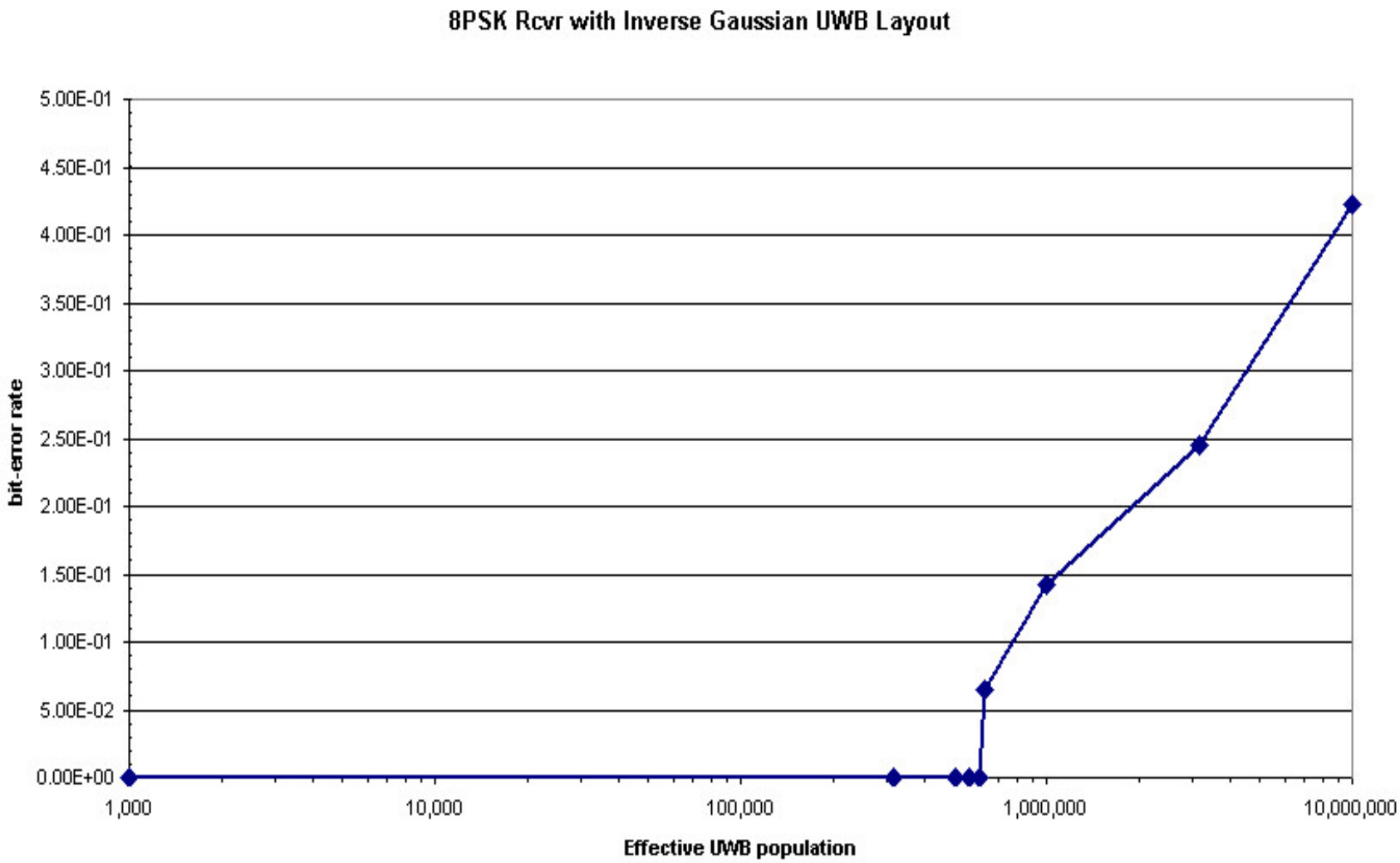

Figure 4-18 8-PSK Receiver Performance (BER vs Effective Population) with 1000 UWB Sources Inverse Gaussian Distributed About Earth Station.

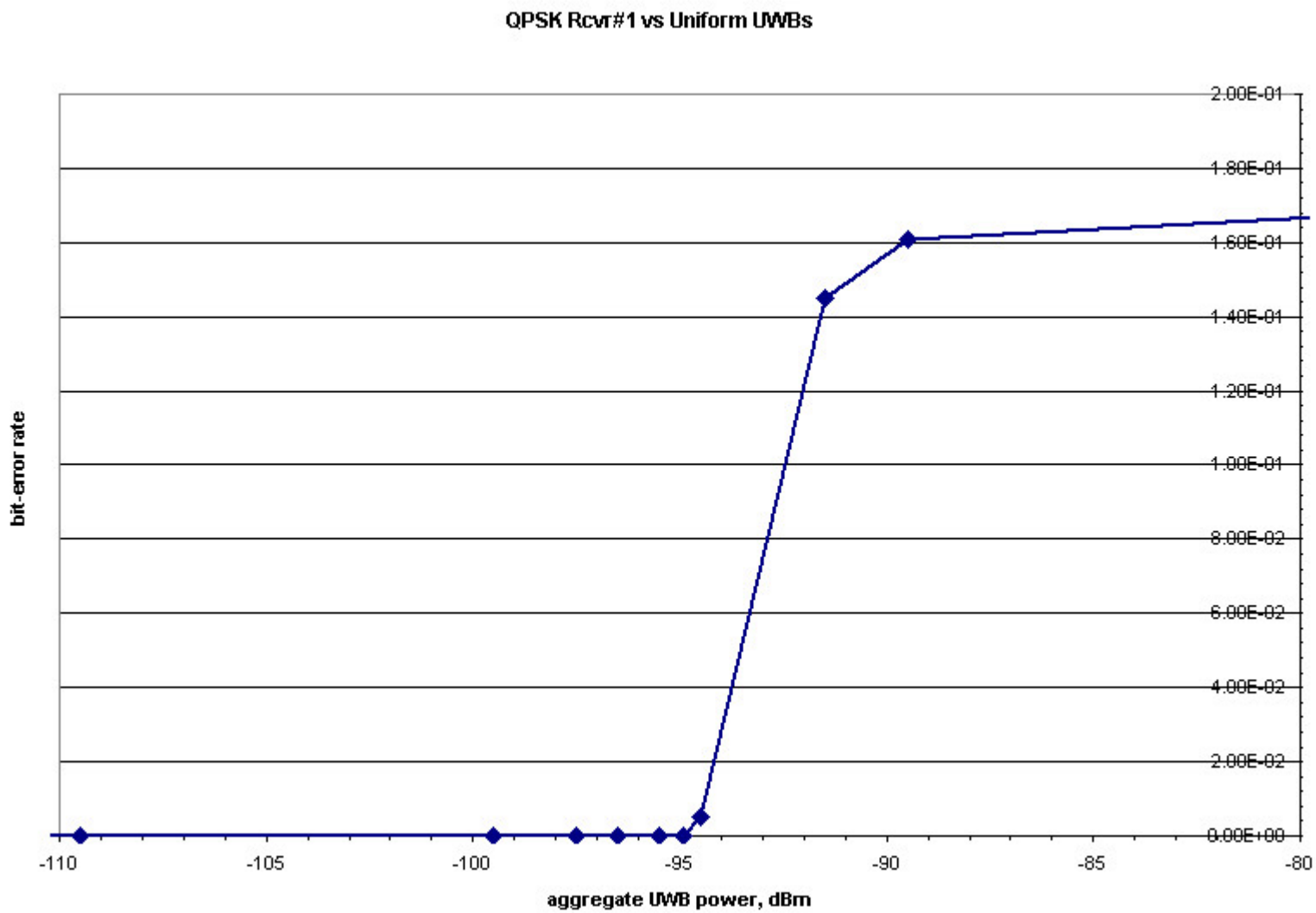

Figure 4-19 QPSK Receiver #1 Performance (BER vs Aggregate Power) with 1000 UWB Sources Uniformly Distributed About Earth Station.

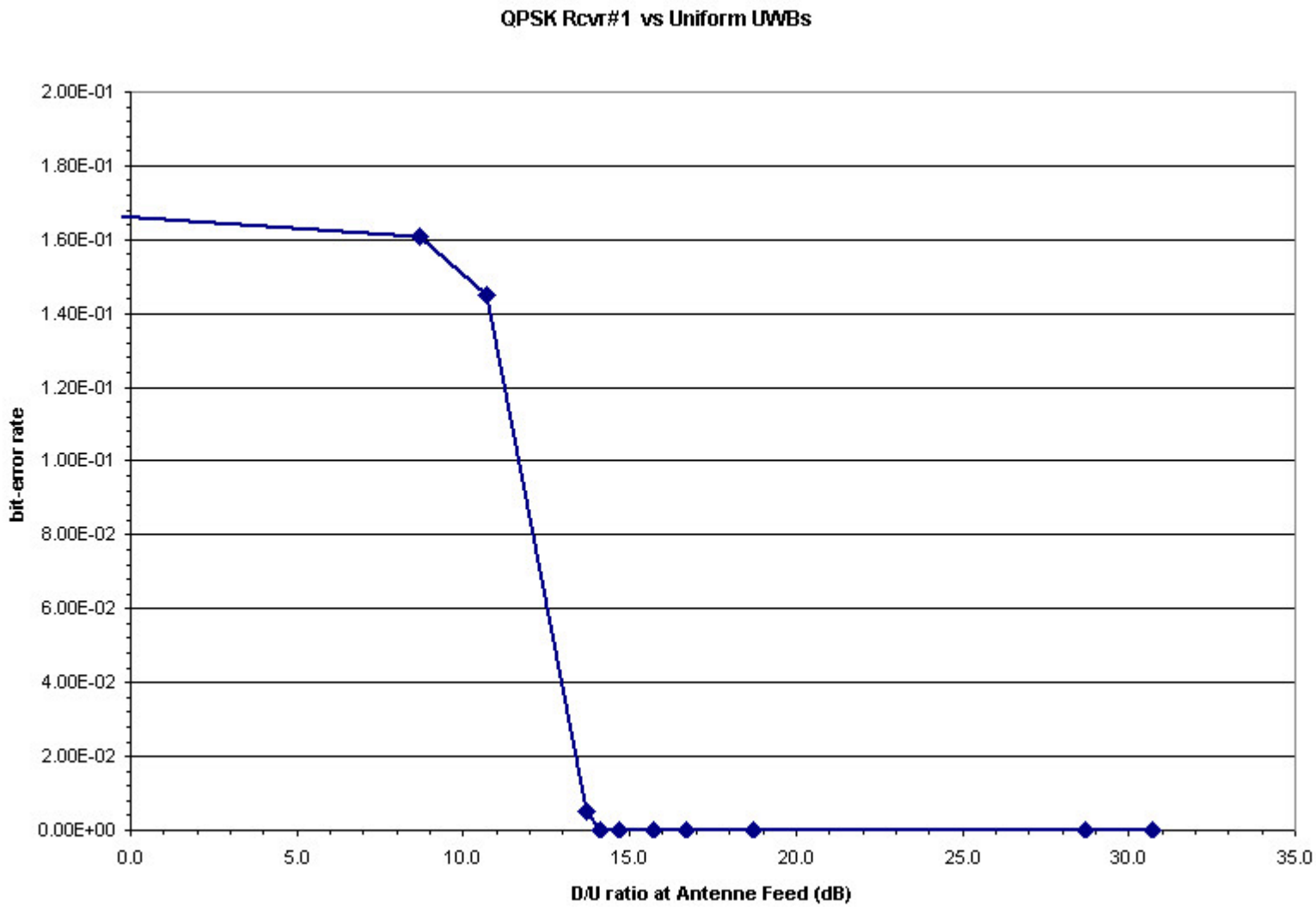

Figure 4-20 QPSK Receiver #1 Performance (BER vs D/U) with 1000 UWB Sources Uniformly Distributed About Earth Station.

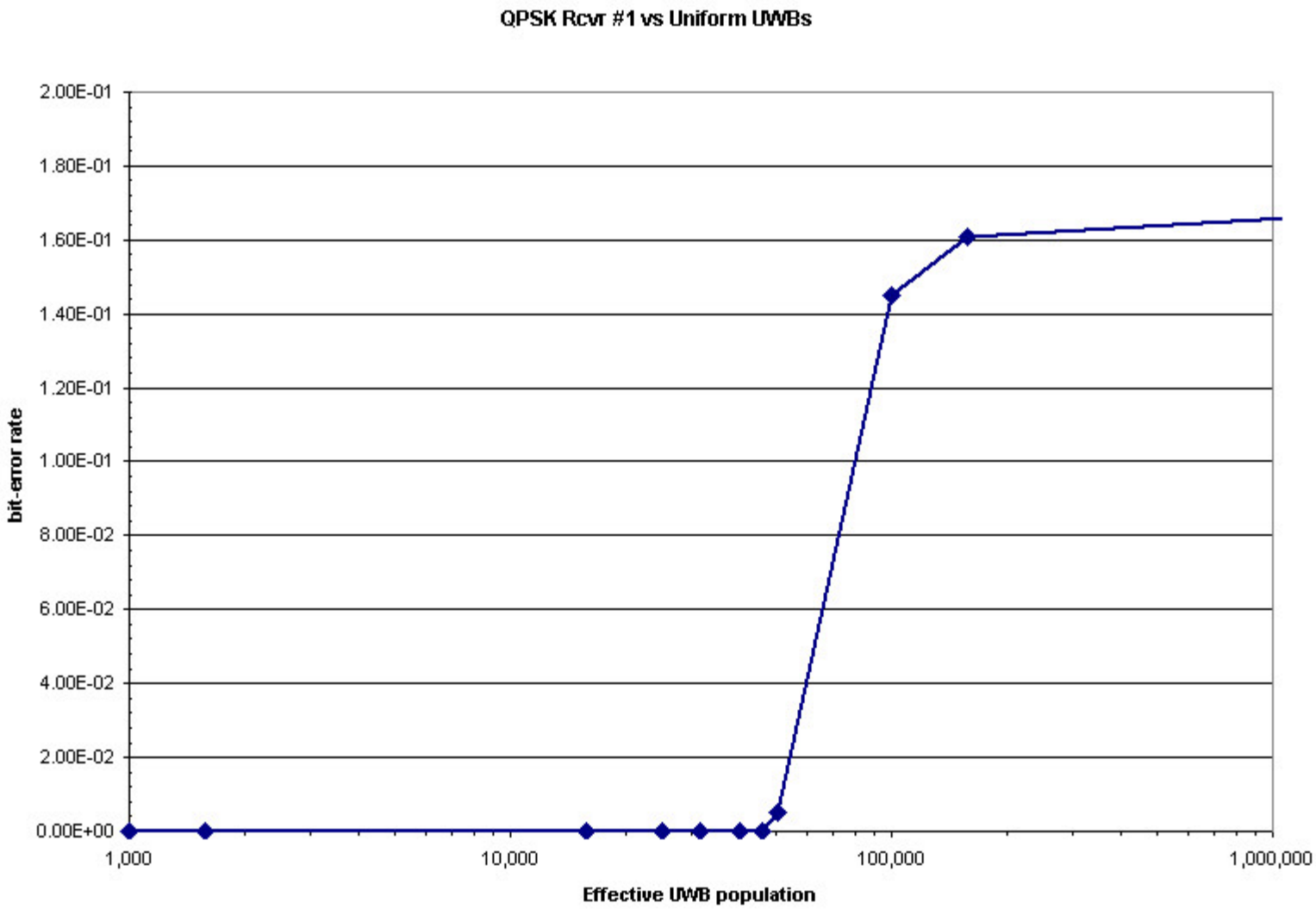

Figure 4-21 QPSK Receiver #1 Performance (BER vs Effective Population) with 1000 UWB Sources Uniformly Dstributed About Earth Station.

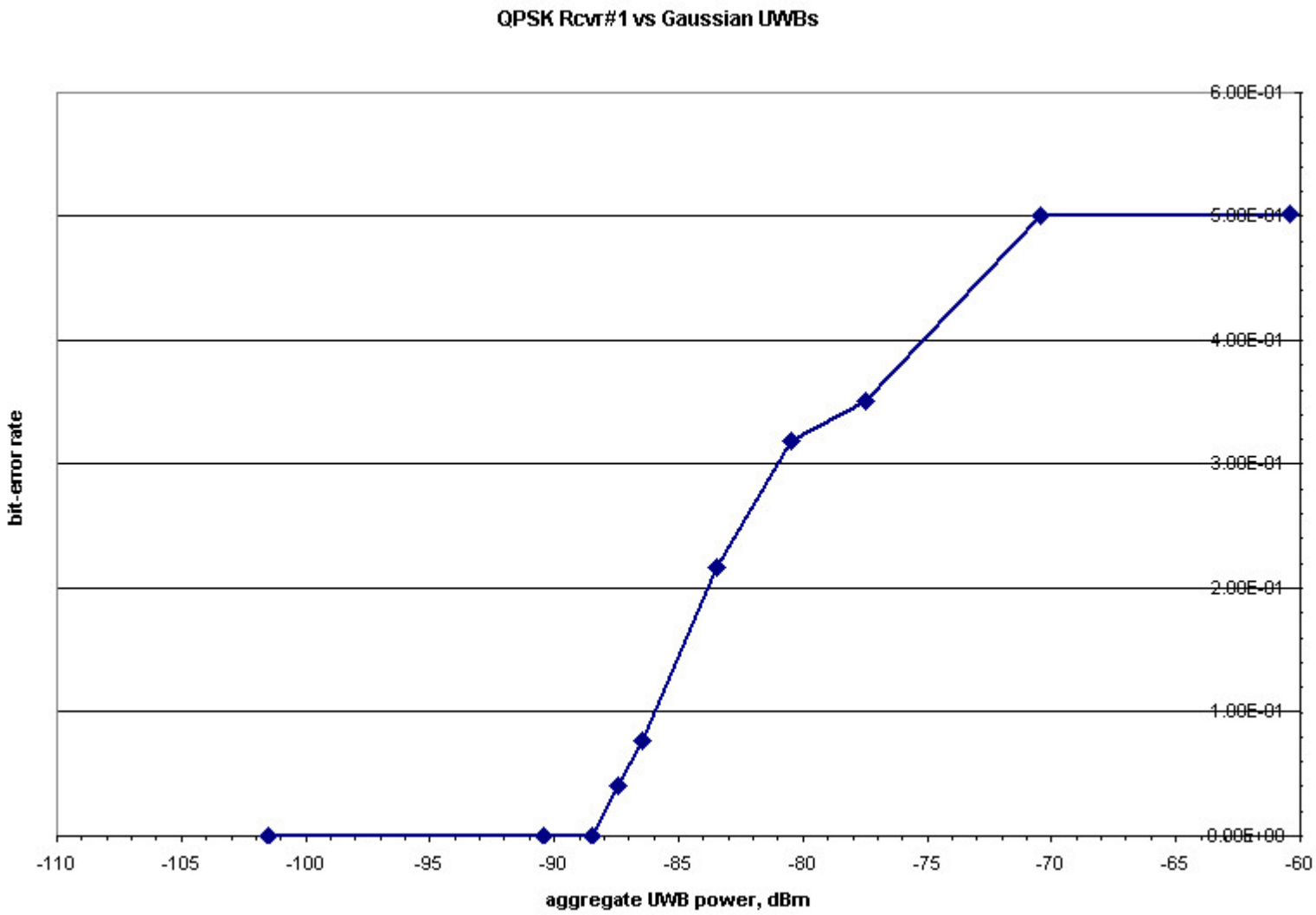

Figure 4-22 QPSK Receiver #1 Performance (BER vs Aggregate Power) with 1000 UWB Sources Gaussian Distributed About Earth Station.

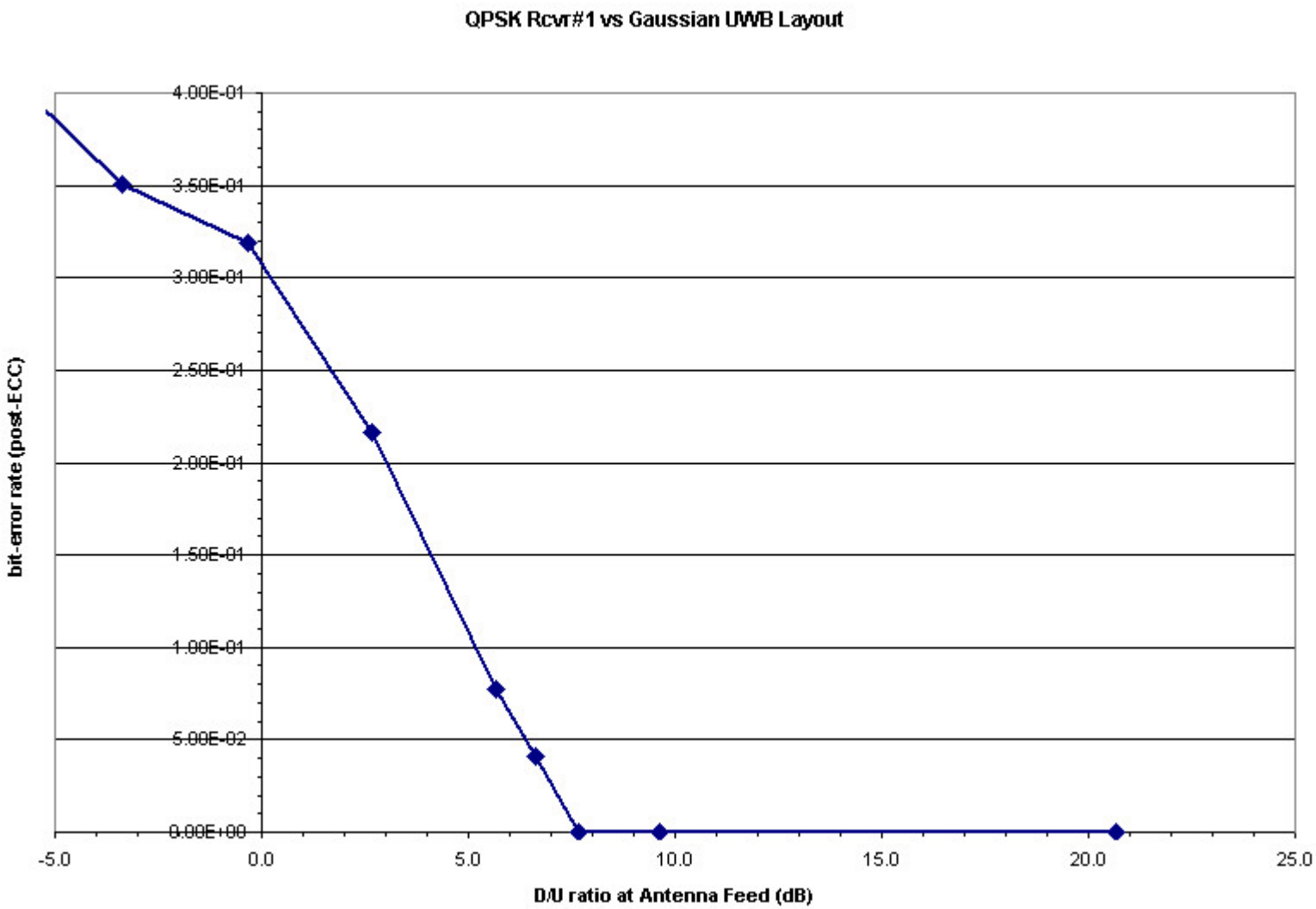

Figure 4-23 QPSK Receiver #1 Performance (BER vs D/U) with 1000 UWB Sources Gaussian Distributed About Earth Station.

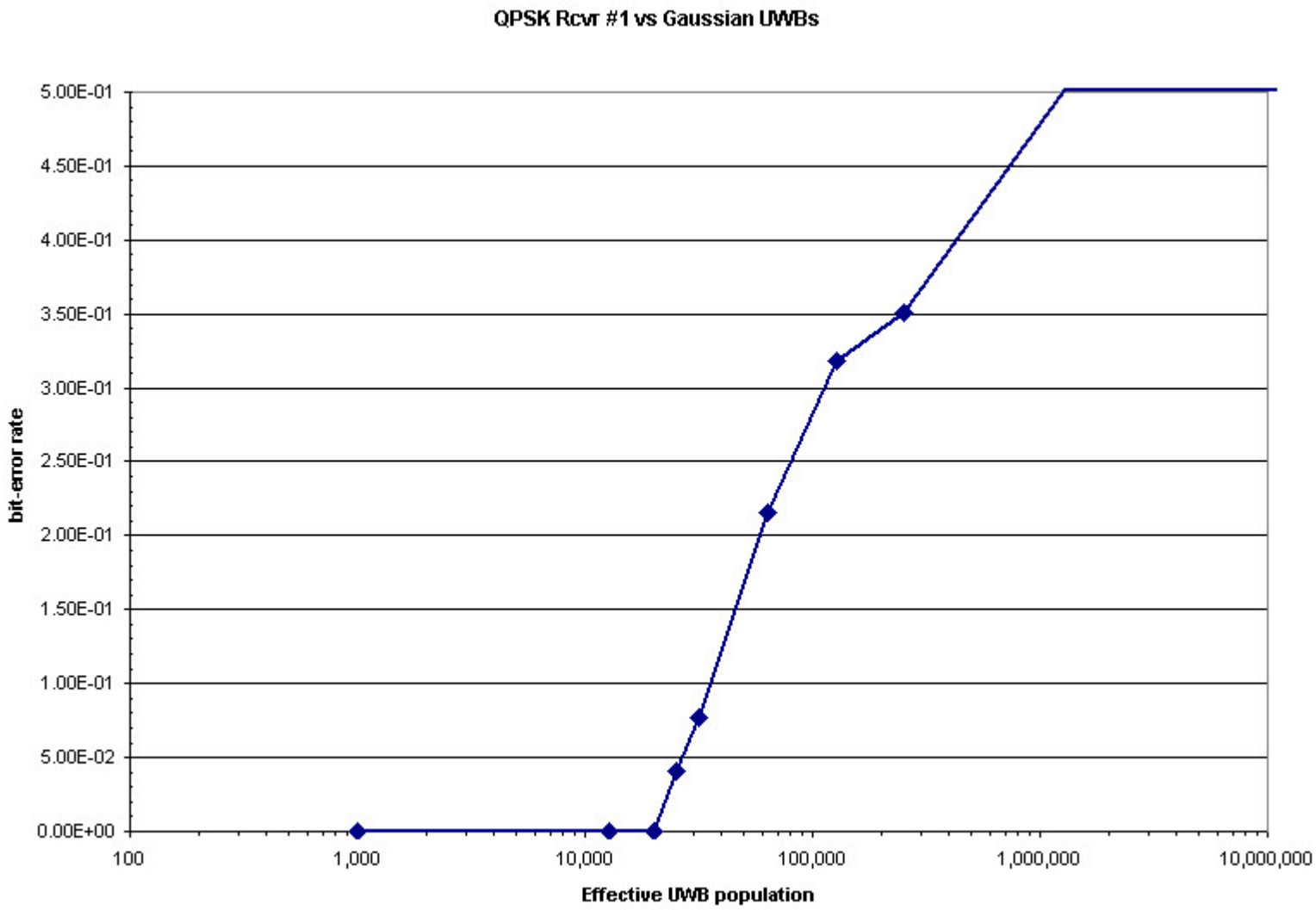

Figure 4-24 QPSK Receiver #1 Performance (BER vs Effective Population) with 1000 UWB Sources Gaussian Distributed About Earth Station.

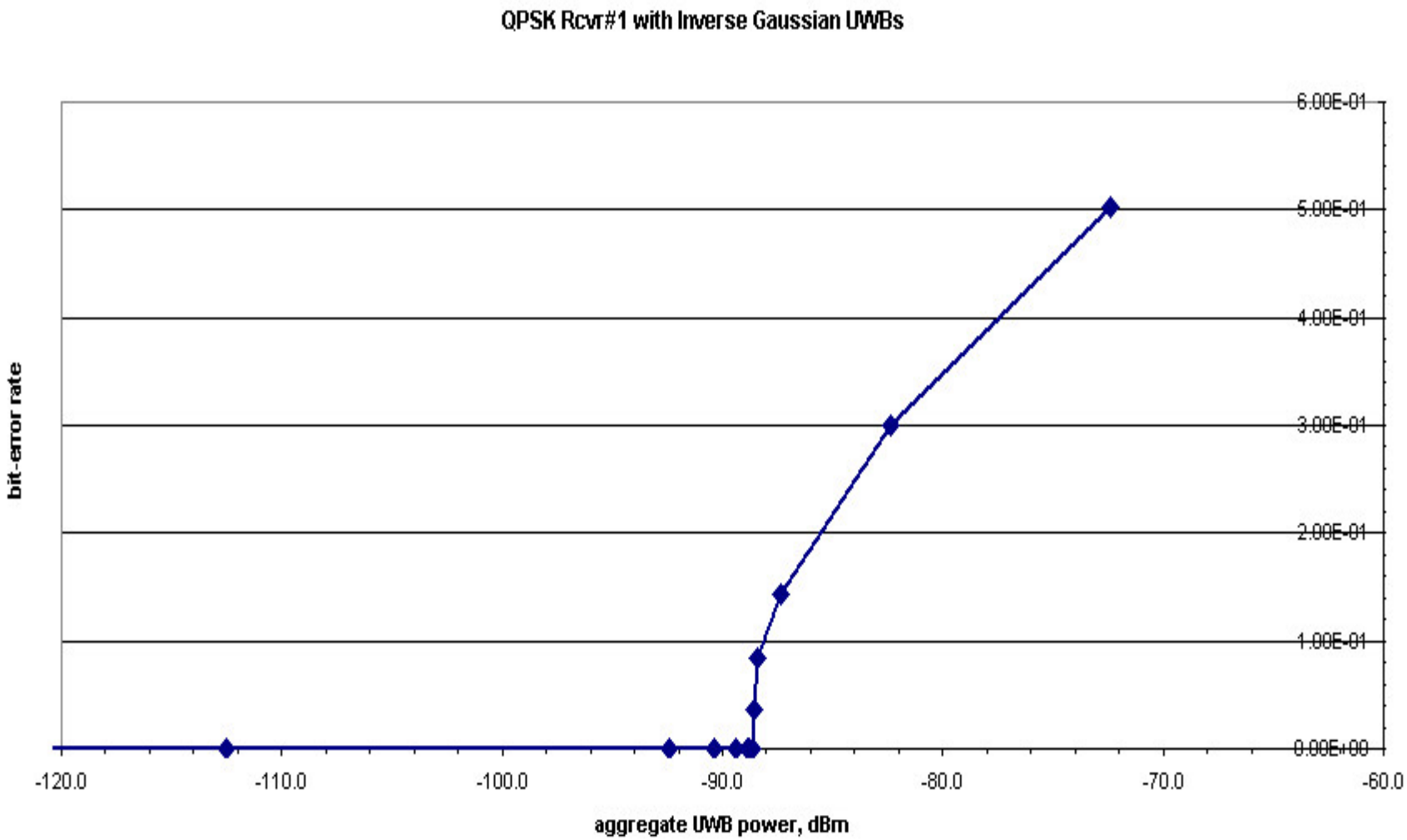

Figure 4-25 QPSK Receiver #1 Performance (BER vs Aggregate Power) with 1000 UWB Sources Inverse Gaussian Distributed About Earth Station.

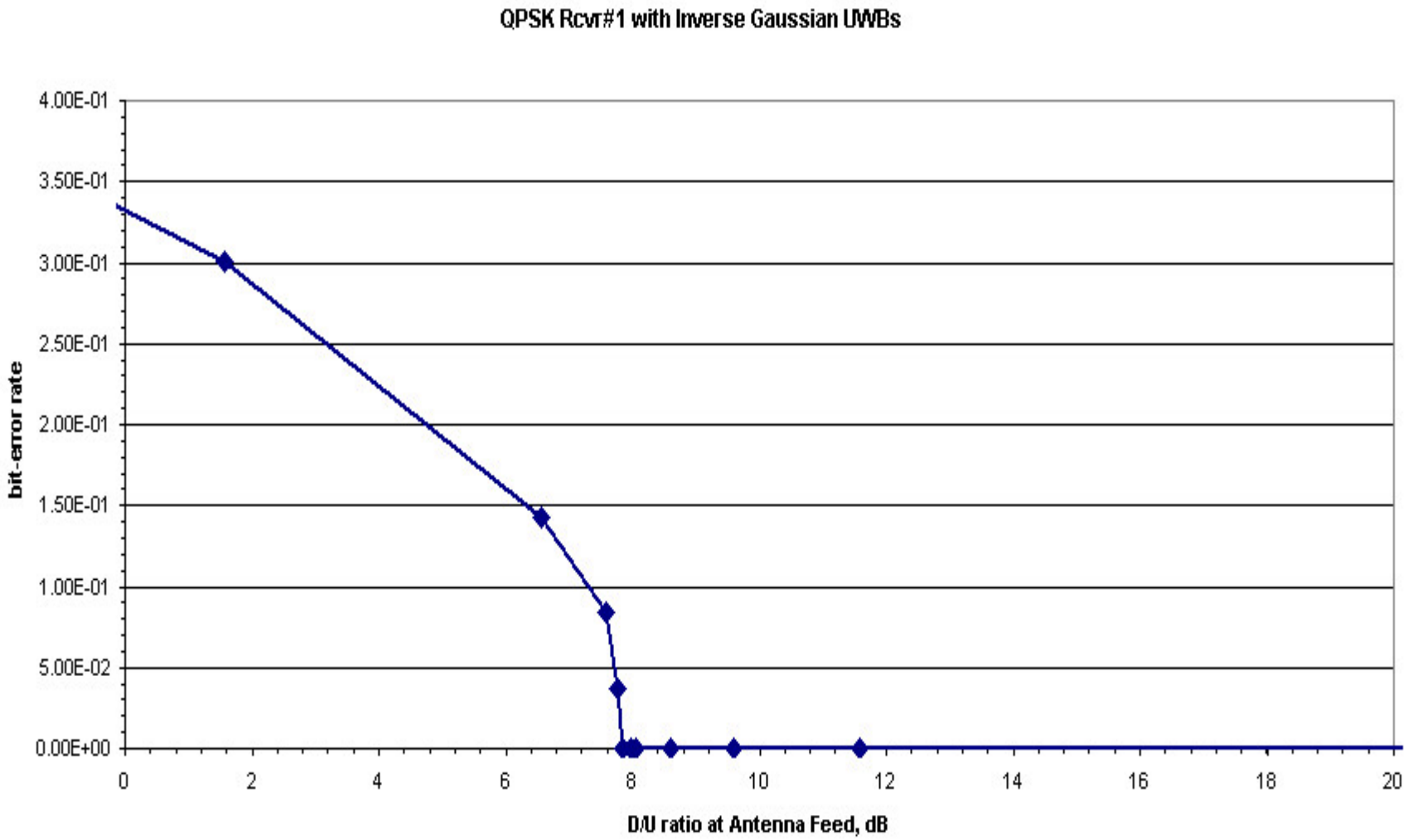

Figure 4-26 QPSK Receiver #1 Performance (BER vs D/U) with 1000 UWB Sources Inverse Gaussian Distributed About Earth Station.

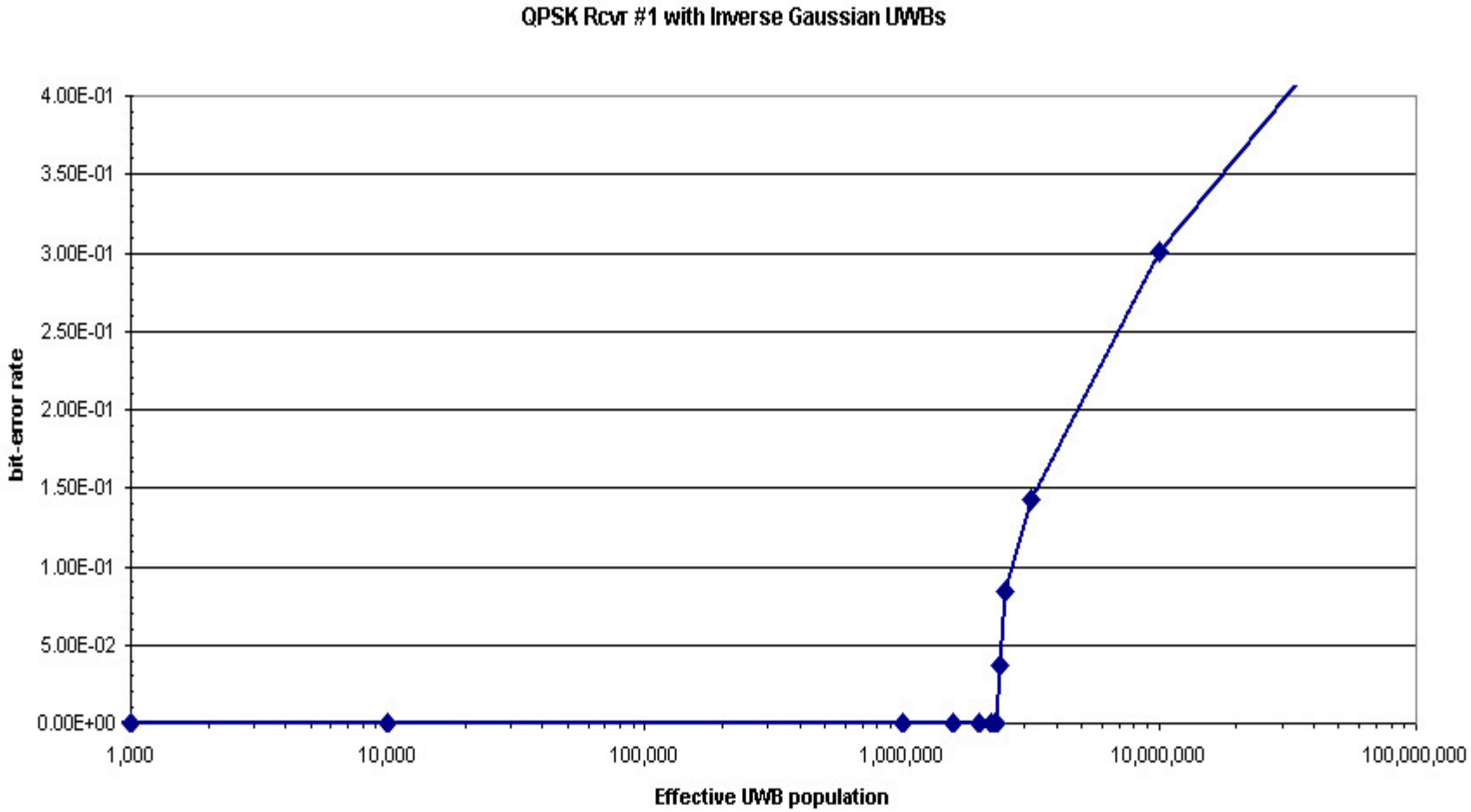

Figure 4-27 QPSK Receiver #1 Performance (BER vs Effective Population) with 1000 UWB Sources Inverse Gaussian Distributed About Earth Station.

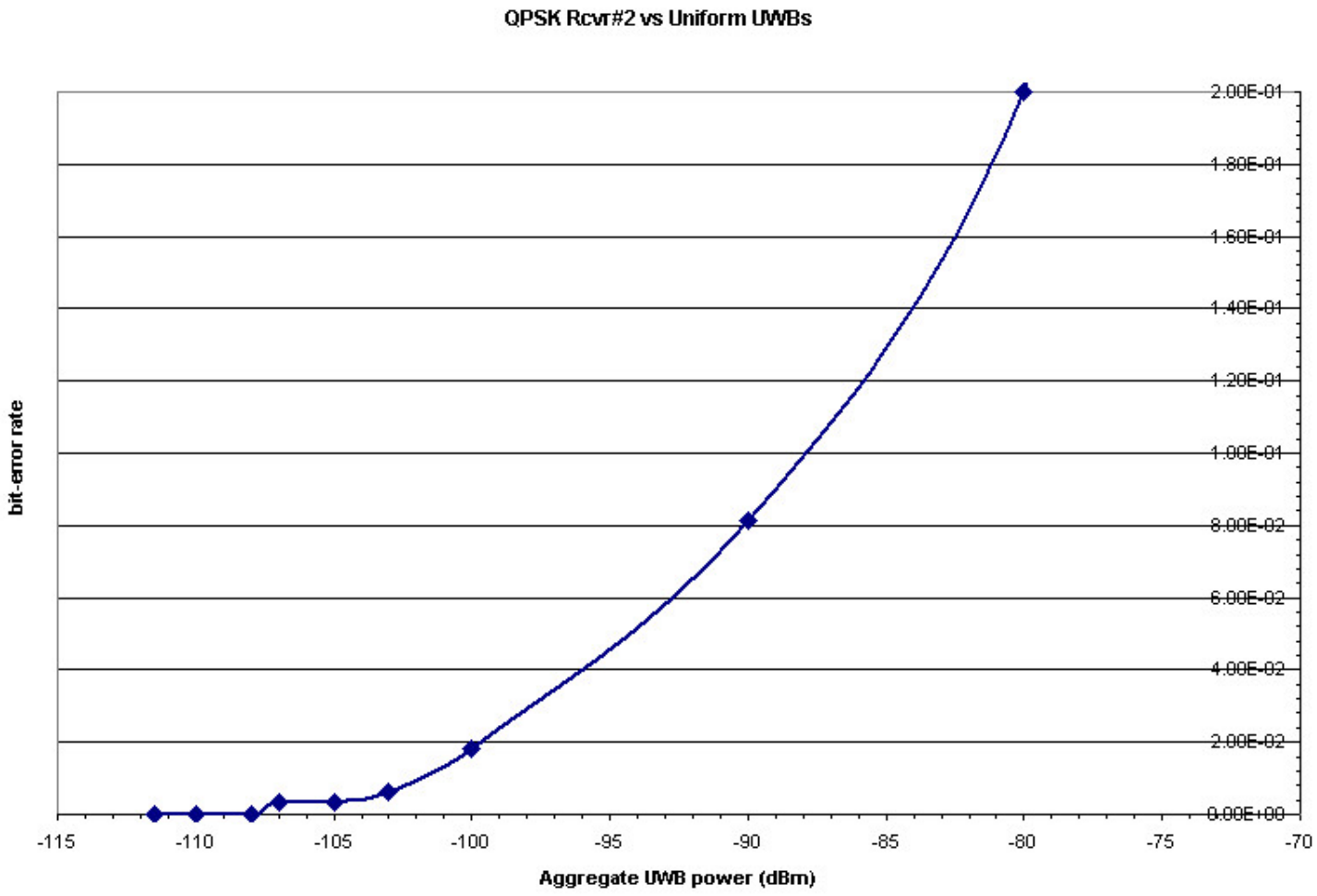

Figure 4-28 QPSK Receiver #2 Performance (BER vs Aggregate Power) with 1000 UWB Sources Uniformly Distributed About Earth Station.

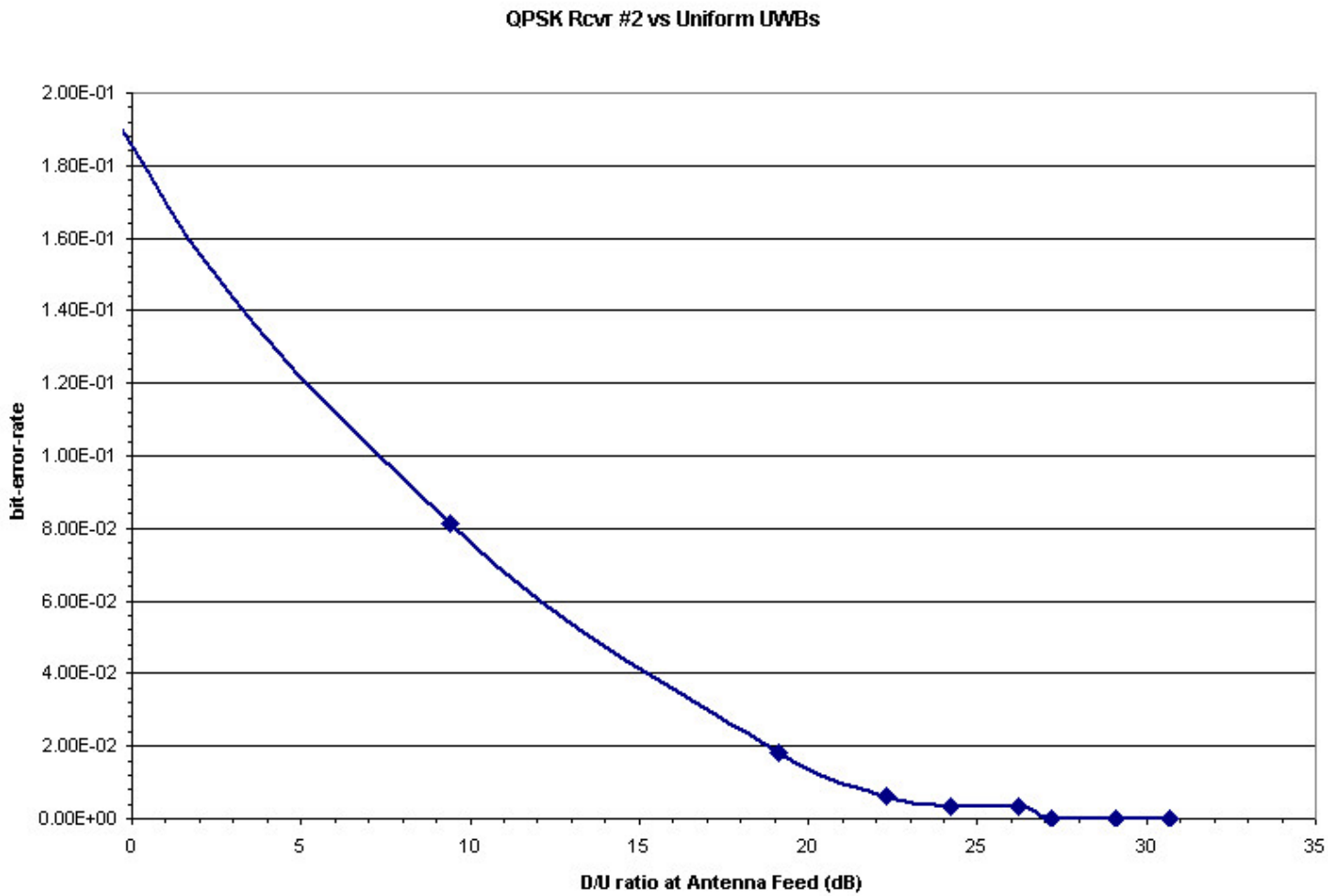

Figure 4-29 QPSK Receiver #2 Performance (BER vs D/U) with 1000 UWB Sources Uniformly Distributed About Earth Station.

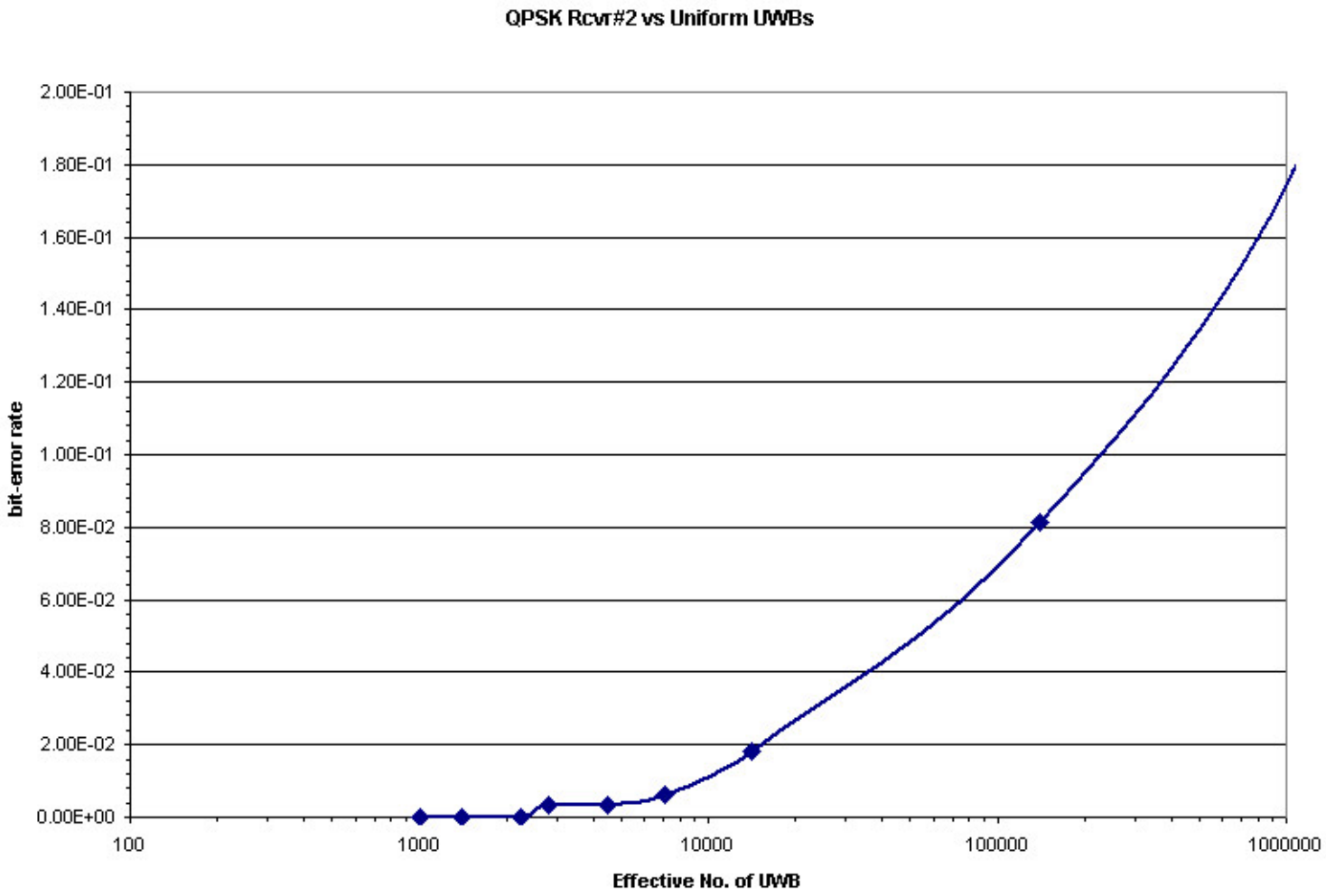

Figure 4-30 QPSK Receiver #2 Performance (BER vs Effective Population) with 1000 UWB Sources Uniformly Distributed About Earth Station.

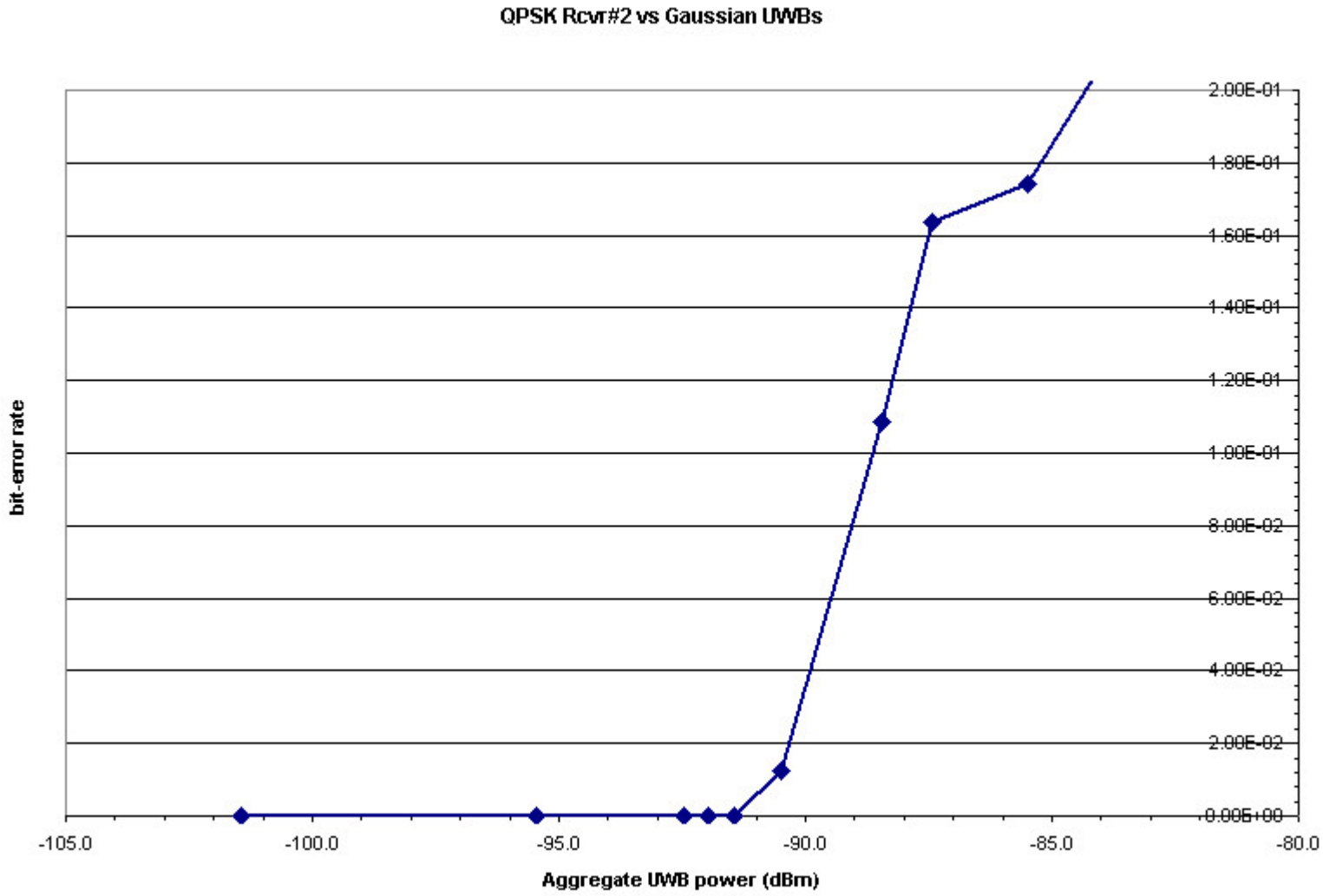

Figure 4-31 QPSK Receiver #2 Performance (BER vs Aggregate Power) with 1000 UWB Sources Gaussian Distributed About Earth Station.

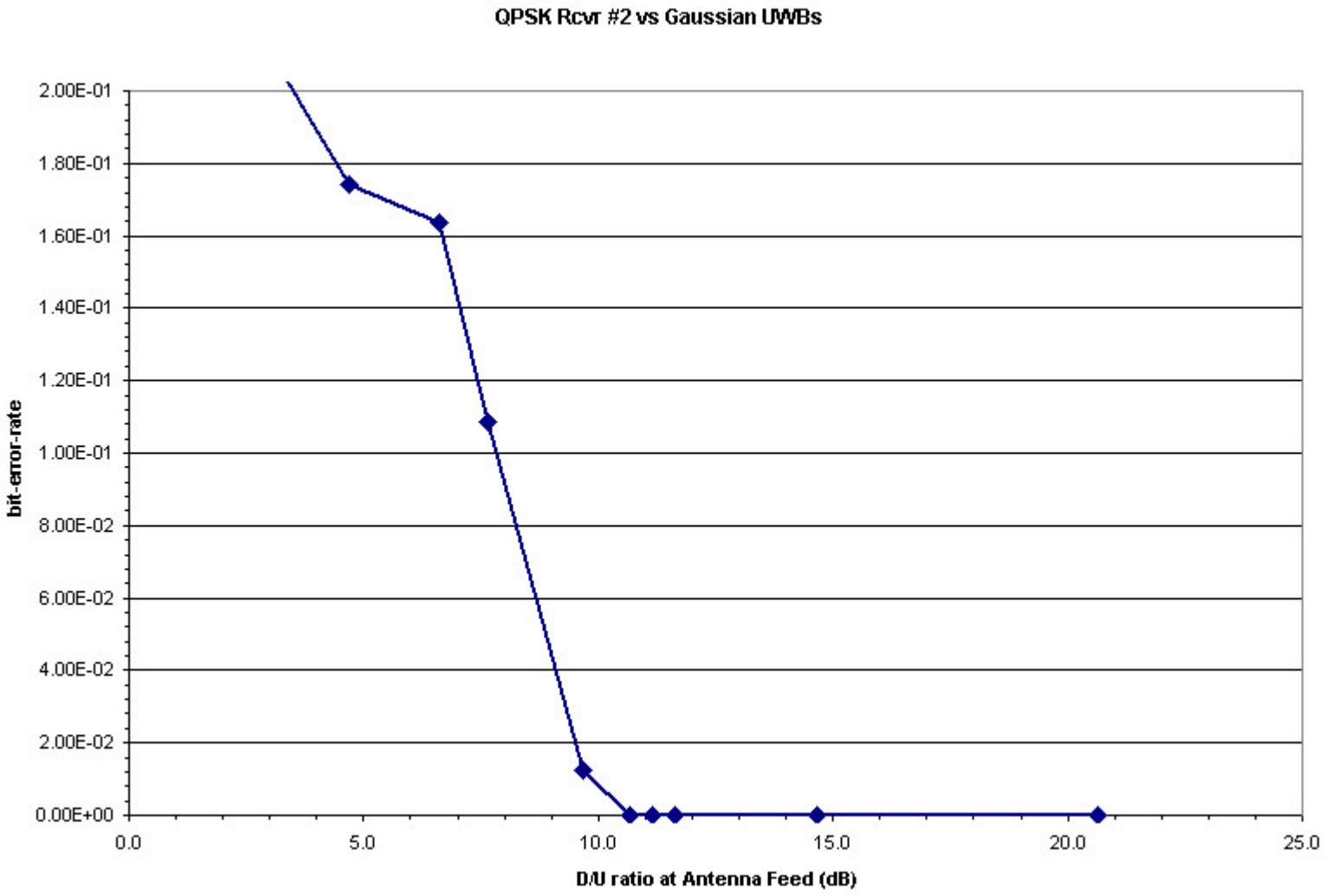

Figure 4-32 QPSK Receiver #2 Performance (BER vs D/U) with 1000 UWB Sources Gaussian Distributed About Earth Station.

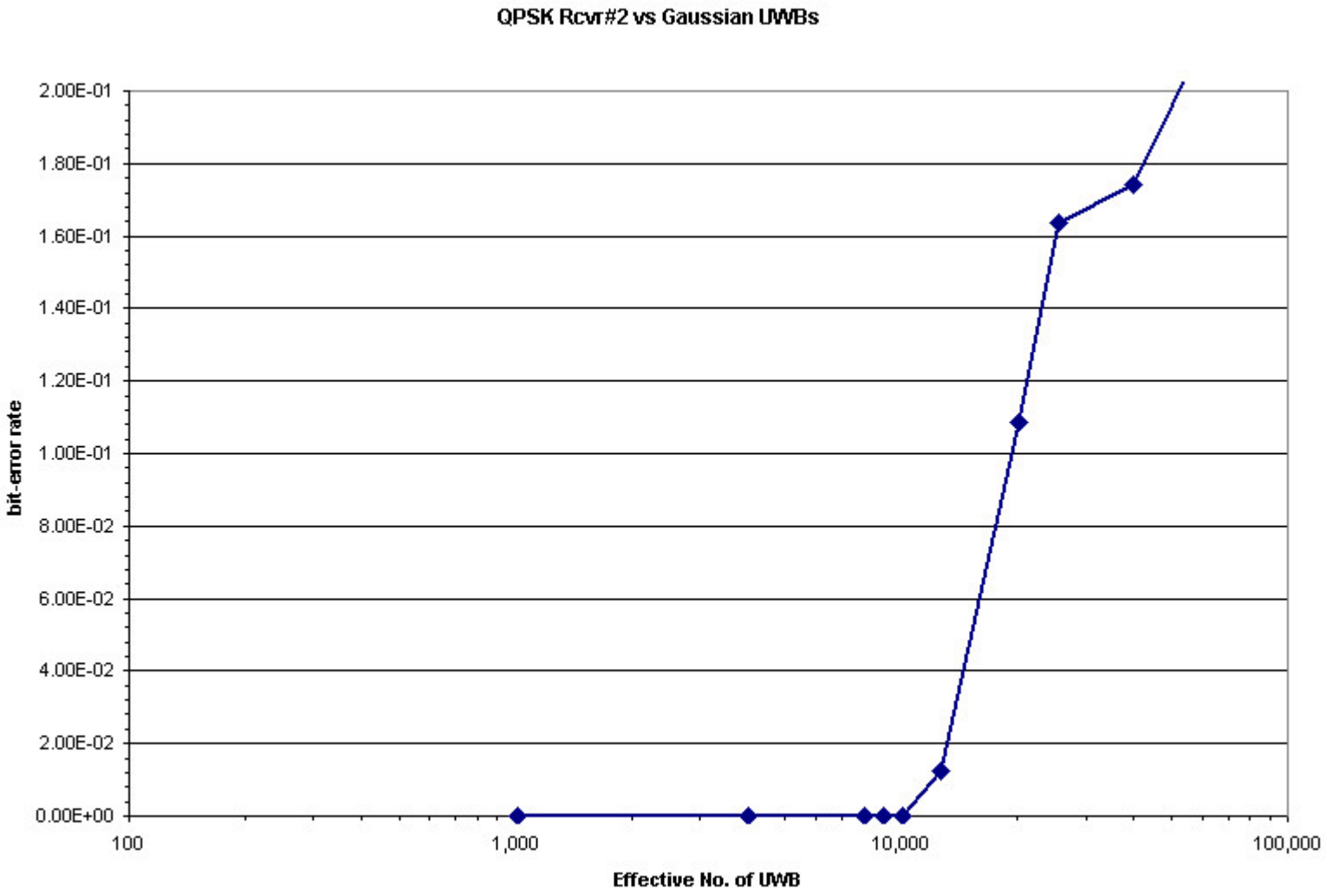

Figure 4-33 QPSK Receiver #2 Performance (BER vs Effective Population) with 1000 UWB Sources Gaussian Distributed About Earth Station.

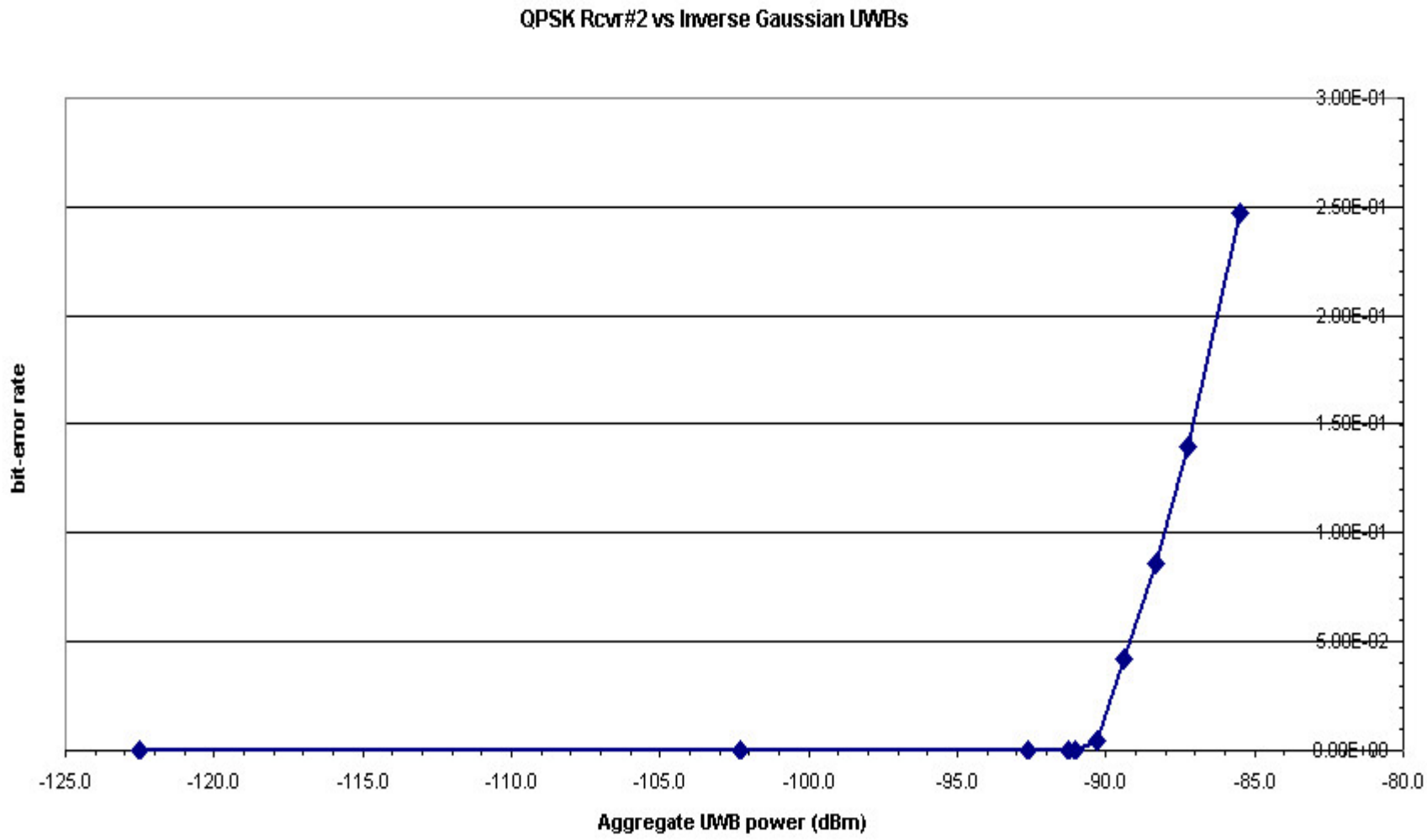

Figure 4-34 QPSK Receiver #2 Performance (BER vs Aggregate Power) with 1000 UWB Sources Inverse Gaussian Distributed About Earth Station.

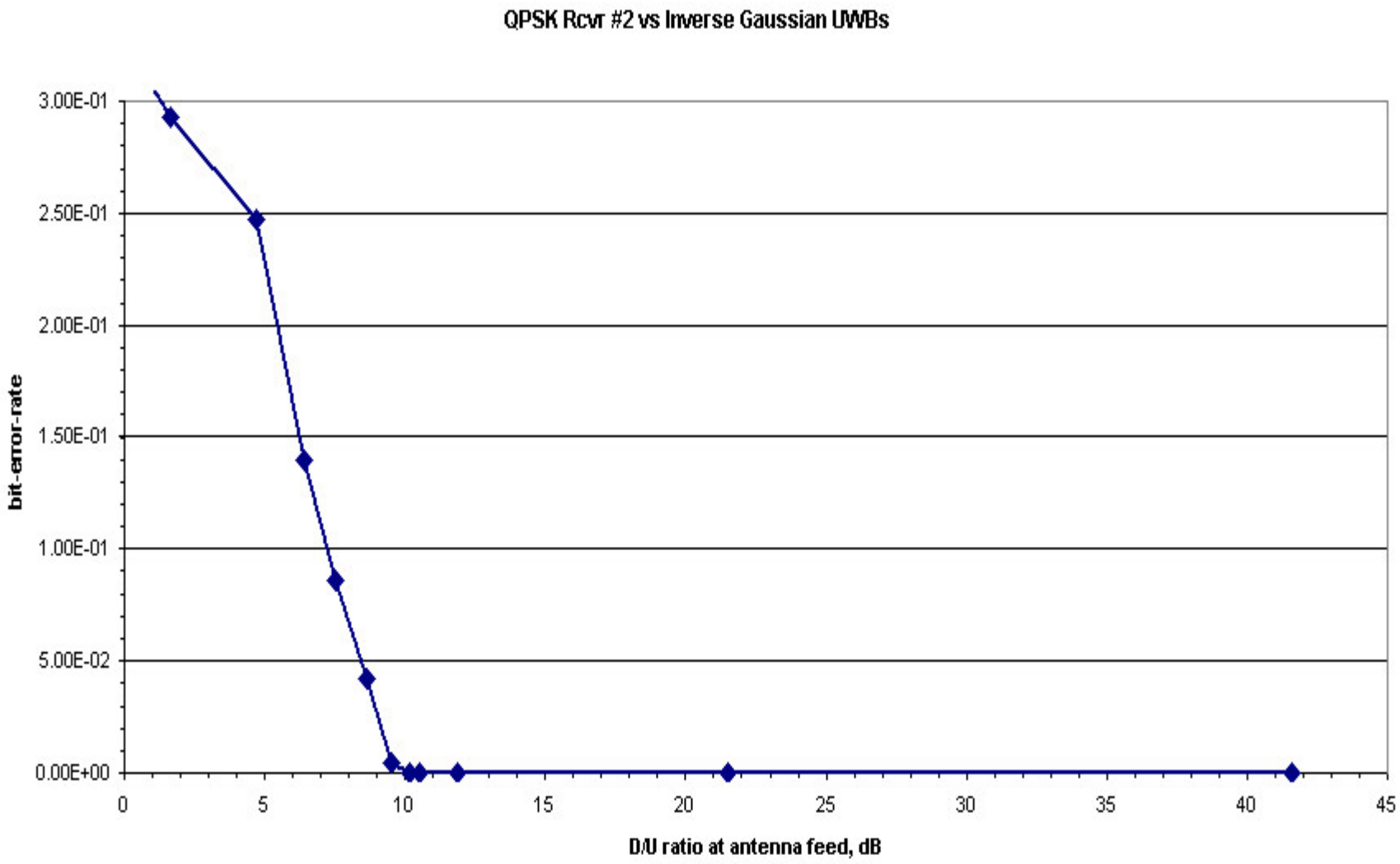

Figure 4-35 QPSK Receiver #2 Performance (BER vs D/U) with 1000 UWB Sources Inverse Gaussian Distributed About Earth Station.

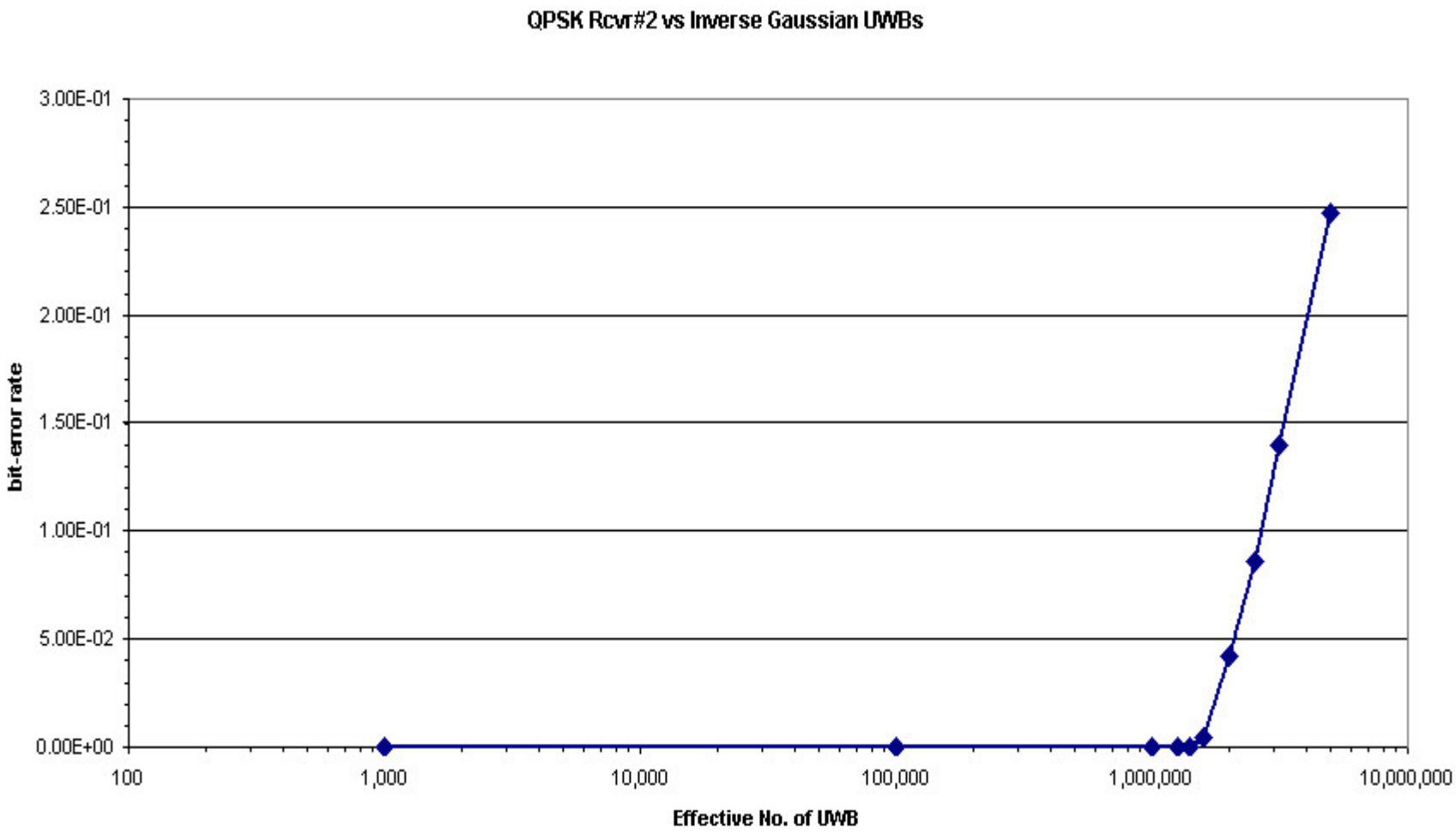

Figure 4-36 QPSK Receiver #2 Performance (BER vs Effective Population) with 1000 UWB Sources Inverse Gaussian Distributed About Earth Station.

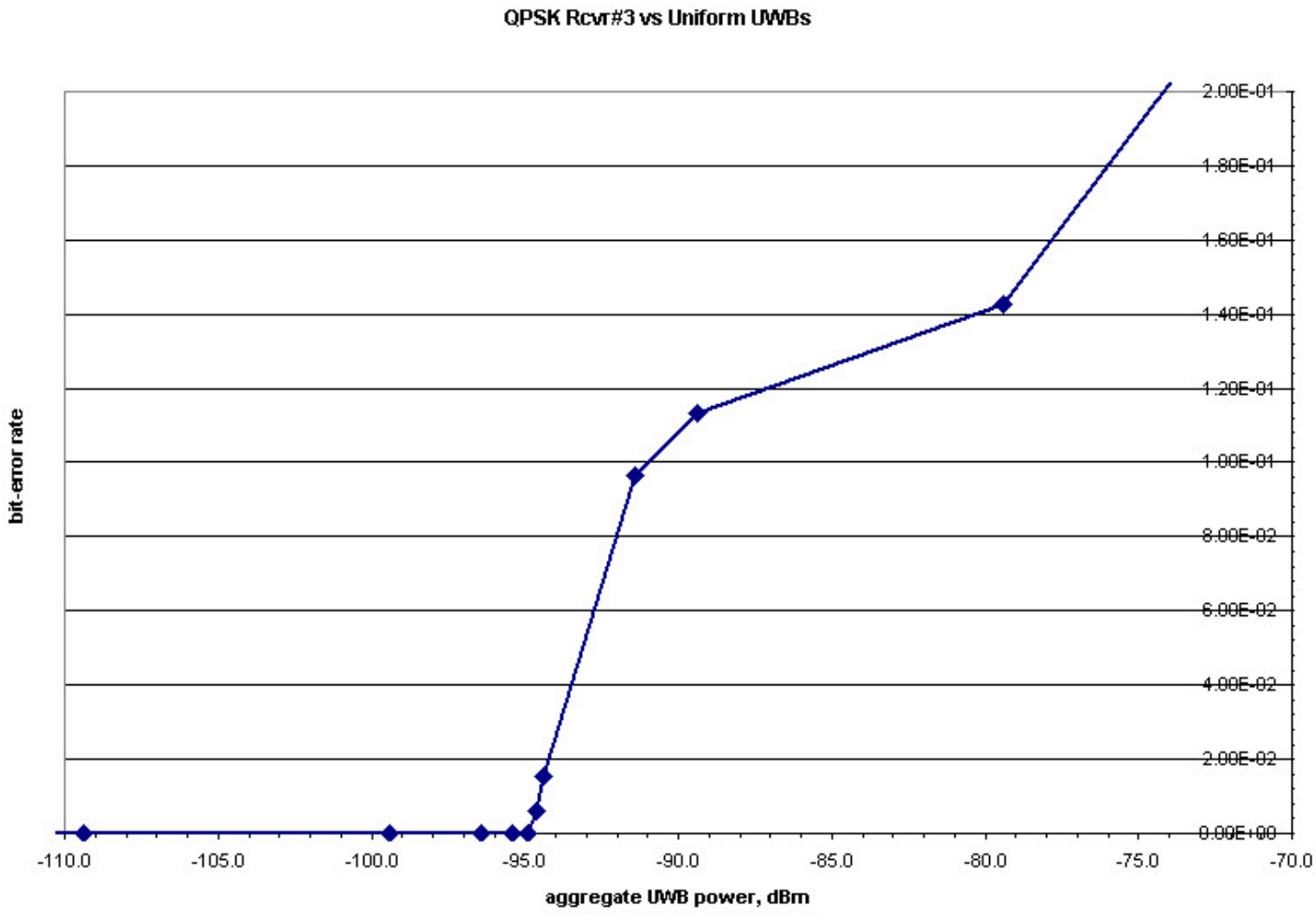

Figure 4-37 QPSK Receiver #3 Performance (BER vs Aggregate Power) with 1000 UWB Sources Uniformly Distributed About Earth Station.

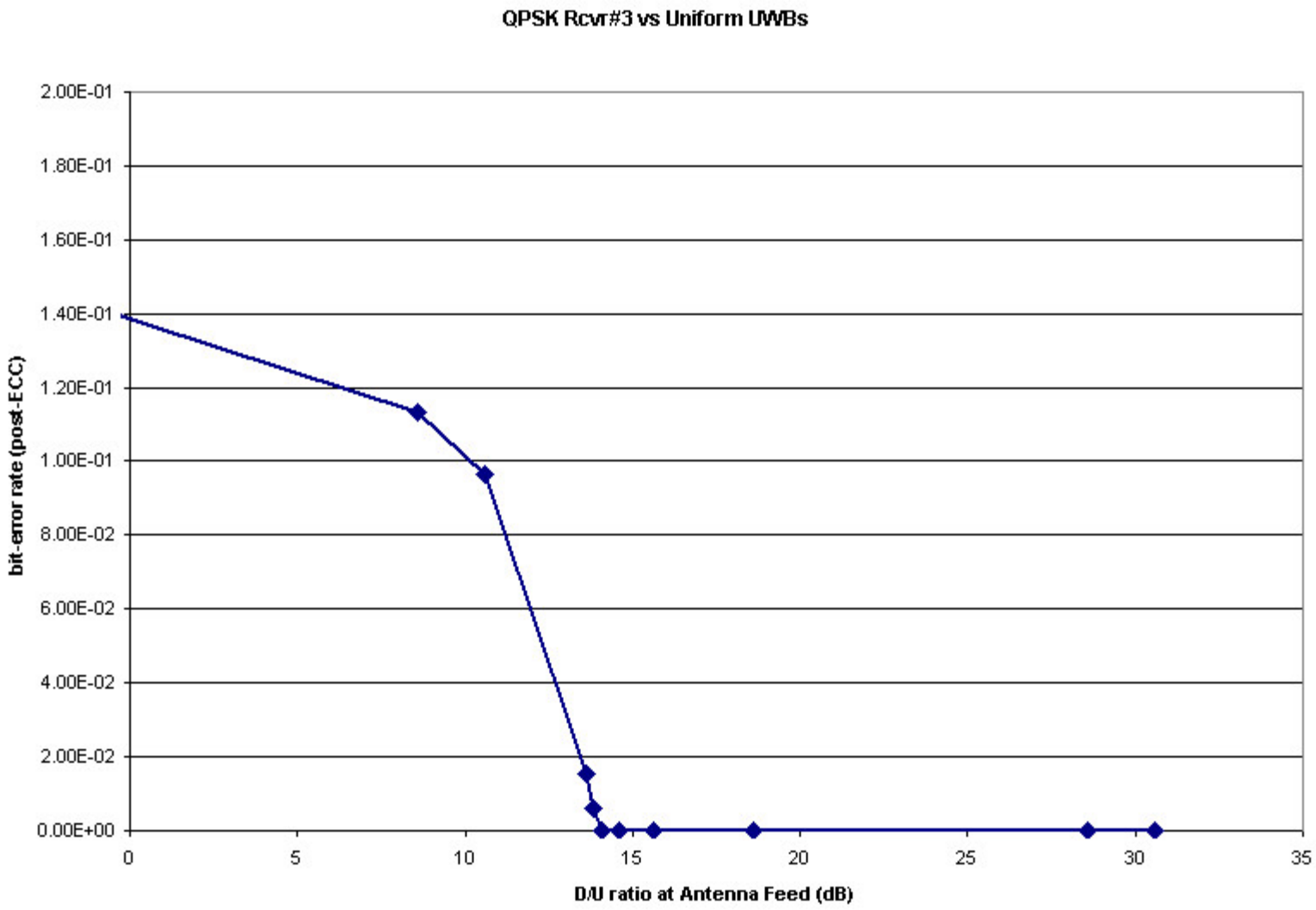

Figure 4-38 QPSK Receiver #3 Performance (BER vs D/U) with 1000 UWB Sources Uniformly Distributed About Earth Station.

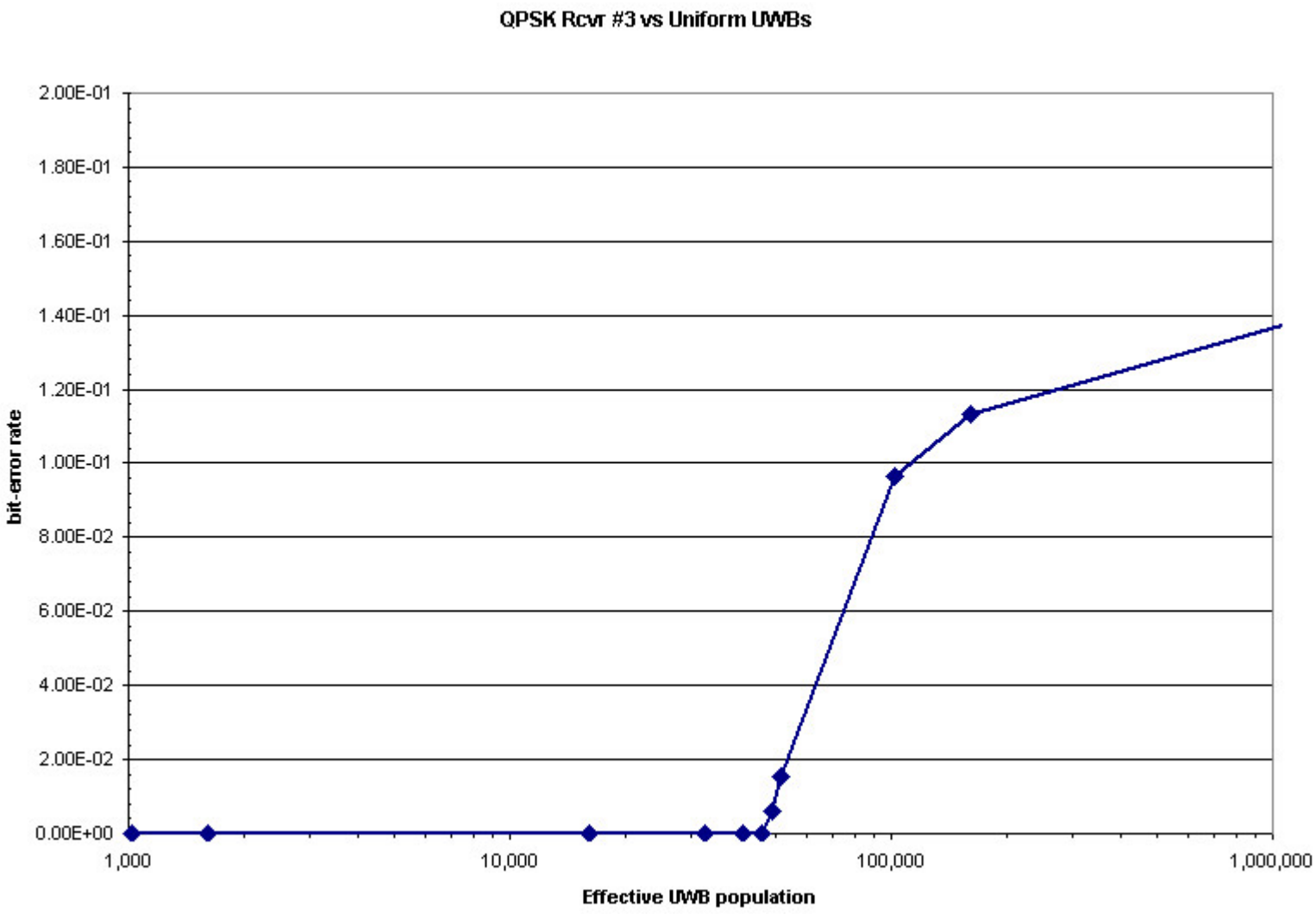

Figure 4-39 QPSK Receiver #3 Performance (BER vs Effective Population) with 1000 UWB Sources Uniformly Dstributed About Earth Station.

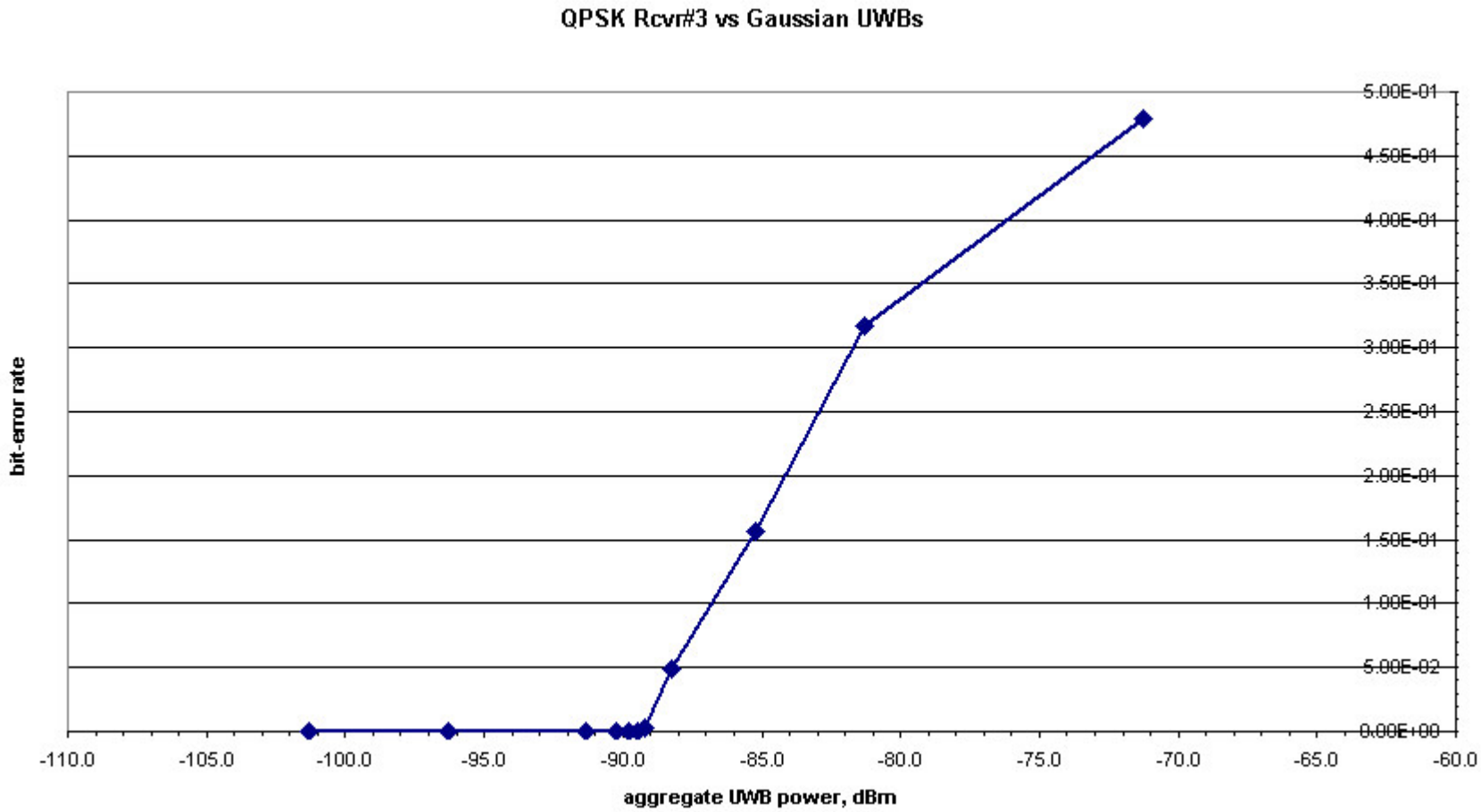

Figure 4-40 QPSK Receiver #3 Performance (BER vs Aggregate Power) with 1000 UWB Sources Gaussian Distributed About Earth Station.

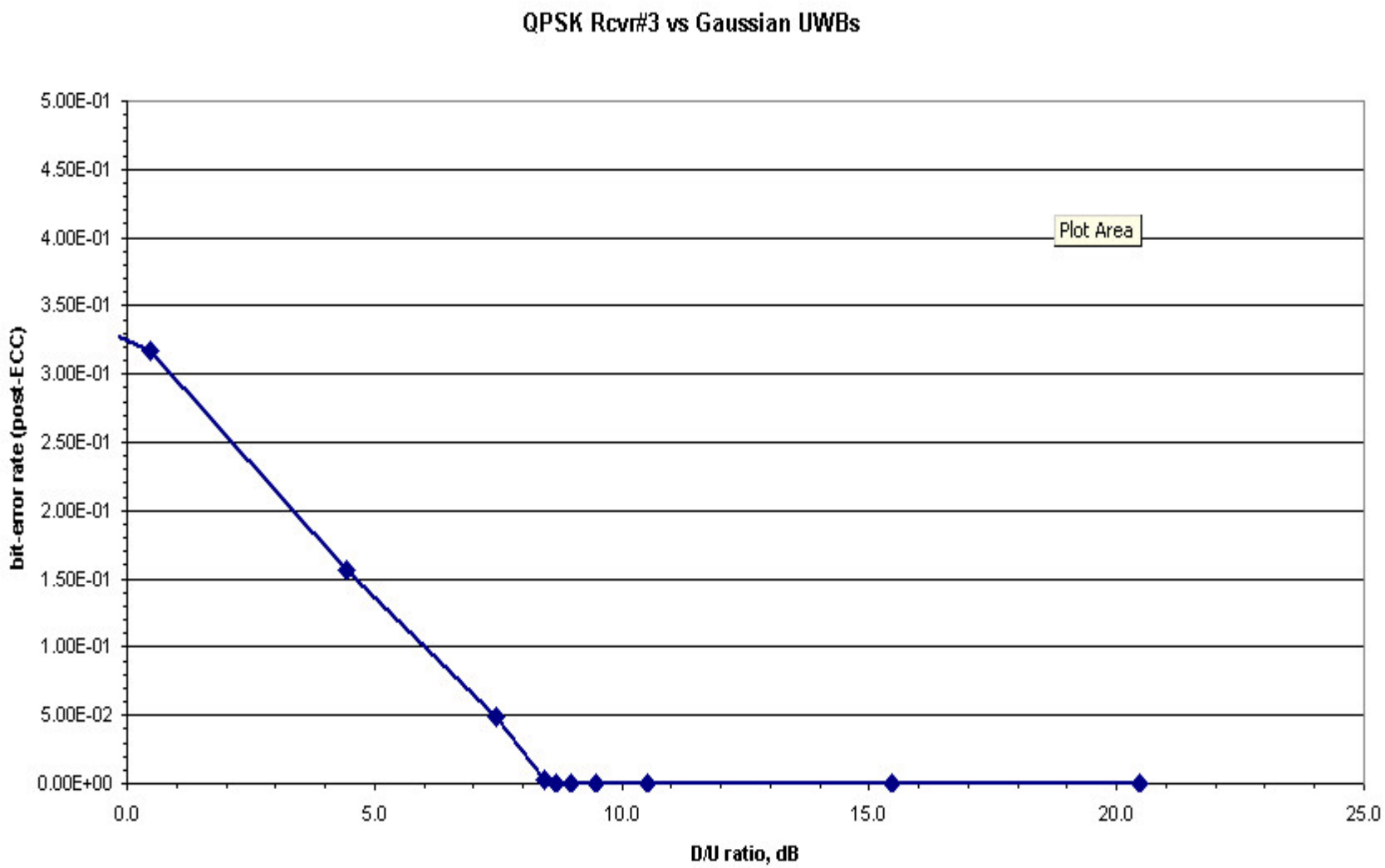

Figure 4-41 QPSK Receiver #3 Performance (BER vs D/U) with 1000 UWB Sources Gaussian Distributed About Earth Station.

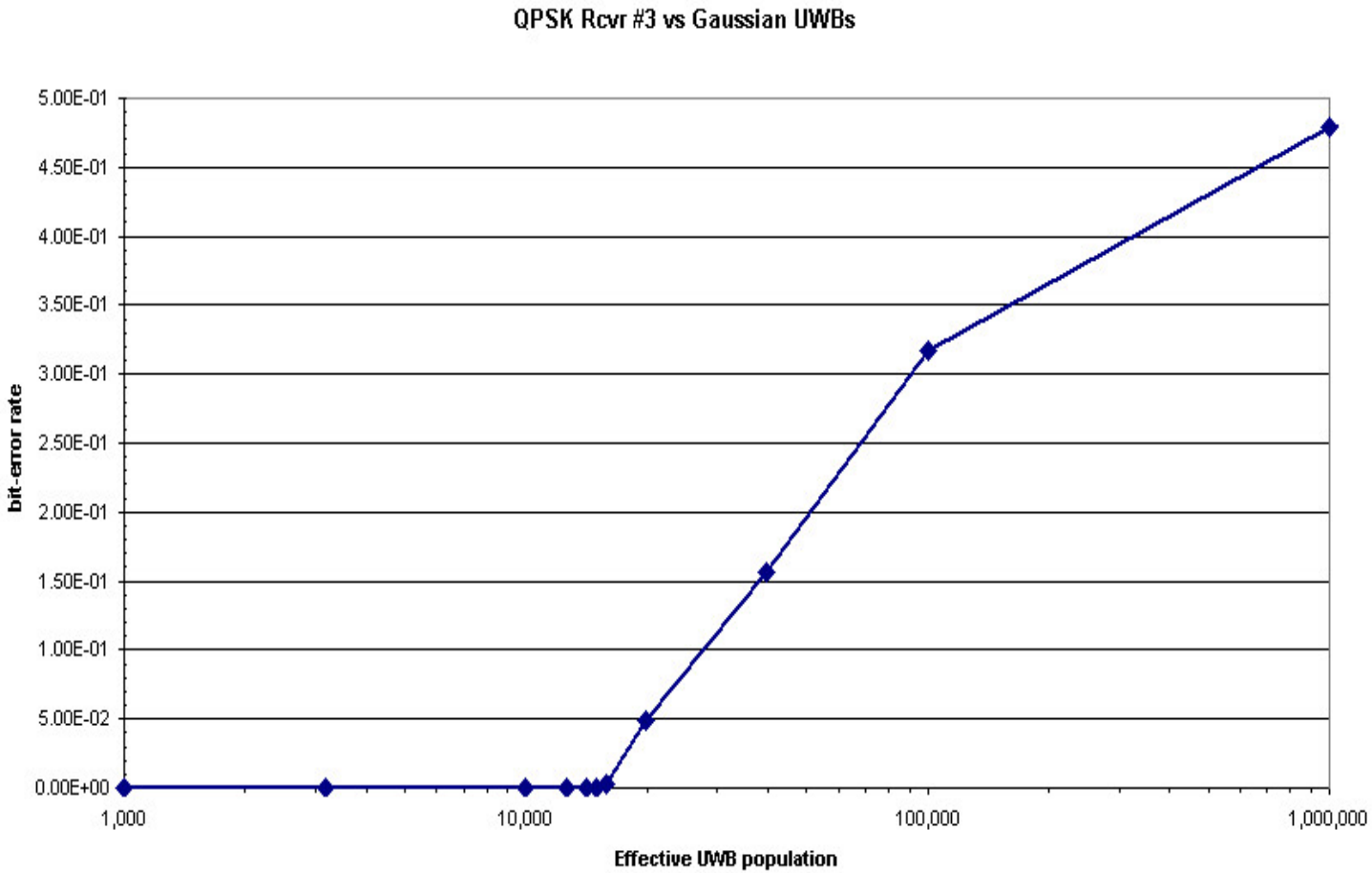

Figure 4-42 QPSK Receiver #3 Performance (BER vs Effective Population) with 1000 UWB Sources Gaussian Distributed About Earth Station.

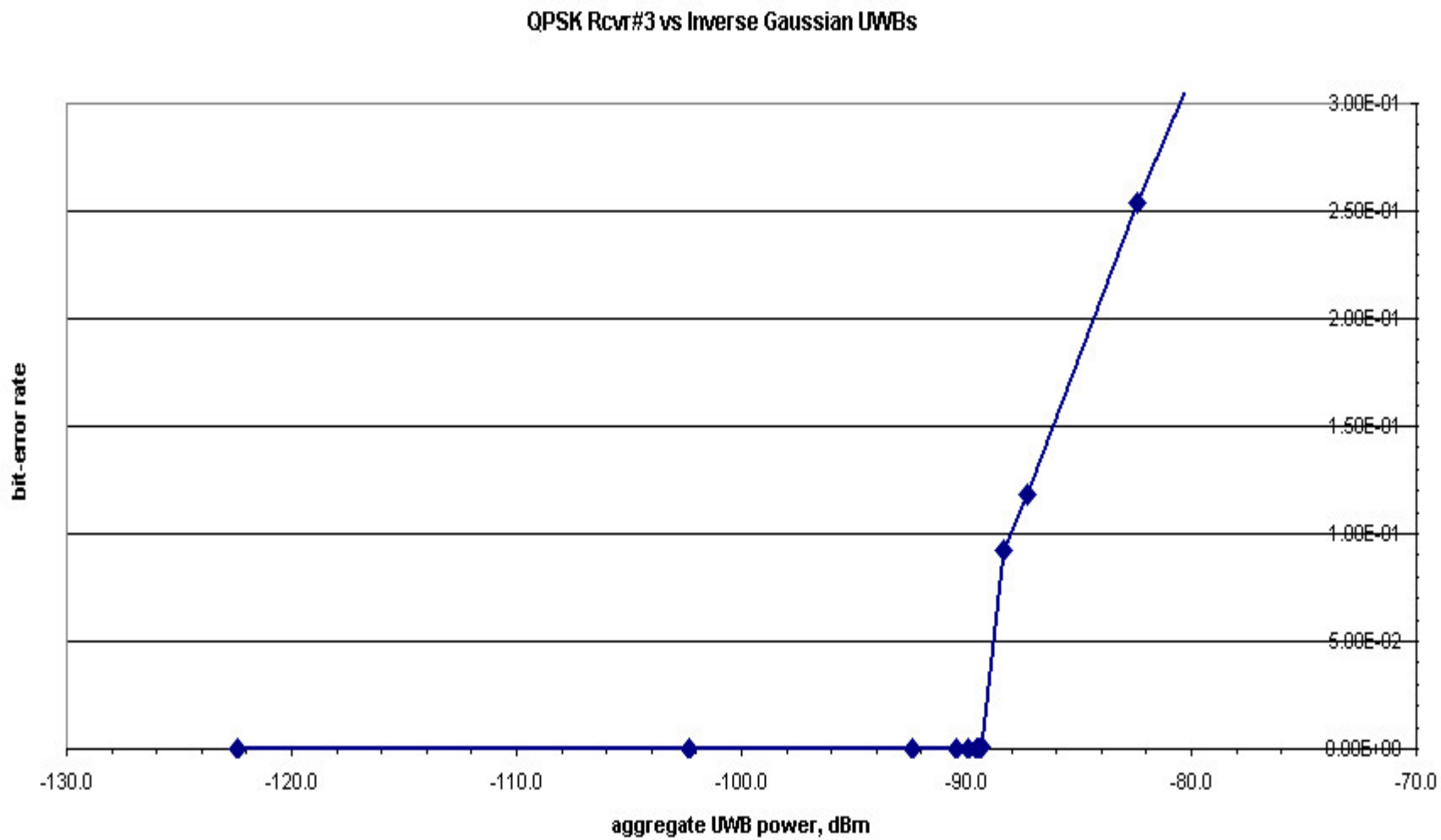

Figure 4-43 QPSK Receiver #3 Performance (BER vs Aggregate Power) with 1000 UWB Sources Inverse Gaussian Distributed About Earth Station.

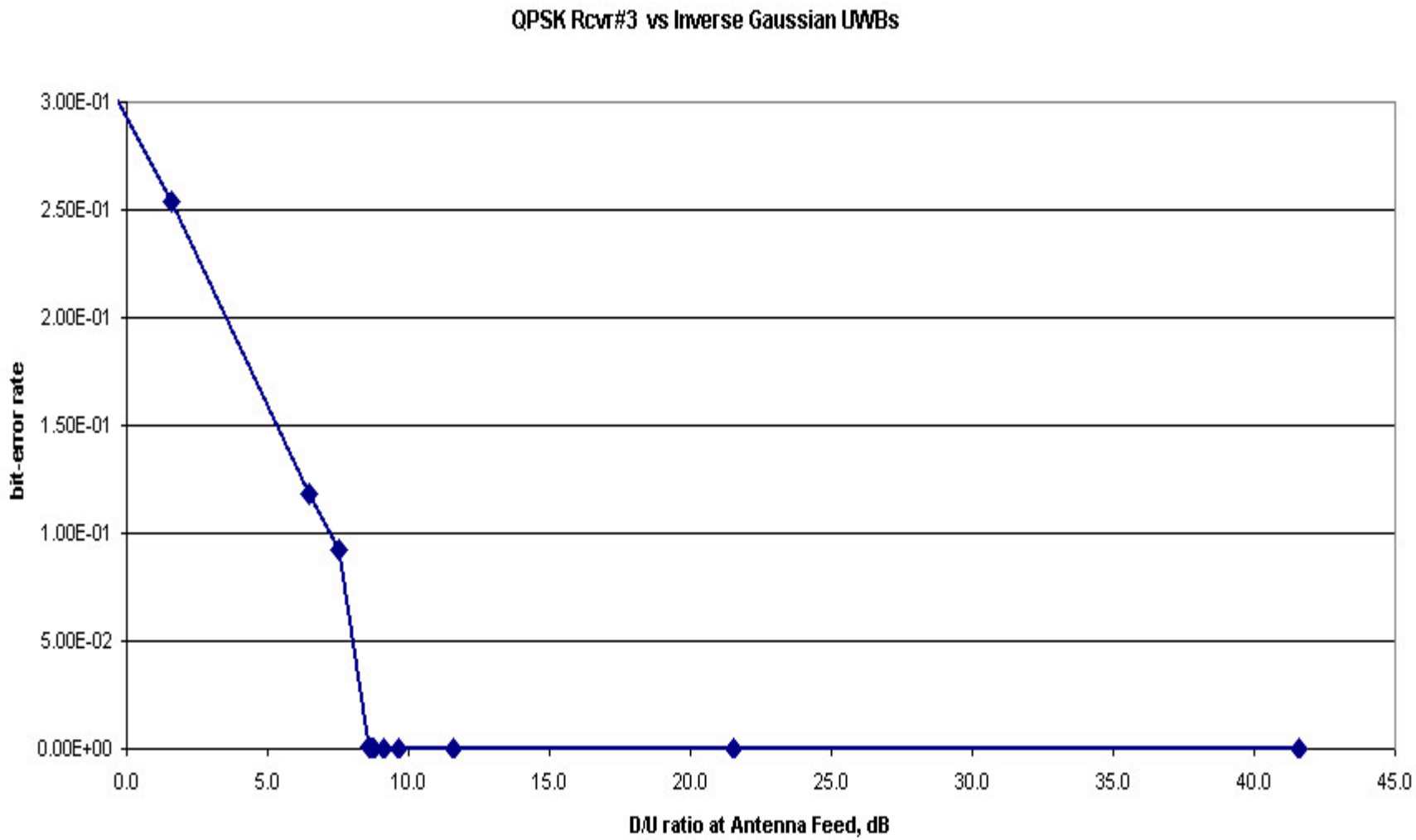

Figure 4-44 QPSK Receiver #3 Performance (BER vs D/U) with 1000 UWB Sources Inverse Gaussian Distributed About Earth Station.

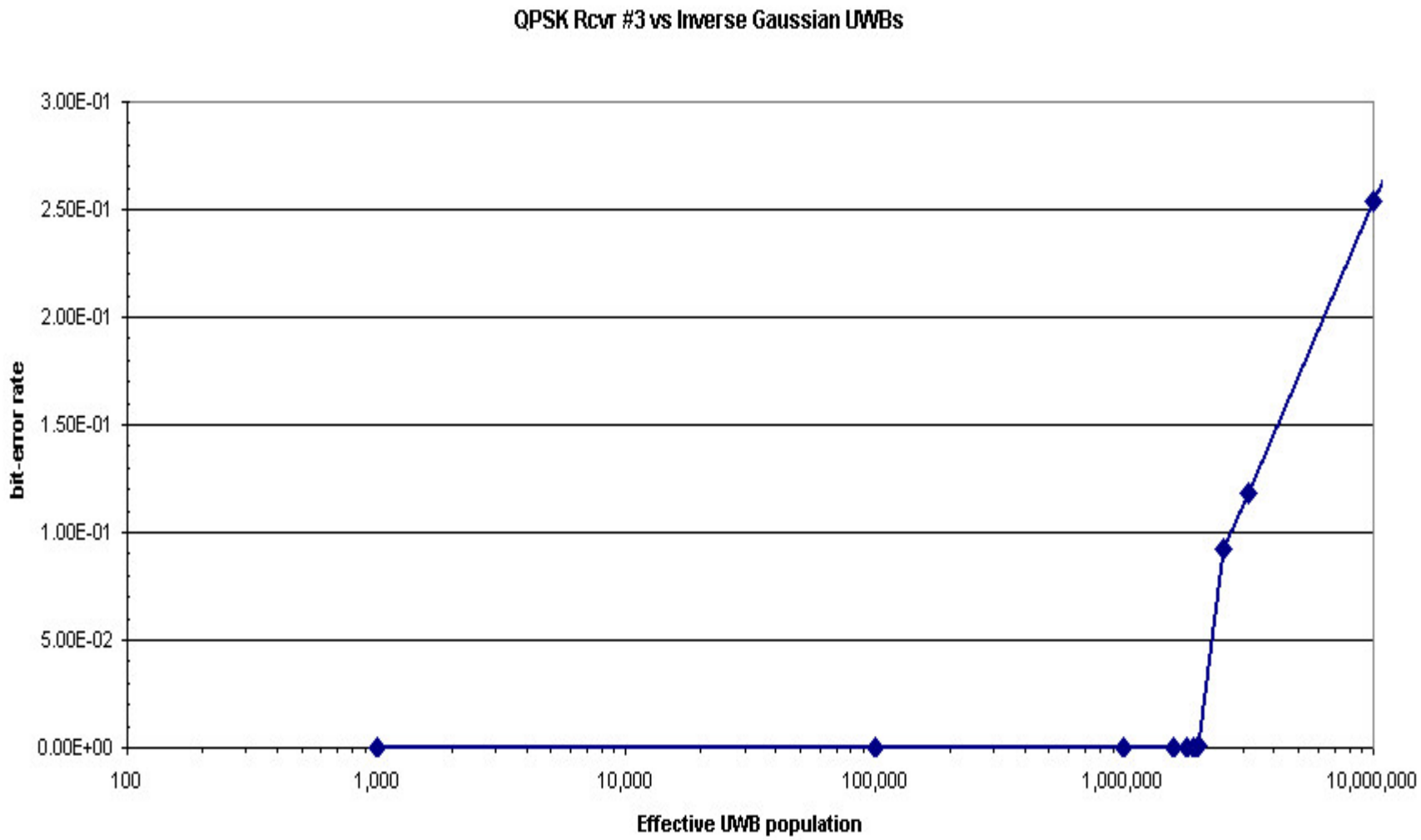

Figure 4-45 QPSK Receiver #3 Performance (BER vs Effective Population) with 1000 UWB Sources Inverse Gaussian Distributed About Earth Station.

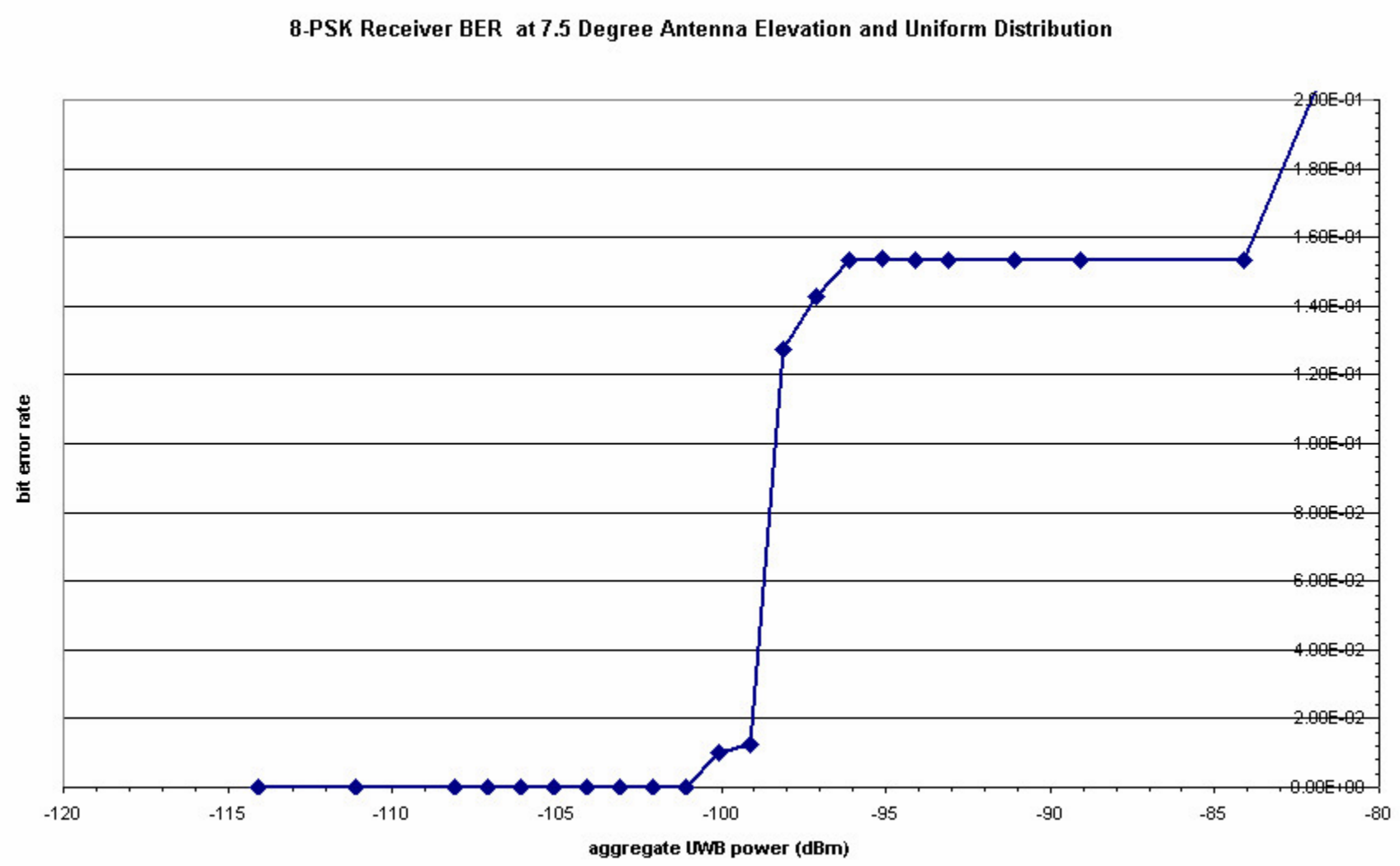

Figure 4-46 8-PSK Receiver Performance (BER vs Aggregate Power) with 1000 UWB Sources Uniformly Distributed About Earth Station and 7. 5° Elevation Angle.

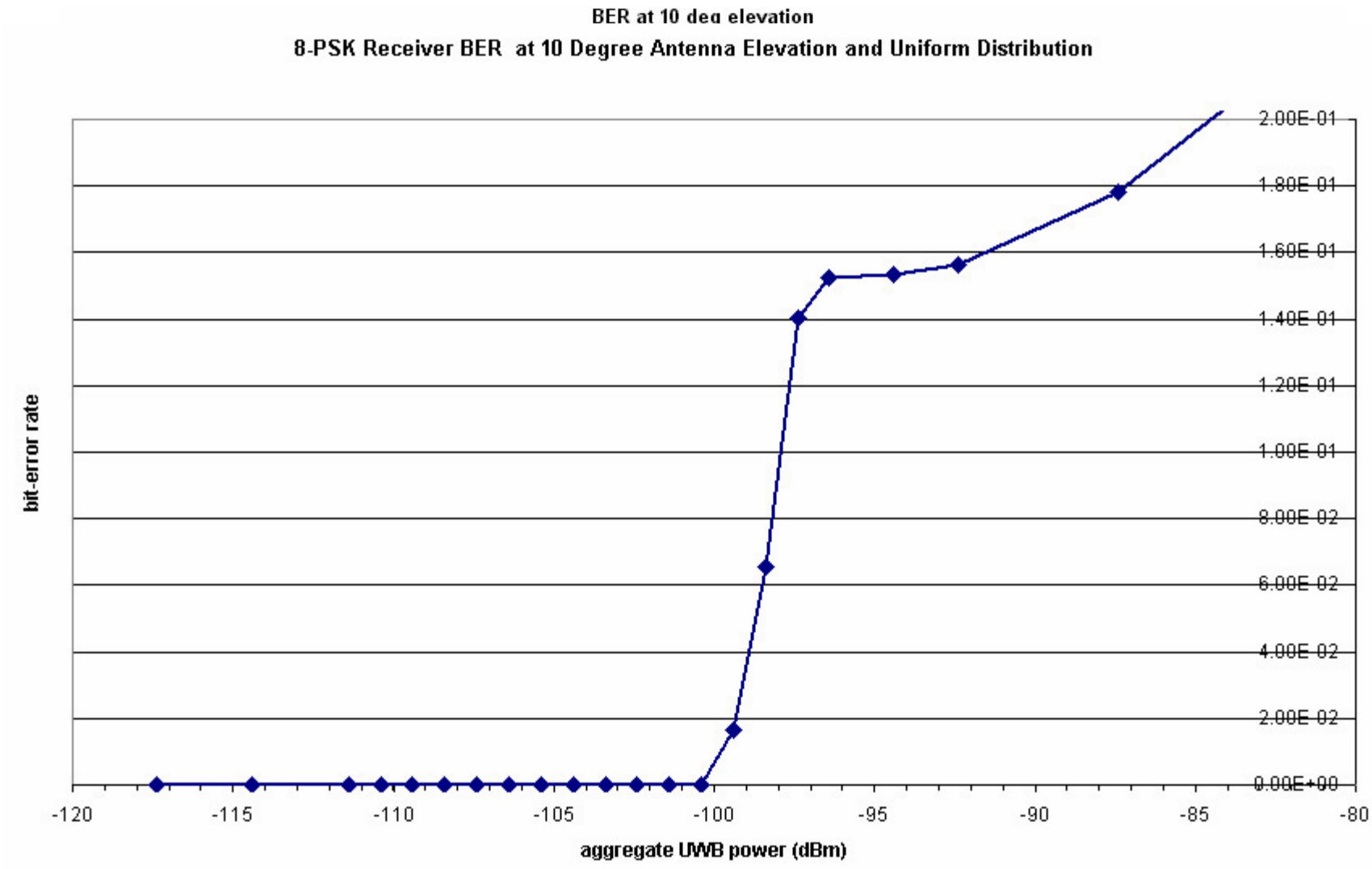

Figure 4-47 8-PSK Receiver Performance (BER vs Aggregate Power) with 1000 UWB Sources Uniformly Distributed About Earth Station and 10° Elevation Angle.

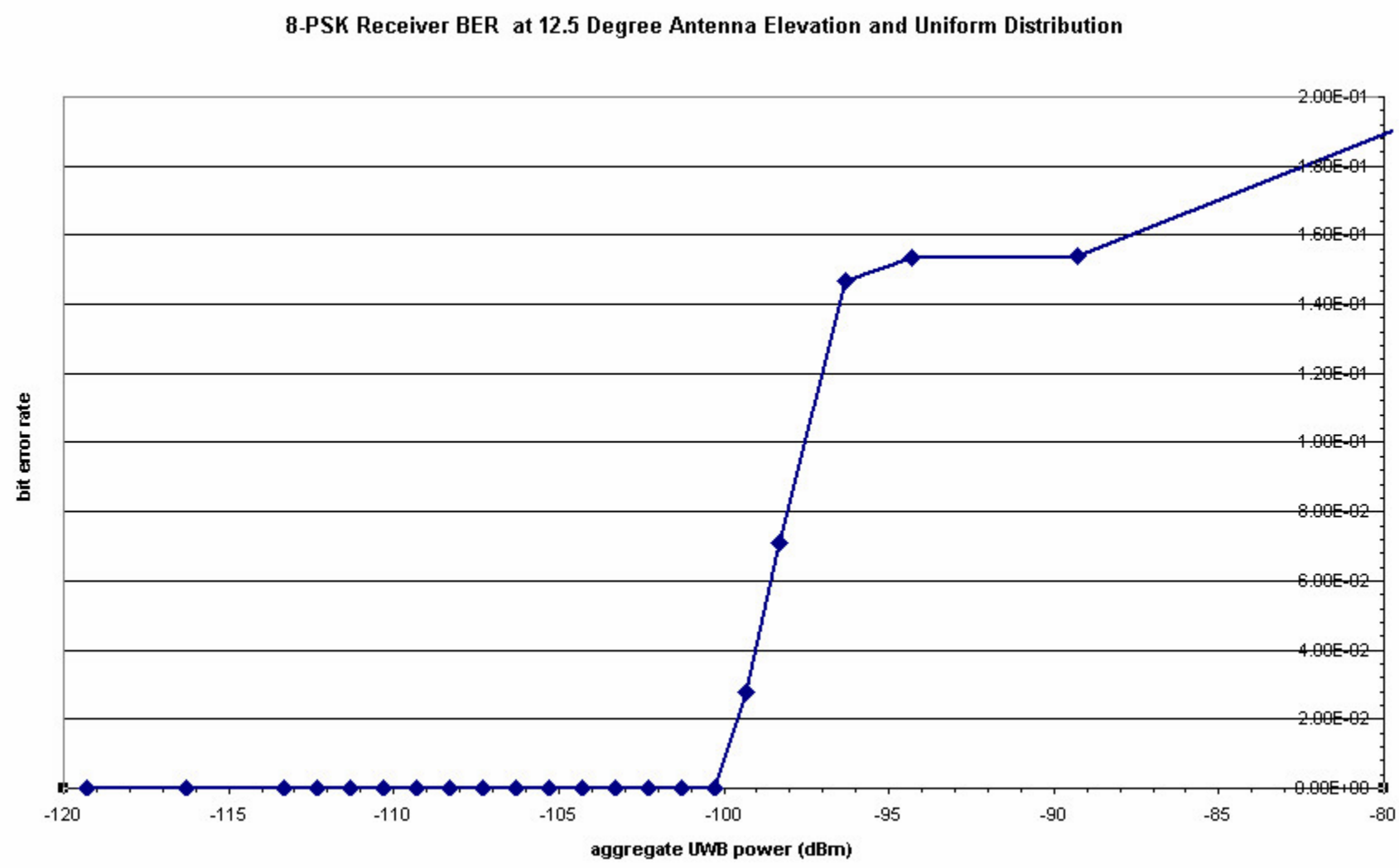

Figure 4-48 8-PSK Receiver Performance (BER vs Aggregate Power) with 1000 UWB Sources Uniformly Distributed About Earth Station and 12.5° Elevation Angle.

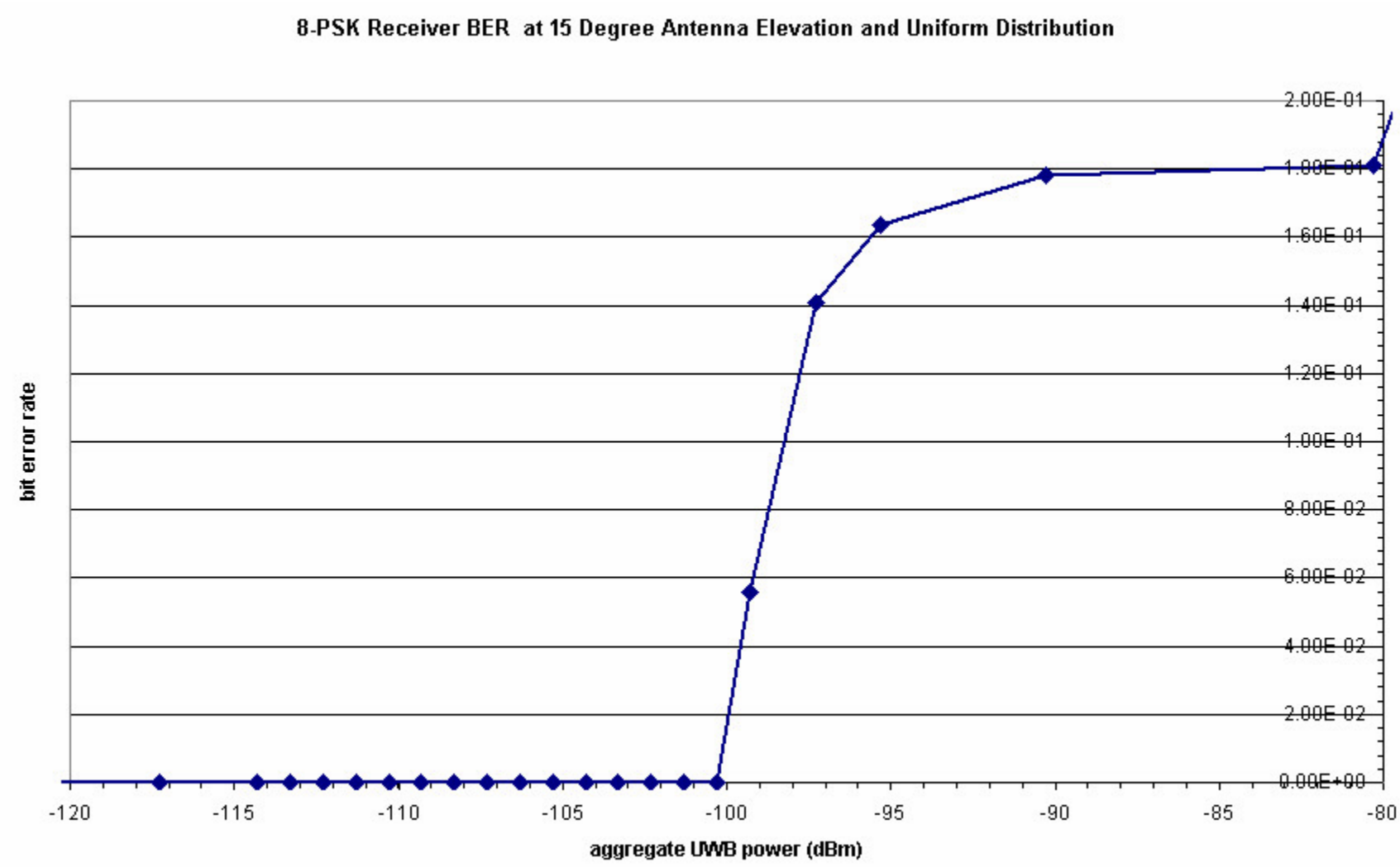

Figure 4-49 8-PSK Receiver Performance (BER vs Aggregate Power) with 1000 UWB Sources Uniformly Distributed About Earth Station and 15° Elevation Angle.

SECTION 5
Validation Testing

5.1 Introduction

The objective of the validation laboratory tests was to characterize the effect of the LNA/LNB on interfering UWB signals, and to collect data to be used to perform validation of the receiver models developed in the modeling and simulation portion of the interference study.

5.2 Testing Methodology

For the receiver model validation tests, a desired C-band signal and varying levels of UWB and lower adjacent band interference were applied to the input of a satellite earth station receiver and the output of the receiver was monitored to identify the degradation produced by the interfering signal. Specific desired signal parameters (modulation, power level at receiver input, and information content) and interfering signal parameters (pulse repetition frequency, power level, and the presence of dithering) were varied. For all of the tests, interference effects on receiver performance were evaluated based on observed degradation in picture quality.

Figure 5-1 is a block diagram of the general test setup for testing interference to the C-Band satellite earth station. The specific configuration illustrated in Figure 5-1 is for testing with UWB interference. The test setup for lower adjacent band interference was similar, except that the UWB signal source was replaced by a lower adjacent band signal source.

The satellite receiver under test was exposed to a combination of desired and undesired (interference) signals. A spectrum analyzer was used to monitor the signals being applied to the receiver under test. The variable attenuators were used to control the power levels of the desired and undesired signals.

The tests characterized interference to both the tracking and acquisition performance of the receivers. At the start of each test, the receiver was permitted to acquire the desired signal before the undesired signal was applied. The undesired signal power was increased, beginning with a power level that was well below the receiver noise floor, until degradation was observed. This first portion of the test established the interference threshold for tracking performance. The desired signal was then attenuated and the undesired signal increased, nominally by 6 dB. The desired signal power was then set back to its original level and the undesired signal was decreased until the receiver was able to acquire the desired signal. This second portion of the test established the interference threshold or acquisition performance.

5.3 Desired Signal Conditions

The desired signal for the tests was obtained from a 4.5-meter dish antenna with an appropriate feed and low-noise block downconverter (LNB) or a low-noise amplifier (LNA). This configuration permitted the desired signal to be combined with the interference in the C-Band radio frequency (RF) range before downconversion to the L-Band intermediate frequency (IF) range. The LNB, which performs the downconversion, was considered part of the receiver for the purposes of these tests.

Tests were conducted for a range of desired signal power levels to include the minimum usable power level and the maximum level that can be provided by the 4.5 meter diameter antenna. The appropriate "minimum usable power level" was determined for each receiver, based on criteria agreed upon by Alion and the C-Band Coalition. For example, the likely criterion for digital receivers is the presentation of a steady, clear picture on the monitor with no visible interruptions of the video stream. The maximum power level for the test was based on a measurement of the IF power level provided by the LNB in a typical configuration, when the LNB was attached to the antenna feed. The equipment configuration for this measurement is illustrated in Figure 5- 2. A plot showing the average power at the receiver input for horizontal and vertical polarization is shown in figure 5-3.

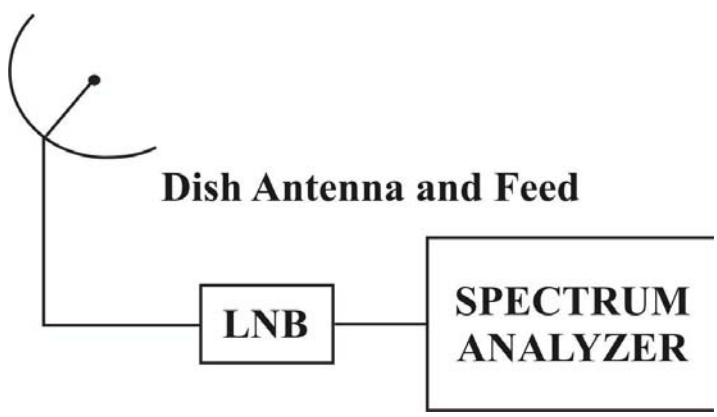

Figure 5-2. Equipment Configuration for Determining Strongest Desired Test Signal Power Level

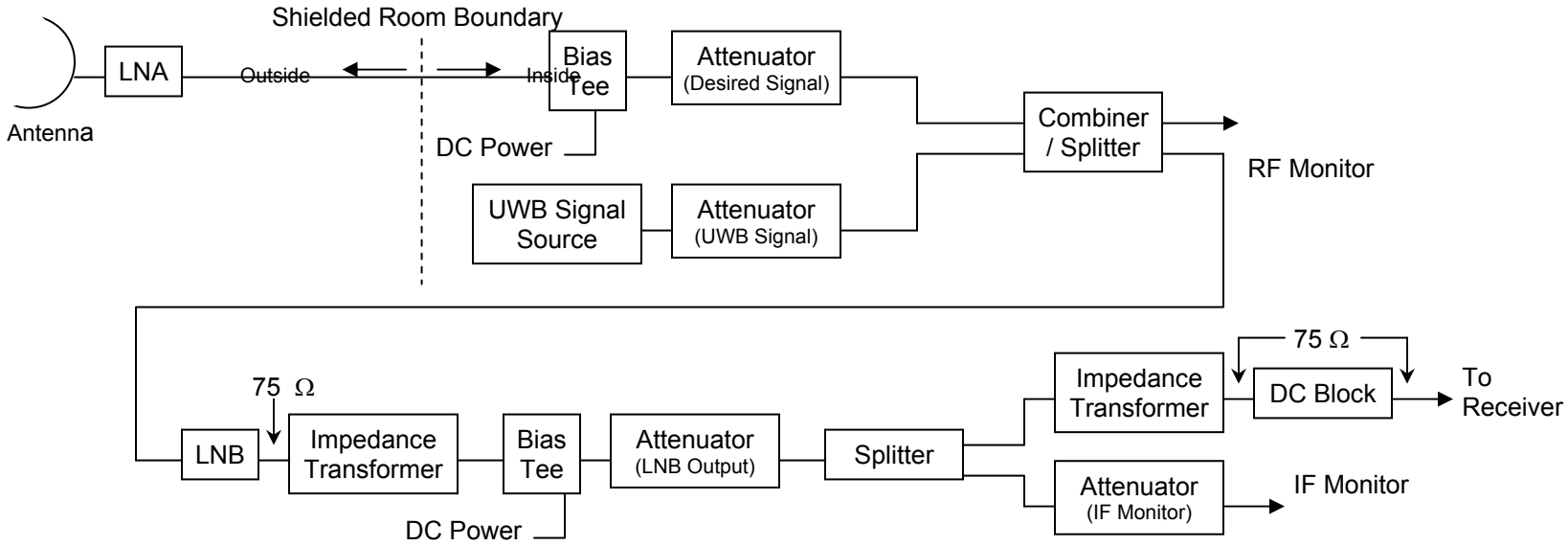

Notes:
- All impedances are 50 Ω unless otherwise indicated.
- RF Monitor output is 1.5 dB weaker than LNB input.
- IF Monitor Attenuator is adjusted so that the signal power level at IF Monitor output is the same as signal power level to Receiver.
- Desired Signal Attenuator and LNB Output Attenuator are adjusted to achieve the necessary desired signal and noise power levels at the input to the Receiver (as seen at the IF Monitor output).
- UWB Signal Attenuator is varied to determine the point at which interference renders receiver unable to track the desired signal.

Figure 5-1. Equipment Configuration for C-Band Satellite Earth Station Receiver Tests

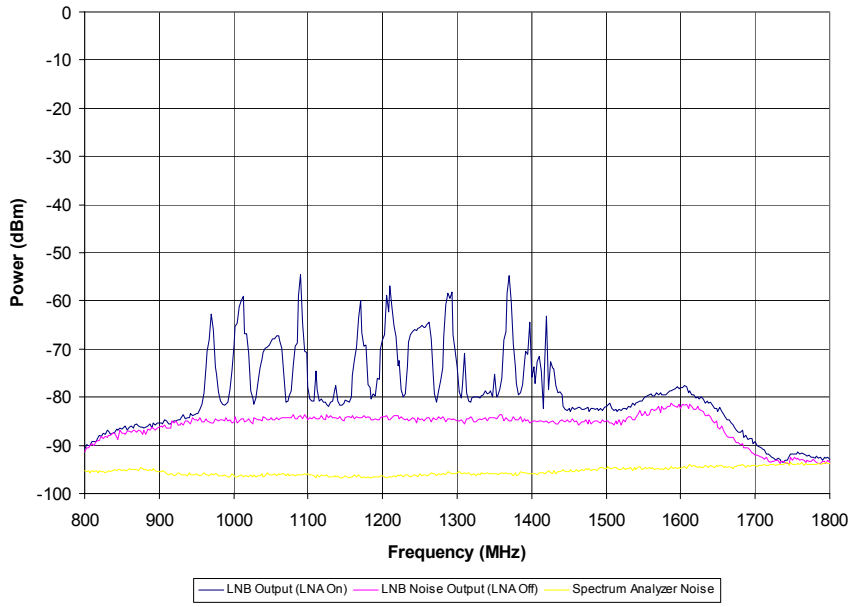

Figure 5-3. Average Power at the Receiver Input with LNB.

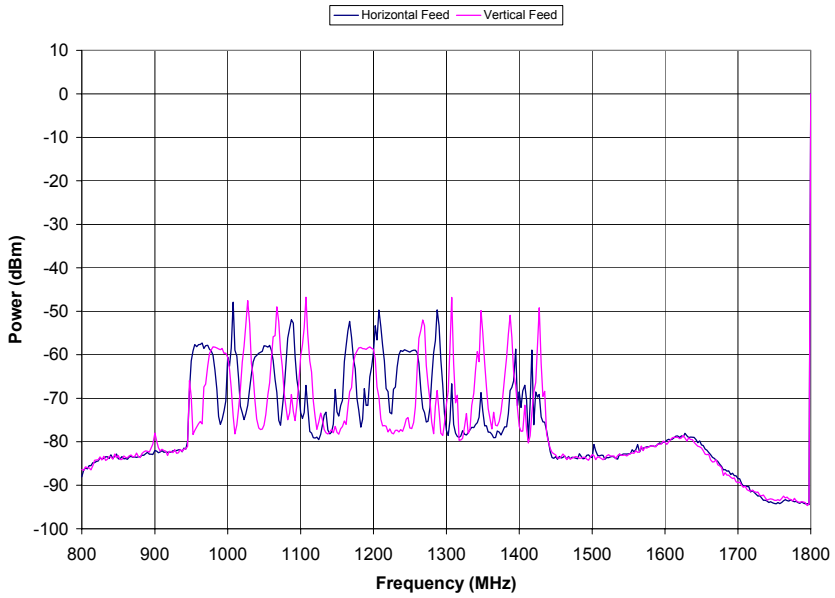

Figure 5-4. Average Power at Receiver with LNA

For tests that used the maximum desired signal power level, the power out of the LNA was attenuated in the test configuration of Figure 5-1 so that the output of the LNB in that configuration matches the IF power measured with the LNB connected directly to the feed as in Figure 5-2/5-3. Care was exercised to ensure that the IF noise floor is also closely matched for the two configurations. This is shown in Figure 5-4.

5.4 Undesired Signal Conditions

Undesired signals included pulsed ultrawideband (UWB) signals and lower adjacent band signals. The lower adjacent band signals consisted of spread spectrum waveforms similar to those presently used by devices operating in accordance with the IEEE 802.11b standards. For all of the undesired signals, the power level was varied as described in the test methodology above. For UWB signals, tests were repeated with a variety of pulse timings, to include pulse repetition frequencies (PRFs) greater than and less than the bandwidth of the desired signal. The PRF variations were intended to investigate UWB signals that appear impulsive in the receiver under test and signals that appear continuous in the receiver. For each PRF, tests were conducted using a steady pulse train and a pulse train in which the pulse timing was (pseudo) randomly dithered. The dither variations were intended to investigate UWB signals that appear periodic in the receiver under test and signals that appear noise-like. Table 5-1 provides a matrix that indicates the UWB signal manifestations within the receiver that result from the various UWB signal characteristics.

Table 5-1
UWB Signal Variations

UWB Signal Parameters	Undithered	Dithered
PRF < Receiver Bandwidth	Evenly Spaced Impulses in Receiver	Impulsive Noise in Receiver
PRF > Receiver Bandwidth	Continuous Tone in Receiver	Continuous Noise in Receiver

5.5 UWB Signal Source

A Multispectral Solutions, Inc (MSSI) Model TFP1001 impulse signal generator was used as the undesired UWB source. The TFP1001 provides separately triggerable, positive and negative impulses having rise times of typically 100 ps, and peak amplitudes of nominally 9 Volts (or +32 dBm) into 50 ohms. It is triggerable at rates in excess of 100 mega-pulses per second.

The impulse outputs from the TFP1001 are doubly-exponential pulses having an extremely fast (sub-nanosecond) rise (fall) time representing the pulse leading edge, and a somewhat slower, although also sub-nanosecond, fall (rise) time (pulse trailing edge). Because of the extremely fast pulse leading edge transition, the resultant waveforms produce significant spectral energy well beyond 10 GHz, permitting UWB system evaluation and testing over the full range of FCC Part 15 Subpart F compliance limits (e.g., 3.1-10.6 GHz). A specification sheet for the TFP1001 from MSSI is provided as Attachment 1, and a screen shot of the UWB waveform in the frequency domain is shown as Figure 5-5.

(*Representative Waveform*)

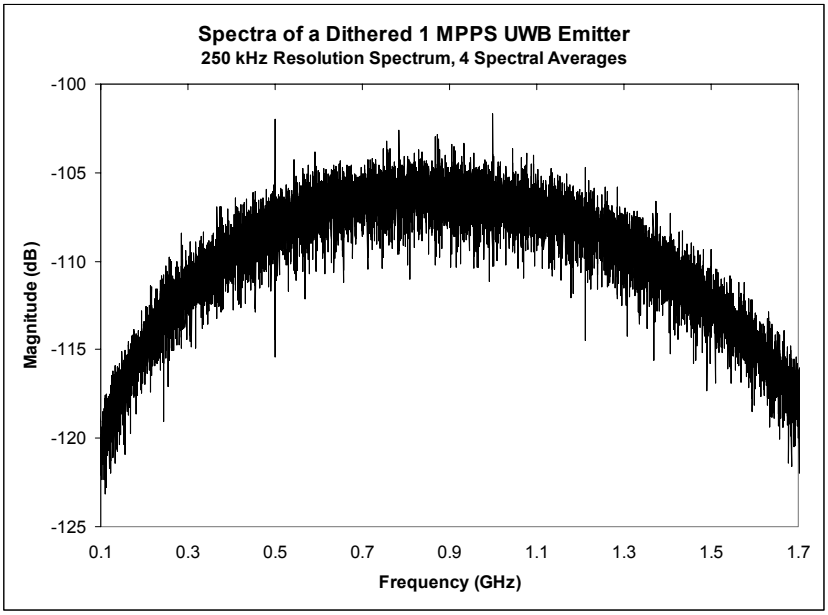

Figure 5-5. UWB Waveform Produced by the MSSI TFP1001

5.6 Receivers Under Test

The C-band satellite signal source and LNA/LNB's and receivers that were tested were provided by members of the C-Band Coalition. The test receivers and LNA/LNB are listed in Table 5-2.

Table 5-2
Analog and Digital C-Band Receivers and LNA/LNB's

Model	Modulation Type	Channel Data Rate	FEC-RS (n,k)	FEC-Viterbi (n,k)	FEC-Turbo	Notes
General Instrument DSR4500 NTSC	QPSK	41.471 Mb/s	(188,204)	3/4	no	alpha=0.35
Wegener Unity 5000	8PSK	73.725 Mb/s	(188,204)	8/9	no	alpha = 0.25
Scientific Atlanta Pwer Vu D9225	QPSK	47.2 Mb/s	(188,204)	7/8	no	alpha = 0.55 ITU-R BO.1516 system C
Standard Intercontinental Model CAD930	Analog FM	10.75 Mhz/V	n/a	n/a	n/a	VideoCipher II analog video; digital audio and multiple audio subcarriers in the 6.2 MHz – 7.1 MHz range ATIS sub-carrier for FCC ID
Vertex RSI Model LCC4S40-X4	N/A	N/A	N/A	N/A	N/A	C-Band LNA
CAP Wireless Inc. Model CA251100	N/A	N/A	N/A	N/A	N/A	C-Band LNB

Both the LNA and LNBs were compatible with the antenna feed so that the test configurations in Figure 5-1 and Figure 5-2 could be implemented. A waveguide-to-coaxial adapter was used to allow a coaxial cable to be connected to the feed end of the LNA and LNBs

Unencrypted program material was used as the desired signal for analog FM tests, and encrypted data streams were utilized for the digital signals. A standard video monitor was utilized to monitor picture quality.

5.7 UWB Test Results for the 8PSK Receiver

The 8PSK digital receiver was considered to be potentially the most sensitive to interference of all models considered. The following constraints were assumed for nominal operation in a UWB environment.

- The EIRP of the UWB emitter just meets the FCC -41.3 dBm/MHz requirement within the earth station receiver passband
- The desired signal into the earth station LNB input is 3 dB stronger than the power level at which noticeable degradation occurs in the absence of interference

The UWB input signal strength was varied to determine the threshold at which significant signal degradation became visible on a standard television monitor. Table 5-3 includes the attenuation values between the UWB antenna and the LNB input that were required to preclude noticeable effects on the earth station receiver. The table also indicates the total average UWB power within the receiver passband at the input to the LNB for each attenuation value.

The laboratory value of attenuation corresponds to the total due to propagation loss, earth station antenna gain in the direction of the UWB emitter, and feed losses.

While the fact that less attenuation is required for the undithered 50 Mpps UWB than for the dithered signal of the same PRF may seem counterintuitive, it is important to note that the undithered signal has spectral lines only every 50 MHz. This means that the power output of the undithered device would need to be reduced to a density of -41.3 dBm/50 MHz. In the lab a 1 MHz filter placed on the spectral line would also provide an output of -41.3 dBm.

Table 5-3
Lab Test of 8-PSK Digital Receivers

UWB PRF (Mpps)	Dithered/ Undithered	Lab Attenuation (dB)	UWB Interference Power (dBm)
50	Dithered	64.8	-88.7
50	Undithered	50.9	-91.1
20.8	Undithered	61.1	-98.0
20	Dithered	72.3	-89.2
20	Undithered	57.8	-96.4
5	Dithered	71.8	-96.7
5	Undithered	67.0	-96.5
1	Dithered	71.8	-94.7
1	Undithered	73.0	-95.7

The total power calculations assumed that the receiver bandwidth was just wide enough to pass all significant components of desired signal that exceeded the noise level. This bandwidth was about 35 MHz. If the actual bandwidth of the receiver were 40 MHz, then the values for dithered UWB signals would increase by 0.6 dB. The values for the 50 Mpps undithered signal would remain virtually unchanged, while the values for other PRFs would increase by up to 0.6 dB (more for the lower PRFs and less for the higher PRFs).

5.8 UWB Test Results for QPSK

Two receivers with QPSK digital demodulation were tested using the same procedure as the 8PSK receiver test described above. Test results for Scientific Atlanta Power Vu D9225 and General Instrument DSR4500 NTSC QPSK-based digital receivers are shown in Table 5-4.

5.9 UWB Test Results for the Analog Receiver

In the tests of UWB effects to the analog receiver, the receiver was operated with a desired signal level 3 dB above the level at which degradation occurs in the absence of

interference. As with the digital receiver, the interference threshold was determined by observing visible degradation on a standard TV monitor. The results with UWB interference are listed in Table 5-5.

Table 5-4
Lab Test Results for Scientific Atlanta PowerVu D9225 and General Instrument DSR4500 NTSC

Receiver	Desired Signal Level (dBm)	UWB Signal Level (dBm)	D/U (dB)	UWB PRF[a]
PowerVu	-85	-101	16	≥5 MHz
	-78	-91	13	≥5 MHz
General Instrument	-84.5	-98	13.5	≥ 1 MHz
	-77.5	-89	11.5	≥ 1 MHz
[a]dithered and undithered				

Table 5-5
Lab Test of FM Analog Receiver

UWB PRF (Mpps)	Dithered/ Undithered	Lab Attenuation (dB)	UWB Interference Power (dBm)
50	Dithered	-91	-96.7
50.1	Undithered	-89	-97.1
5	Dithered	-91	-96.7
5	Undithered	-91	-97.2
1	Dithered	-91	-100.7
1	Undithered	-88	-94.9
0.1	Dithered	-91	-87.7

5.10 WiFi Test Results

In the next round of tests, the interference source was an 802.11b (WiFi) signal, amplified and translated in frequency to operate near the lower edge of the receiver passband. The frequency offsets were chosen to simulate the condition in which the desired signal is near the lower edge of the 3.7-4.2 GHz band and the WiFi signal is near the upper edge of the 3.65-3.70 GHz (lower adjacent) band. The receiver was operated with a nominal desired signal level 3 dB above the level at which degradation occurs in the absence of interference. The results of the WiFi interference tests are shown in Table 5-6.

Table 5-6
Lab Test of Earth Station Receivers: WiFi Interference

Desired Signal Type	Desired Signal Level (dBm)	WiFi Frequency Offset (MHz)	WiFi Power (dBm)
Standard Intercontinental	-91 -91	31 42	-84 -69
Wegener	-85 -85	31 42	-86 -73
PowerVu	-85 -85 -78 -78	51 62 51 62	-61.5 -62.4 -59.5 -59.4
General Instrument	-84.5 -84.5 -77.5 -77.5	51 62 51 62	-81.6 -74.8 -74.6 -70.8

5.11 Computer Receiver Model Validation

Validation of the receiver simulation models was performed by comparison of the test output with simulation output, with the simulated UWB interference comparable to the 50+ Mpps dithered case described in the test procedures. The simulated desired signal power was held at –81 dBm, which matches the product of the spectral density and bandwidth defined above for the digital receiver test. Meanwhile the undesired (UWB)

signal power was varied parametrically to find the "knee" of the simulated receiver's performance curve. The results of this procedure are provided in Table 5-7. A positive deviation value indicates that the experimental receiver was slightly more sensitive to UWB interference than the simulation predicted. On the whole the variation between predicted and observed receiver sensitivities to UWB interference were considered to be well within the range of experimental precision.

Table 5-7
Receiver Model Validation Results

Receiver Simulation Designation	Metric of Comparison	Test value	Simulation value	Deviation (dB)
8-PSK	D/U ratio (dB)	8.1	13.2	+5.1
QPSK-1	D/U ratio (dB)	13	7.8	-5.2
QPSK-2	D/U ratio (dB)	11.5	10.7	-0.8
FM Analog	D/U ratio (dB)	5.7	6.5	+0.8

SECTION 6
SUMMARY OF RESULTS AND CONCLUSIONS

6.1 Summary of Results

A combination of laboratory testing and computer simulation was utilized to investigate the effect of UWB and lower adjacent band unlicensed devices on C-Band FSS ground station receiver performance. A representative sample of analog and digital receivers of interest were identified. Simulink models of these receivers were then developed, verified, and validated (V&V) using laboratory testing with appropriate desired and undesired interfering UWB and lower adjacent band signals. Three specific interfering signal deployments were considered starting with 1000 UWB devices uniformly distributed, normally distributed, and inverse normally distributed within a 5 km radius of the receiver of interest.

From this measurement/analysis effort, it is predicted that the impact of UWB and lower adjacent band devices on the performance of FSS receivers is dependent on the distribution and density of emitters in the environment in the vicinity of C-Band earth stations. FSS receivers will experience complete reception failure at currently regulated UWB power levels assuming emitter densities currently found in the environment of common wireless-based consumer items.

For the purposes of this analysis, complete reception failure is defined as loss of video and/or audio for digital receivers and the appearance of "snow," or impulsive artifacts for analog receivers. For example, the simulated 8-PSK earth station, the most sensitive receiver considered in this effort, failed when the aggregate UWB power reached –102.4 dBm. This is equivalent to approximately 8,000 emitters uniformly distributed within a 5 km radius or about 0.8 devices per acre for an antenna elevation angle of 5 degrees. At antenna elevation angles of 7.5°, 10°, 12.5°, and 15° the critical densities in a uniform UWB environment are 1.9, 4.7, 7.4, and 9.3 devices per acre respectively. These densities are considered achievable in the early stages of an UWB-based network deployment or usage paralleling that of cordless telephones.

Market Influence on UWB Environment

The market for UWB based applications is in its infancy, but familiar trends in affordability and popularity of other networking technologies and wireless communications devices indicate the potential growth will impact earth station viability.

If, for instance, UWB becomes as ubiquitous as the cordless telephone, a market density of two per ¼-acre residential lot is a reasonable projection. This is more than ten times the critical density we have previously identified. Deployment within an industrial park, for example, one UWB per 10'x10' office, introduces significantly greater interference potential.

Vehicular UWB applications also represent a potentially significant source of interference for earth stations in the vicinity of major highways. For example, rush hour traffic density along a six-lane highway through a major metropolitan area like Los Angeles can reach concentrations of 150 to 190 vehicles per acre. If even a small fraction, say 10%, of these cars and trucks carried UWB transmitters, the aggregate interference could be twenty times (13 dB) or more above the functional tolerance of nearby earth stations.

If UWB and lower adjacent band-based applications behave as other similar technologies in the marketplace, there is considerable precedent for anticipation of rapid growth in the density of these devices:

- Between 1998 and 2000 the fraction of U.S. households with computers grew from 42% to 51%. During the same period households with Internet access grew from 26.2% to 41.5%. (U.S. Dept. of Commerce, National Telecommunications and Information Administration, *Falling Through the Net: Defining the Digital Divide*, July 1999 and October 2000)

- Between 1985 and 2002 the fraction of U.S. households with cordless telephones grew from 11% to 81%. During the same period households with cellular telephones grew from 0.1% to 56%. (Consumer Electronics Association, reprinted in *World Almanac 2004*)

- Cellular telephone subscribers in the U.S. grew from 11 million in 1992 to over 140 million in 2002. *(CTIA Semiannual Wireless Industry Survey)*

- Population in major metropolitan areas (1-5 million) grew by 19% during the 1990s. *(Population Reference Bureau: Ameristat.org)*

- Typical urban population and housing densities (Table 6-1) indicate a potential market for household UWB applications far above the critical level indicated by this analysis. *(US Census Bureau 1990, 2000)*
- Population and housing statistics for several counties within the Washington DC metropolitan (Figures 6-1 and 6-2) show that even the suburban market may be a critical source of UWB interference, when both household and mobile applications are taken into account. The majority of suburban housing in this region consists of single detached homes and townhouses (Figure 6-3), leading to lower densities than nearby cities, but still above the critical threshold. *(US Census Bureau 1990, 2000)*

Table 6-1
Representative Urban Population and Household Densities

City	Land area (sq. mi)	Population (2000 Census)	Persons per acre	Households per acre (est.)
Los Angeles, CA	469	3,694,820	12.3	4.7
Washington, DC	68	572,059	13.1	5.1
Minneapolis, MN	55	382,618	10.9	4.2

Based on population trends cited above and market data for previous wireless applications, projections of future density for consumer UWB devices were developed, as shown in Figures 6-4 through 6-6.

If the minimum device density that can significantly interfere with digital TVRO is less than one emitter per acre, then the analysis clearly indicates that consumer UWB and lower-adjacent-band applications should not be ignored for their potential impact on C-band earth station operations.

Figure 6-1. Suburban population densities near Washington, DC

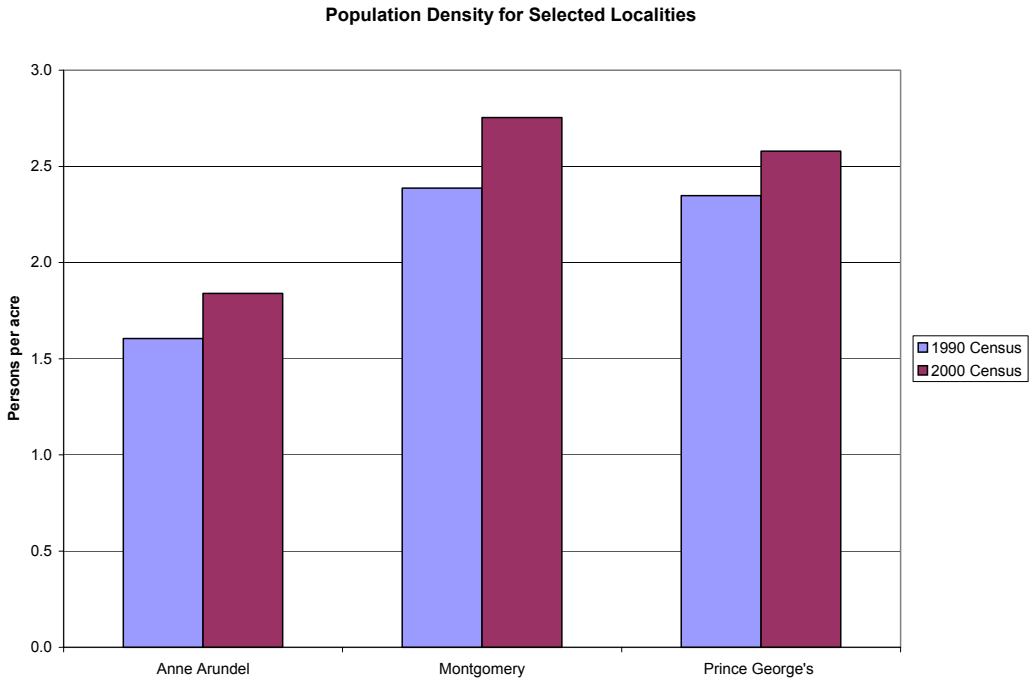

Figure 6-2. Suburban housing densities near Washington, DC

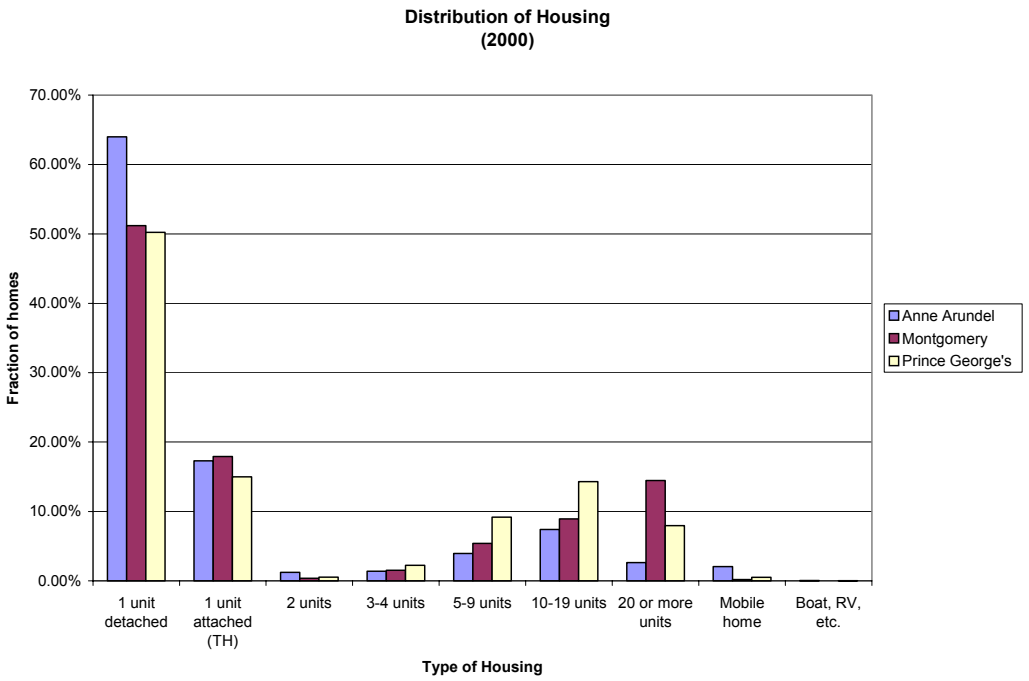

Figure 6-3. Suburban housing distribution near Washington, DC

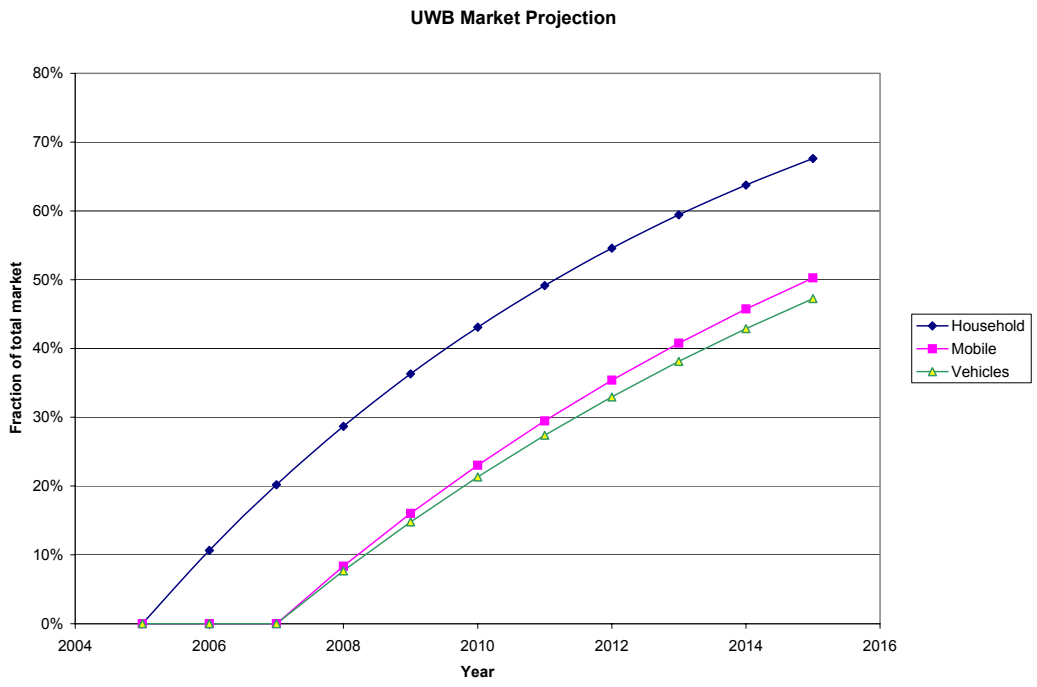

Figure 6-4. Projected UWB consumer market penetration

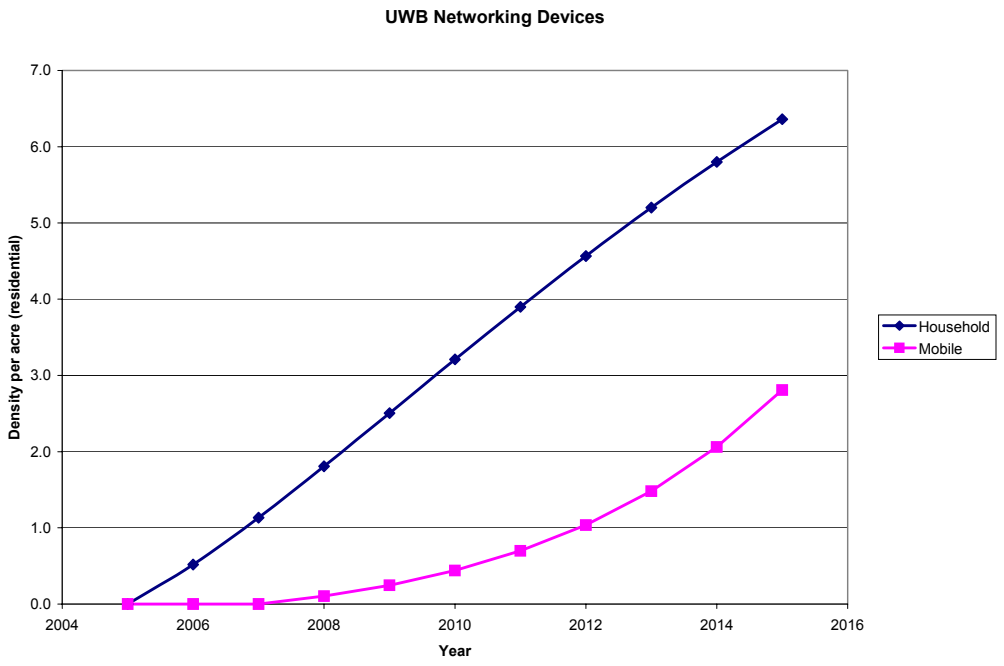

Figure 6-5. Projected UWB residential densities

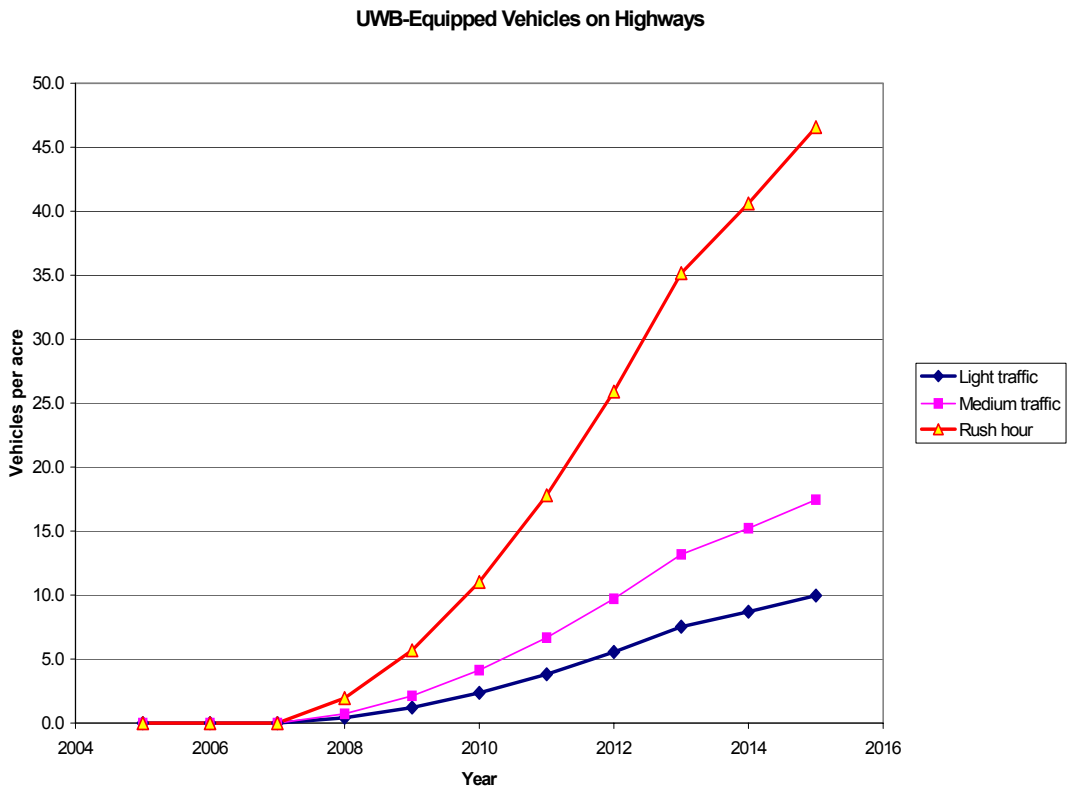

Figure 6-6. Projected UWB vehicular densities.

6.2 Conclusions

Every metropolitan area in the United States has numerous C-band ground stations associated with network television affiliates, cable television head-ends, and private television receive-only (TVRO) systems. From this measurement/analysis effort, it is predicted that the impact of UWB and lower adjacent band devices on the performance of FSS receivers is dependent on the distribution and density of emitters in the environment in the vicinity of C-Band earth stations. FSS receivers will experience complete reception failure at currently regulated UWB power levels assuming emitter densities currently found in the environment of common wireless-based consumer items.

For the purposes of this analysis, complete reception failure is defined as loss of video and/or audio for digital receivers and the appearance of "snow," or impulsive artifacts for analog receivers. For example, the simulated 8-PSK earth station, the most sensitive receiver considered in this effort, failed when the aggregate UWB power reached –102.4 dBm. This is equivalent to approximately 8,000 emitters uniformly distributed within a 5 km radius or about 0.8 devices per acre for an antenna elevation angle of 5 degrees. At antenna elevation angles of 7.5°, 10°, 12.5°, and 15° the critical densities in a uniform UWB environment are 1.9, 4.7, 7.4, and 9.3 devices per acre respectively. These densities are considered achievable in the early stages of an UWB-based network deployment or usage paralleling that of cordless telephones.

A combination of reduction in the power of individual interfering devices and a PRF limit would provide a balance against the earth station interference potential imposed by market growth. Based on the simulation analysis results, curves of recommended reductions in UWB power (in decibels) as a function of projected market density (in emitters per acre) was developed for the 8-PSK receiver (Figure 6-7). These curves are indexed by the earth station's antenna elevation angle (5° to 15°). As an example, an adjustment of approximately 9.5 dB in the UWB emitter power would allow 16 devices per acre at an earth station antenna elevation angle of 7.5°. Similarly, a 5.5 dB reduction would be required to allow the same 16 devices per acre with an elevation angle of 10°. This corresponds to a UWB usage of four in every household in a typical urban housing development (1/4 acre lots). Much higher UWB densities are likely in townhouse or apartment complexes, or commercial office parks.

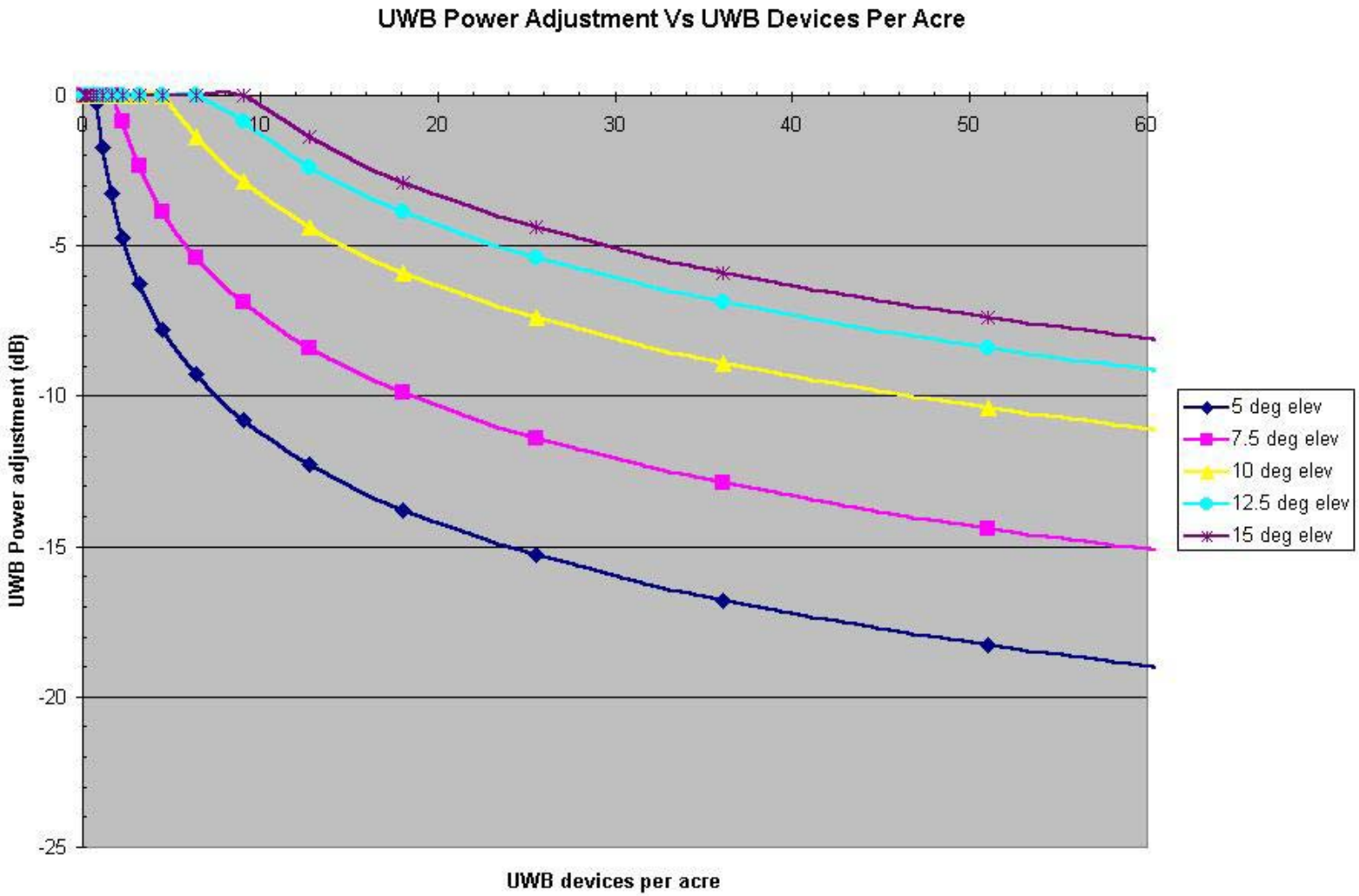

Figure 6-7. UWB Power Adjustments Versus Antenna Elevation Angle to Prevent Disruption of Service

ATTACHMENT 1

MULTISPECTRAL SOLUTIONS, INC.

Model TFP1001 Impulse Source User Instructions

1. Introduction

The MSSI Model TFP1001 is a dual output, impulse signal generator for use in applications ranging from

time domain reflectometry (TDR) to Ultra Wideband (UWB). The TFP1001 provides separately triggerable, positive and negative impulses having rise times of typically 100 ps, and peak amplitudes of nominally 9 Volts (or +32 dBm) into 50 ohms. Triggerable at rates in excess of 100 megapulses per second, the TFP1001 is ideally suited to a wide range of UWB systems analyses and measurements.

The impulse outputs from the TFP1001 are doubly-exponential pulses having an extremely fast (subnanosecond) rise (fall) time representing the pulse leading edge, and a somewhat slower, although also subnanosecond, fall (rise) time (pulse trailing edge). Because of the extremely fast pulse leading edge transition, the resultant waveforms produce significant spectral energy well beyond 10 GHz, permitting UWB system evaluation and testing over the full range of FCC Part 15 Subpart F compliance limits (e.g., 3.1-10.6 GHz).

2. Operational Requirements

Power:

The TFP1001 is supplied with a 12 Volt AC-to-DC adaptor; however, the instrument will operate with DC voltages in the range 9-18 Volts (center post Positive +), with a minimum current requirement of 300 mA (at 100 MHz toggle rate).

Trigger Inputs:

The negative and positive impulse outputs are separately triggerable from the BNC connectors on the back panel. Trigger input circuitry consists of a CMOS input gate (flip-flop) and a 50 ohm resistor to ground. Trigger inputs respond to the rising edge of the clocking source.

The minimum HIGH voltage required is 2.5 volts, for which the LOW voltage must be 0.5 volts or less. A minimum pulsewidth of 3 nanoseconds is required. However, for reliable operation at high pulse repetition frequencies (PRF) up to 100 MHz, it is recommended that the HIGH voltage be at least 3.3 Volts and have a pulse width of at least 5 nanoseconds.

Note 1: The maximum trigger input voltage should not exceed +7 Volts.
Note 2: If the trigger is supplied from a 50 ohms source impedance, the voltage will be halved at the trigger input to the TFP1001 (voltage divider effect). For example, a CMOS line driver chip operating from 5 Volts with a 50 ohms output impedance will not be able to reliably trigger the TFP1001 at all PRFs since typical power supply droop and coaxial cable losses will put the trigger input level at the TFP1001 slightly below the required minimum.

3. Specifications:

Output Voltage (Magnitude): 8.0 Volts (minimum), 9.0 Volts (typical) into 50 ohms
Rise Time: 125 ps (maximum) Positive Pulse (110 ps typical)
Fall Time: 125 ps (maximum) Negative Pulse (100 ps typical)
Pulsewidth: 250 ps (RMS) typical
Maximum PRF: 100 MHz (minimum)
Typical Output Responses

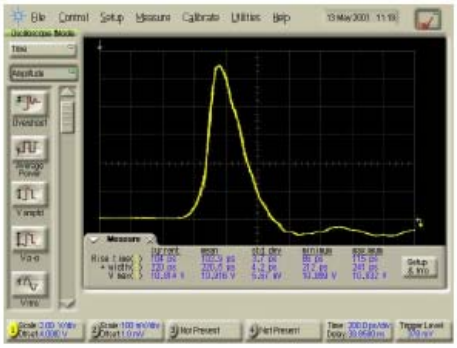

Typical Positive Output Pulse (200 ps/div)

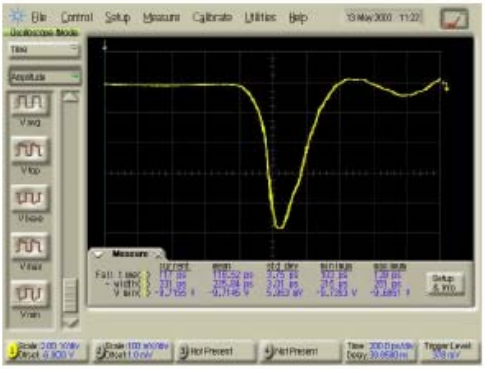

Typical Negative Output Pulse (200 ps/div)

Multispectral Solutions, Inc., 20300 Century Boulevard, Germantown, MD 20874 USA
(301) 528-1745 FAX: (301) 528-1749 email: info@multispectral.com
A Tradition of Excellence in Innovation